The Glencoe caldera ring fault(s) as a detailed record of a magmatic sub-surface transport system and its collapse mechanics.

FRANCESCA LILY HAYWOOD

A thesis submitted for the degree of Master of Science (by research)

The Glencoe caldera ring fault(s) as a detailed record of a magmatic sub-surface transport system and its collapse mechanics.

Francesca Lily Haywood

Earth Sciences, Durham University, Durham, DH1 3LE

Primary supervisor: Fabian B. Wadsworth

Secondary Supervisors: Richard J. Brown, Dave McGarvie (The Lancaster Environment Centre, Lancaster University, Lancaster)

With thanks to: Annabelle Foster, Alex Iveson, Bob Holdsworth, Madeleine Humphreys

Abstract

Some of the largest and most hazardous natural events on Earth are silicic caldera-forming volcanic eruptions, where the eruption of vast volumes of magma results in the collapse of crustal material that forms the magma reservoir's roof (Cole *et al*., 2005; Geyer and Martí, 2014; Sigurdsson *et al.*, 2015; Kennedy *et al.*, 2018; Geshi *et al.*, 2021). Volcanic eruptions include 3 key regions of activity: magma storage, sub-surface magma transport, and surface magma eruption. The behaviour of the sub-surface transport system throughout a caldera-forming eruption is poorly constrained due to limitations in methods of study available, and because it suffers from being complicated by its interaction with the structural caldera collapse system (Wiebe *et al.*, 2021). Along caldera ring fault surfaces the two separate movements occur (the upwards transport of magma, and the downwards collapse of the caldera block), so, it is difficult to unpick the relationship between these two processes and whether this interaction causes any changes to the mechanics of caldera-forming eruptions.

In order to address the poor understanding of caldera transport systems, this thesis addresses two questions. (1) How do the processes of caldera slip and magma transport initiate and interact with one another when both occurring along the common surface of the caldera ring fault? (2) In what state is magma transported through the crust? This study applies these questions to the ancient Glencoe caldera (Scotland) where erosion has allowed for exposure of the caldera on many levels including the ring fault/conduit fill (Kokelaar and Moore, 2006). Therefore, this study uses field, textural, petrological, geochemical, and theoretical evidence to discuss these key questions in order to build a model for the evolution of the sub-surface transport system throughout an eruption which is applicable to calderas worldwide where this exposure cannot be seen.

Here we show that friction along caldera ring faults is not high enough to produce frictional melts, as proposed by previous 'superfault' theories (Spray, 1997; Kokelaar, 2007; Han *et al.*, 2019; Kim *et al.*, 2019). Instead, we suggest that collapse is incremental, piecemeal, and dilational, and that ring faults are dominated by magma transport processes throughout an eruption. Hence, this provokes the idea that the naming of such ring faults may have a misleading emphasis. This work also shows that the subsurface transport of pyroclastic magma is deep, widespread and long-lived during caldera eruptions which progressively tap deeper magma chamber components. We anticipate this thesis will encourage future research to not focus on caldera models which rely on high friction along caldera ring faults, but instead understand that these systems are long lived and dominated by eruptions of pyroclastic material.

Acknowledgements

I would like to thank my supervisors Fabian Wadsworth, Rich Brown and Dave McGarvie for their support and advice throughout every stage of my masters. It has been a particularly challenging time due to social isolation and restrictions in work access so their effort has been especially valuable. Also, thank you (and Annabelle Foster) for doing fieldwork in Glencoe without me present, I couldn't have done this without your work! Fabian's effort to meet me in person despite covid restrictions has been a massive help to making everything seem a bit more normal. Fabian has gone over and beyond by providing me support outside of my masters, with PhD plans and writing what will hopefully become my first published paper, I am so appreciative of this.

Thank you to Annabelle Foster, Alex Iveson, Bob Holdsworth and Madeleine Humphreys at Durham who helped me at stages throughout this work. This support was really needed due to the wide range of topics my work covered therefore I would have been lost without their expertise and guidance.

Leon Bowen and Diana Alvarez-Ruiz have been a huge help during my masters, so thank you. Their dedication to teaching me on the SEM and EDS (despite my many questions…) as well as their good spirits despite long days in the labs is so massively appreciated.

I want to say a huge thank you to my Dad, Tim Haywood, who journeyed out to Glencoe with me in the middle of winter to brave the torrential rain in order to make sure that I had seen the area I was due to study for the next year (and no thanks to covid for causing me to miss the original fieldtrip).

Thank you to my friends, family and Jamie who kept me sane despite the struggles of covid, which at times became quite overwhelming, especially when we were stuck isolating in our grotty student house for 4 weeks.

Contents

Chapter 1: Thesis introduction

Silicic caldera-forming eruptions have great capacity for destruction. Silicic caldera-forming eruptions are considered to be among the largest and most hazardous natural events on Earth, with the ability to erupt 5,000 km^3 of lavas (recorded as the Fish Canyon Tuff associated with La Garita caldera, US) and pyroclastic material (Cole et al., 2005; Geyer and Martí, 2008; Sigurdsson *et al.*, 2015; Kennedy *et al.*, 2018). Caldera-forming volcanoes also represent a large portion of the world's total volcanism (for example, there are >60 known calderas in North America (Newhall and Dzurisin, 1988; Geyer and Martí, 2008; Browning and Gudmundsson, 2015). Motivated by this hazard, research has resulted in coherent understanding of the processes occurring in the magma reservoir and eruption at the surface. However, the sub-surface transport of magmatic material along caldera ring faults between the reservoir and the surface remains poorly constrained. In order to address this outstanding problem, this thesis studies a rare example in Glencoe caldera, Scotland, U.K. where erosion has exposed the crustal magma transport system and therefore presents an opportunity to test hypotheses associated with magma transport. This study addresses two main questions which aim to contribute towards filling this gap in our knowledge applicable to caldera systems worldwide (1) how do the processes of caldera slip and magma transport initiate and interact with one another when both occurring across the common surface of the caldera ring fault? And (2) in what state is magma transported through the crust? Therefore, at what stage does fragmentation occur during the transport of large masses of magma along ring faults at caldera-forming eruption?

1.1 Caldera-forming eruptions

Calderas are volcanic depressions created by the collapse of crustal material that forms the roof of the magma reservoir into the space created below by the removal and eruption of magma, through the volcanic sub-surface transport system (Cole et al., 2005; Sigurdsson *et al.*, 2015; Kennedy *et al.*, 2018). This results in a wide variety of caldera sizes (up to 75 km in approximate diameter) and a range of eruptive volumes (1-5000 km^3 of ejecta) of which the predominant product is pyroclastic (Cole et al., 2005; Geyer and Martí-, 2014; Kennedy *et al.*, 2018). Caldera forming eruptions have a magma storage region, crustal transport region and surface eruption/deposition region as expected with other volcanic systems, however the key difference is the size, complexity and structural configuration associated with the caldera collapse system (figure 1.1).

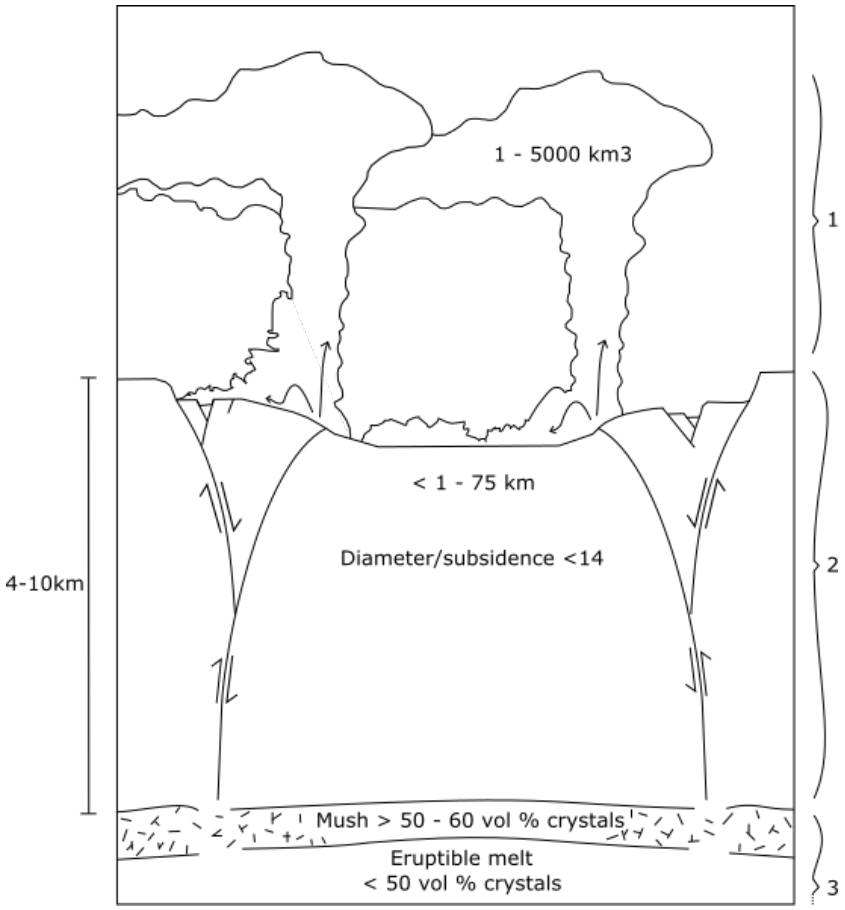

Figure 1.1. *A simplified cartoon model of a cross section of a volcano during a caldera-forming eruption shown to demonstrate the 3 important subsystems of a caldera during eruption: (1) the surface eruption, (2) the magma transport zone through the crust, and (3) the magma reservoir. The lack of drawing for how magma moves from the reservoir into and along the ring fault transport system demonstrates the relatively poor understanding for how this subsystem behaves during an eruption. Note that this is not accurately drawn to scale although some indicative scales are given for portions of the system.*

Here I will describe the current popular model for caldera-forming eruptions, which aligns with the evidence that exists today. This is written to provide context to the wider picture for the study's focus on calderas, however, I will later reveal that this model is very generalised and there still remains great complexity and uncertainties. Refer to Kennedy *et al.,* (2018) for a detailed account of the current overall model of caldera structure and the complexities not reviewed here in detail.

Silicic caldera-forming eruptions initiate via large Plinian eruptions which progress through multiple vents along the caldera ring fault structure. The ring fault is typically an annular system of intersecting faults that facilitate the downwards collapse of the caldera floor as well as the sub-surface transport of magmatic material to the surface (Sigurdsson *et al.*, 2015). Caldera-forming eruptions produce abundant ignimbrite deposits which result from sustained pyroclastic density currents (PCDs) erupted

from ring fault vents. The eruption styles, deposit styles, and timescales are well understood via fieldwork studies of deposits and modelling (Branney and Kokelaar, 2003; Brown and Branney, 2004; Wilson, 2008; Brown et al., 2012). Caldera fault collapse dynamics are generally dilational due to the outward or sub-vertical dipping structure of ring faults and the intrusion of magma exploiting the fault surfaces as a vent often prior to collapse (Geshi *et al.*, 2021). These processes are often piecemeal and incremental, and are accompanied by the ejection of abundant lithic debris shed from the fault planes (Cole et al., 2005; Segall and Anderson, 2021). Caldera block mapping and sandbox modelling provides evidence for this structure (Acocella, 2007; Geyer and Martí-, 2014; Segall and Anderson, 2021).

1.2 In brief: What we know about caldera-forming eruptions

A large-scale, silicic caldera-forming eruption has never been witnessed, and we rely on reconstructing events from field studies, textural studies of deposits, analogue modelling, and numerical modelling (Geyer and Martí-, 2014). However, understanding caldera-forming eruptions is complicated by their size and because calderas are often buried by their own deposits (Browning and Gudmundsson, 2015). Existing models of caldera-forming volcanic processes will often focus on the two ends of its eruptive sequence, with information gathered from erupted materials (table 1):

1. The storage conditions of melt in a caldera's shallow crustal reservoir and the processes that prime magma for eruption (Figure 1.2a), including constraint of parameters and processes such as storage depth, volumes, melt extraction from a crystal mush or mush rejuvenation, and magma evolution in the Earth's crust with a focus on magma accumulation and eruption timescales. Evidence is given by plutonic equivalents and geochemical/petrological studies (Acocella, 2007; Bachmann and Bergantz, 2008; Wilson, 2008; Cashman and Giordano, 2014; Parmigiani *et al.,* 2014; Wilson *et al*., 2021).

2. The production and deposition of materials at the Earth's surface during caldera-forming eruptions (Figure 1.2b), including constraint of parameters and processes such as mass flux, ignimbrite plumes, eruptive product emplacement, steadiness of flow, and the waxing or waning of eruption rates. Evidence is given by field and sample structures and compositions (Branney and Kokelaar, 2003; Brown *et al.,* 2012; Devenish, 2013; Costa *et al.,* 2018).

This understanding has developed because there are widespread deposits of material erupted from silicic calderas which are easily accessible for studies of these regions.

Table 1 *A table to demonstrate the 3 key regions of a caldera system and the degree of current-day knowledge of their structures and processes. The relative scale provided is subjective, based on a thorough investigation into present day literature on topics at time of writing.*

Region of a caldera-forming eruption	Degree of current-day knowledge of this region's structure and processes	Best methods of study available to understand this region	How easy those study methods are to use	Key references for previous research into this region
Surface eruption and deposition processes	Good	Fieldwork into surface deposit structure and analysis of deposit samples	Easily accessible	Branney and Kokelaar, 2003; Brown *et al.,* 2012; Devenish, 2013; Costa *et al.,* 2018
		Direct observations	Limited for calderas but abundant for other comparable eruptions	
		Modelling of surface processes	Complicated by size and shape but still informative	
Crustal sub-surface magma transport	Very limited	Fieldwork into deeply eroded ancient calderas that exposure the sub-surface	Effective but few examples of this exist	Cole et al., 2005; Kokelaar, 2007; Acocella, 2007; Holohan, 2015; Browning and Gudmundsson, 2015; Kennedy *et al.*, 2018; Wiebe *et al.*, 2021
		Analogue models	Large uncertainties due to size and shape of calderas making the processes hard to model	
		Application of knowledge for non-caldera forming eruptions	Often needed due to the limit of other methods of study, but leaves large unknowns due to relative simplicity	
Magma storage region	Quite good	Analysis of surface deposits and plutonic equivalents that reveal insights into storage region processes (e.g. crystal inclusions, dating methods…)	Easily accessible and wide array of opportunities which reveal effective and quantitative insights to the system	Acocella, 2007; Bachmann and Bergantz, 2008; Wilson, 2008; Cashman and Giordano, 2014; Parmigiani *et al.,* 2014; Wilson *et al.*, 2021
		Fieldwork into deeply eroded ancient calderas that exposure the sub-surface	Effective but few examples of this exist	

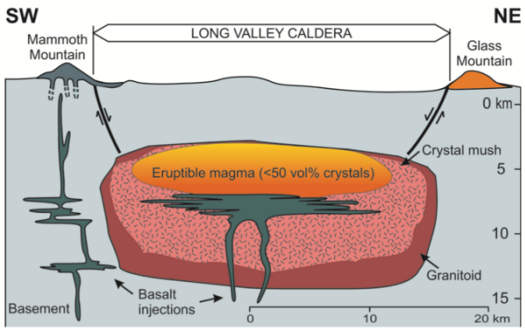

A

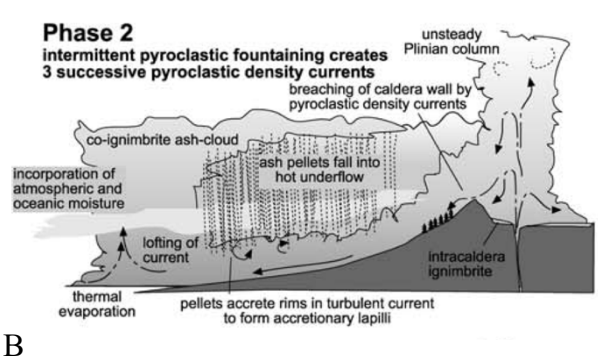

B

Figure 1.2. *Examples of the areas of focus in previous work on caldera-forming systems. (a) The focus given to, and detailed understanding of, caldera magmatic reservoirs (taken from Bachmann and Bergantz, 2008). (b) The focus given to, and detailed understanding of explosive volcanic eruption dynamics at the Earth's surface (taken from Brown and Branney, 2004)*

At least 5000 km^3 of magma (which parallels the largest volume of magma known to erupt during a single event, Bachmann and Bergantz, 2008) resides within reservoirs beneath caldera-forming volcanoes. The magma reservoirs of large silicic eruptions are known to be distinct and display great diversity - from their timescales (of accumulation and eruption of magma), to their subsurface structure, and their style of eruption, trigger and collapse (Kennedy *et al.*, 2018; Wilson *et al.*, 2021). The state of magma prior to eruption is transient and dynamic. Caldera systems will mostly erupt the shallower (4-10 km below the surface), more evolved, younger crystal poor magmas (figure 1.1, 1.2a). However eruptible magmas may reside at depths up to 17 km (Kennedy *et al.*, 2018). The reservoirs containing these large volumes of eruptible magmas (silicic melt) that source caldera systems are short lived (sometimes just a few centuries in age after the onset of accumulation) and evolve through the progressive fractionation of their deeper mantle-derived basaltic magma roots, mafic influx, as well as assimilation of country rock and melt extraction (Wilson *et al.*, 2021).

Shallow silicic magmas reside mostly within, and are fed by, a vertically extensive magma mush which is dominantly in a crystalline state (Bachmann and Bergantz, 2008; Parmigiani et al., 2014; Bachmann and Huber, 2016; Kennedy *et al.*, 2018). The mush zone extends furthest below the melt rich body, known as the trans-crustal magmatic system, where it becomes gradually more differentiated and evolved with elevation. Minor volumes of these crystal rich (50-60 vol.% crystals), deep (>10 km), basaltic 'magma mush' roots may also contribute to eruptions when it is remobilised through thermal inputs, to produce crystal rich deposits (25-55 vol.% crystals) (Kennedy *et al.*, 2018). The mush may interact with melt bodies through remobilisation and eruption of its whole crystal rich body, or extracted interstitial melts, which may still result in crystal poor magmas (Holness, 2018). The reservoir structure for magma storage for large silicic systems is very variable: they can consist of one or multiple bodies, which may be simultaneously or sequentially tapped, and might be compositionally zoned or vigorously convecting (Bachmann and Bergantz, 2008; Huber, Bachmann and Dufek, 2011; Wilson *et al.*, 2021). Compositional variations (which may or may not be systematic) can occur due to crystal abundance and/or melt phase composition. External tectonics may also play a great control in the architecture of magmatic reservoirs (Wilson *et al.*, 2021). Magmatic activity producing intrusions at calderas will often exploit structures produced by faulting, subsidence and regional tectonism, as seen at the Glencoe ring faults (Kokelaar and Moore, 2006; Kennedy *et al.*, 2018). Venting of magma along ring faults will change significantly as faulting and

subsidence (therefore the stress regime) develops, highlighting the complex sub-volcanic transport system present.

1.3 The gap in our knowledge of calderas: the sub-surface transport system

A simplified view of the sub-surface transport system for caldera-forming eruptions consists of a sub-circular ring fault which accommodates slip of the downfaulted block and acts as a conduit for magma transport, to produce a ring fault dyke. There are often other smaller faults and conduits also present surrounding this. This system connects the magma storage and eruption regions. The transport system must therefore play a key role in caldera eruption dynamics.

The focus on storage processes or eruptive processes leaves out a key missing piece of information concerning the sub-surface transport system that links the two regions (Table 1; figure 1.1) (Sigurdsson *et al.*, 2015; Wiebe *et al.*, 2021). An explanation for why this gap in our knowledge has developed can be attributed to the limitations of the methods of study available when being applied to caldera transport systems: (1) there is a paucity of good field examples, (2) we have never witnessed a large, high-energy caldera-forming eruption, (3) the dynamics are so energetic and on such a large scale, that they are difficult, if not impossible, to forward-model numerically, and (4) the system is difficult to scale-down to analogue laboratory experiments because the large-scale structure matters, as does the local flow regime in the transport system (Wilson, 2008; Geyer and Martí-, 2014; Costa *et al*., 2018; Kim *et al.*, 2019), making dynamic scaling via dimensional analysis a challenge. The gap in our knowledge has become increasingly noticeable as recent studies modelling the storage zones of caldera-forming systems have made progress in the understanding of mush storage. However, these models do focus on the long term systematics of producing silicic melt, whereas fewer developments have been made towards the short term behaviours of these large rhyolitic melt bodies, such as how they respond to the sudden and complex pressure changes they undergo during periods of volcanic or faulting activity (Bachmann and Bergantz, 2008; Cashman and Giordano, 2014; Parmigiani et al., 2014; Bachmann and Huber, 2016; Kennedy et al., 2018; Wilson et al., 2021).

The spatial and temporal scales of large silicic caldera-forming eruptions are so large that it is not possible using standard computers or analogues to model their full behaviours, as there are too many variables to make this tractable. Due to the uncertainties around models for sub-surface caldera structures (Cole et al., 2005; Acocella, 2007; Holohan, 2015; Kennedy *et al.*, 2018), field studies of dissected terrains (that expose contemporaneous volcanic and plutonic rocks) that are then used to underpin geochemical studies provide the most reliable route to understanding these catastrophic systems (Browning and Gudmundsson, 2015; Wiebe *et al.*, 2021). Studies using fieldwork, samples

and geochemistry must however account for the fact these methods will only display the final result of a long-standing complex system which may overprint deposits, textures, and geochemical signals. Therefore, there is large opportunity for misinterpretation because the temporal evolution cannot be immediately recognised. The end result of these studies must be to understand what the evidence implies for the system over time to create a sequential theoretical model.

While the dynamics of magma transport in conduits and fissures at caldera-forming eruptions have received relatively little attention, it is prodigiously studied for non-caldera-forming eruptions (Melnik and Sparks, 1999; Mastin *et al.*, 2009; Polacci *et al.*, 2017). Lots of research has tackled the movement of magma in non-caldera-forming systems and this has allowed for various advancements in understanding of those systems. However, in order to produce these models, the physics has suffered the consequences of being simplified and steady-state (such as considering single cylindrical and isothermal conduits or steady state flow systems). Therefore, applying any knowledge drawn from these simple-models to the not-quite-so-simple (due to the scale, geometry and coeval caldera block subsidence) caldera system presents additional limiting challenges. Having said that, fundamentally similar physical processes occur at caldera-forming eruptions as do in non-caldera-forming eruptions (such as decompression and ascent; bubble growth; fragmentation; granular transport above the fragmentation transition) yet no clear quantitative model exists that accounts for the scale and geometry of calderas (Wilson, 2008).

During explosive silicic eruptions magma fragments (in this thesis the term fragment/fragmented refers to a volcanic pyroclastic which has formed by magma fragmentation, unless stated otherwise) on ascent to the surface from the molten or mush reservoirs to erupt, and ultimately to form ignimbrite and fall deposits (for example, previous research proposes that fragmentation occurs at depths of 2 km or less for simple single vent conduits) (Wolff, 1986; Branney and Kokelaar, 2003; Degruyter *et al.*, 2012; Bachmann and Huber, 2016; Wilson *et al.*, 2021). Large volumes of dominantly fragmented magma (up to 5,000 km^3) are erupted at the surface of large silicic eruptions, therefore these volumes must have at one point travelled through and fragmented within the crust, exploiting caldera ring faults as conduits (Figure 1.1; Wilson, 2008). Fragmentation of a continuous volume of decompressing magma occurs when gases cannot escape easily, causing bubble overpressure and fragmentation, ripping apart the magma to produce discrete pieces: pyroclasts (Gonnermann, 2015). This process results from the conversion of potential energy into the surface energy of the pyroclasts created as well as kinetic energy of the growing mixture of gases and pyroclasts. Caldera-forming eruptions pose a special example of this phenomena because the effect of caldera collapse structure and style (such as the size of the structure and the creation of large underpressure at magmatic depths due to the opening of faults) on the fragmentation process is unclear.

Large volumes of magma (at least 5000 km^3) reside within the crustal reservoir and are subsequently known to erupt at the surface often during a single, sustained event (Brown and Branney, 2004; Bachmann and Bergantz, 2008). This demonstrates that during an eruption(s) great volumes of material must be transported through the transport system. However, the ring fault dykes that remain of transport systems are comparatively much smaller in volume than the deposits produced at the surface, therefore the conduits are likely to have once been active for extended periods, dilated in size, and transported large volumes of material quickly.

Calderas are structurally complex systems. Any model of a subsurface caldera transport system must explain the dynamic relationship between the processes of structural subsidence and the related volcanism. The ring fault plays a key role in the sub-surface transport of magmatic material as well as the slip of collapsing calderas, therefore it is important to study yet simultaneously more complex. Due to the dynamic relationship that must exist between slip and magma transport sharing this common fault/conduit, studies into a sub-caldera transport system must address these concurrently in order to understand the ring fault as a whole. It is poorly understood how the processes of slip along ring fault surfaces interact with the upward movement of magma exploiting these surfaces as conduits, and whether this interaction causes any changes to the expected mechanics on the fault surfaces.

1.4 Caldera structure

A long-standing debates exists about the structure of the fault system of calderas, such as the initiation, propagation and configuration of the faults (Geyer and Martí-, 2014). Various approaches have been deployed to understand calderas collapse structures (such as analogue models, numerical models, and geophysical studies), which have produced a wide range of outcomes for the structure of their ring faults. At the forefront of developing ideas is sandbox modelling, where analogue models provide important insights into how host rocks may collapse and deform under the expected volume changes (Roche *et al.,* 2000; Kennedy *et al.*, 2004; Acocella, 2007). It is now widely accepted that collapse occurs principally on steeply outward dipping reverse faults accompanied by an outer set of inward dipping normal faults and an intervening tilted block (Figure 1.3; Kennedy *et al.*, 2004; Cole *et al.,* 2005). Collapse can also be accommodated by ductile downsag (the crustal reorganisation of the reservoir roof). The extent to which downsag (ductile) or faulting (brittle) accommodation of subsidence occurs is denoted by the mechanical and geometric crustal properties (Kennedy *et al.*, 2018).

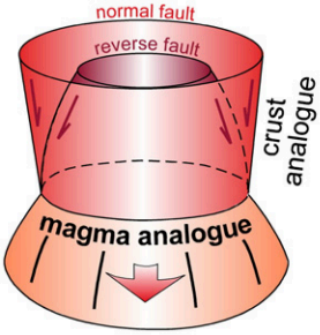

Figure 1.3. *The now widely accepted model for general caldera structures is a set of outward dipping to vertical reverse ring faults, with subsidiary set of inward dipping normal faults. It is currently believed that subsidence along these faults (roof reservoir collapse) occur due to magma reservoir underpressure and the main outward dipping set of faults propagate upwards from the reservoir. This is the basic structure which acts independently from roof aspect ratio, shape of crust-reservoir interface strength of crust, viscosity of reservoir, velocity of collapse, topography, and regional tectonics (taken from Acocella 2007).*

Despite this apparently simple model for basic fault structures, there is still a range in final caldera morphology expressed at the surface. This variability is influenced by: (1) the geometry of the magma reservoir, (2) the number of collapse events, (3) whether collapse is continuous or intermittent, (4) how the caldera floor breaks, (5) how uniform block collapse is, (6) the directions and distribution of crustal stress, (7) the tectonic setting, (8) pre-existing structures, (9) the magma composition, (10) the size and duration of eruption, and (11) the occurrence of resurgence and/or tumescence (Roche *et al.,* 2000; Bosworth *et al.,* 2003; Cole *et al.,* 2005; Kennedy *et al.*, 2018). Often the resulting caldera structure is asymmetric.

Consequently, the variety of caldera structures is considerable, and these have been classified into four end-member collapse styles which encapsulates this variety: piston collapse, piecemeal collapse, trapdoor collapse, and downsag collapse. Despite the basic structure of caldera faults being well understood, the effects of piecemeal breakup, downsag, rotation and asymmetry result in calderas often being more complex and broken up than the basic model implies (Figure 1.4). It is unlikely a caldera example will fit perfectly into these end-members, instead calderas often present hybrid or evolving styles. It is also debated how the collapse of calderas is triggered. Whether it occurs as a result of reservoir over or under pressure, whether the ring faults propagate upwards or downwards, and at what angle these faults lay (Geyer and Martí-, 2014). It is becoming increasingly accepted that magma reservoirs develop ring faults due to an underpressured reservoir caused by the rapid extraction of magma which exceeds the roof blocks threshold of fracturing, therefore producing upward propagating reverse ring faults. There may be multiple concentric sets of these reverse ring faults that become progressively steeper and further from the caldera centre (Kennedy *et al.*, 2004; Burchardt and Walter, 2010; Geyer and Martí-, 2014; Browning and Gudmundsson, 2015).

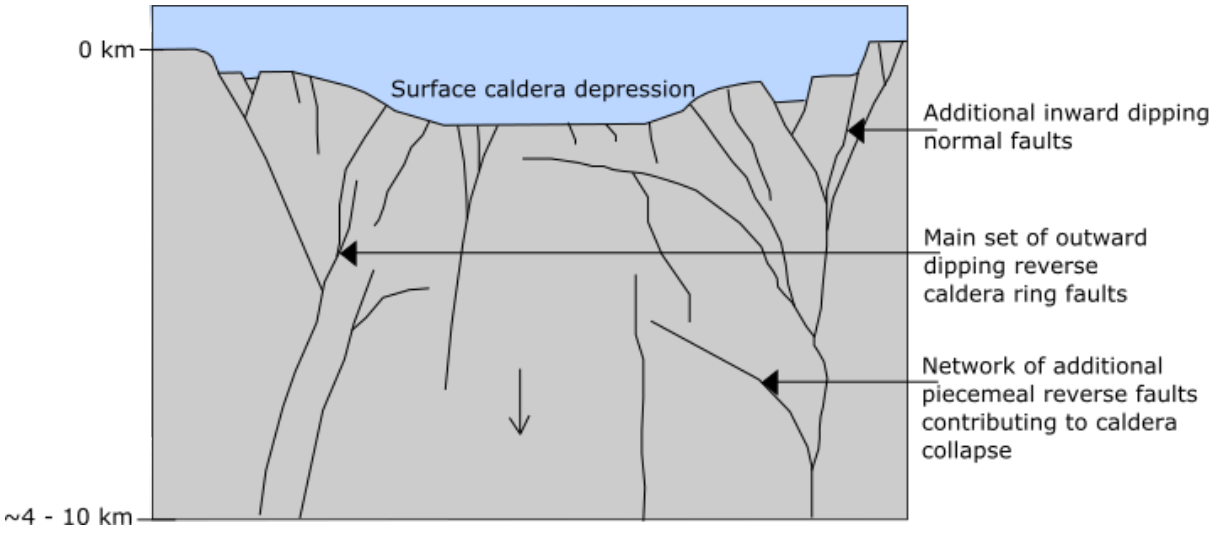

Figure 1.4 *A model to show the highly piecemeal, incremental, and rotational behaviour of a lot of caldera systems. Therefore, do calderas contain one key set of superfaults or is strain partitioned amongst many blocks? Is it likely for slip and friction to become high enough to allow for melting, as proposed by the superfault hypothesis (Spray, 1997)? (Model adapted from Acocella, 2007; Burchardt and Walter, 2010; Geyer and Martí-, 2014; Holohan, 2015).*

Calderas can subside by depths in excess of a kilometre during eruption (for example Glencoe caldera, Scotland, Kennedy *et al.*, 2018), leaving deep, wide depressions at the surface. However, whether collapse is accommodated by ring fault slip in one catastrophic event (Spray, 1997; Kokelaar, 2007; Han *et al.*, 2019) or by intermittent stick-slip and piecemeal breakup of the reservoir roof remains unclear (Wilson, 2001; Stix and Kobayashi, 2008; Gudmundsson *et al.*, 2016; Segall and Anderson, 2021). Some research proposes that catastrophic slip on ring faults can result in the production of frictional melts, naming them to be caldera 'super faults' – a fault characterised by very large displacements (of over 100 m) which occurs during a single slip event at seismogenic velocity (>0.1 m/s) (Spray, 1997).

1.5 Unpicking the relationship between transport and slip on caldera faults

As volcanic products move towards the surface, a central crustal block(s) moves downwards. The fault surfaces which accommodate slip are commonly believed to be shared with the conduit surfaces that feed ongoing eruption. This means that there is an intimate relationship between initiation, slip, subsidence and magma transport which must be unpicked (Kim *et al.*, 2019). Understanding when friction is dominant along fault surfaces, versus when dilation and magma transport dominates, is critical to the temporal understanding of these systems. Constraining the role of friction becomes more difficult because its effects are not necessarily reflected in the eruptive products. Spray (1997) argued

for the existence of superfaults at calderas with large (>100 m) displacements and high slip velocities (>0.1 $m.s^{-1}$), is sufficient to melt the local rock, and generate pseudotachylytes in the fault fill (Figure 1.5). Since, many models of caldera systems have developed a focus on the importance of friction, such as the work of Kokelaar (2007) and Kim *et al*., (2019).

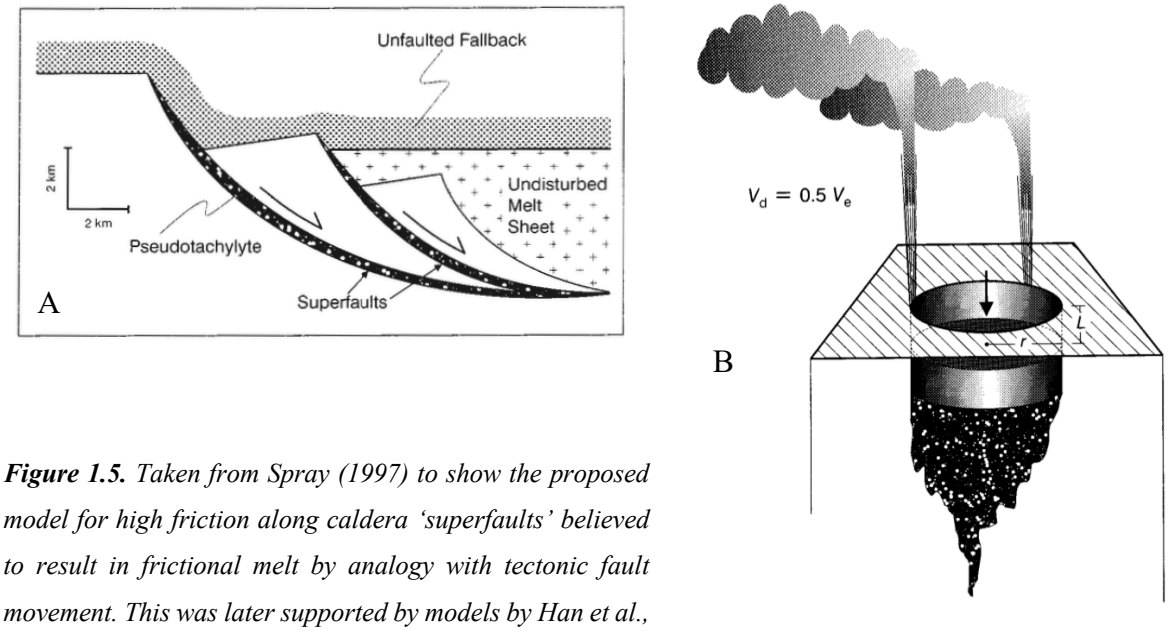

Figure 1.5. *Taken from Spray (1997) to show the proposed model for high friction along caldera 'superfaults' believed to result in frictional melt by analogy with tectonic fault movement. This was later supported by models by Han et al., (2019); Kokelaar and Moore (2006); Kokelaar (2007); Kim et al., (2019).*

However models involving substantial friction along caldera ring faults are not universally accepted (Reynolds, 1956; Garnham, 1988; Burt and Brown, 1997) due to outward dipping (dilational) configuration of ring faults (Figure 1.3), debatable evidence of pseudotachylytes, or the common piecemeal collapse structure considered to reduce strain along single fault surfaces (Figure 1.4; Roberts, 1966; Holohan, 2015). Any model of friction along caldera faults must be sensitive to the newly understood fault geometry (Acocella, 2007; Geyer and Martí-, 2014).

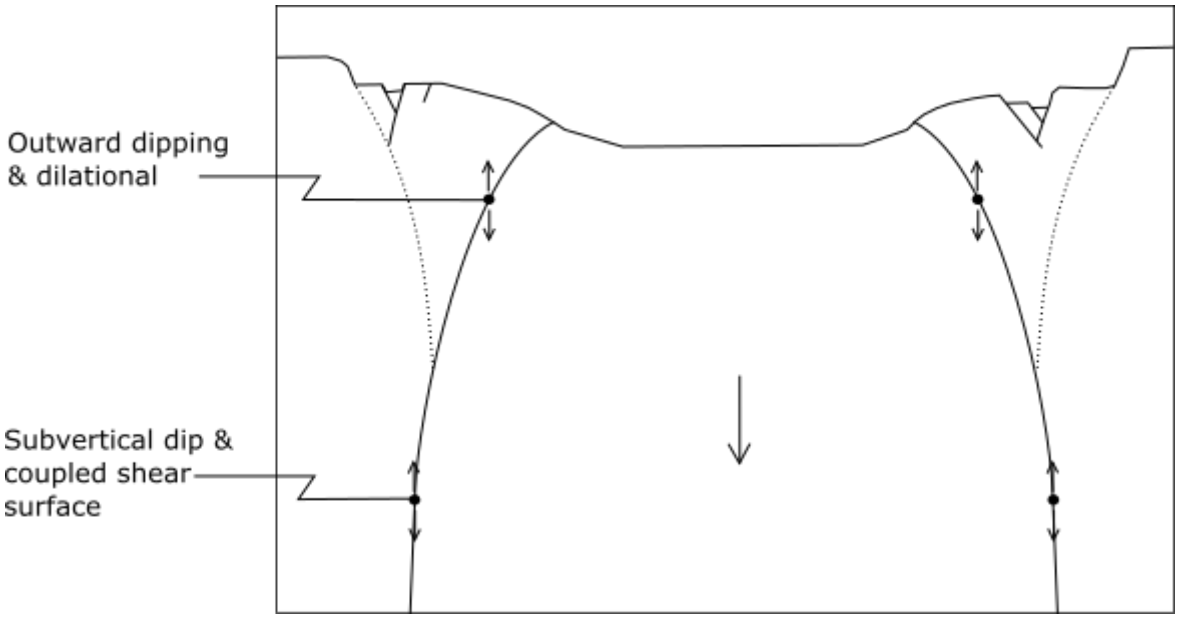

Figure 1.6. *Friction models at calderas must be sensitive to the geometry of the fault systems – are they superfaults? A model to show how the outward to vertical dipping fault planes at calderas may result in dilational or coupled shear fault surfaces, therefore, is the normal stress high enough to produce a frictional melt? (Caldera model shape adapted from (Burchardt and Walter, 2010).*

Therefore, due to the complex nature of intertwining subsidence and magma transport along shared ring faults, research into ring fault transport systems is best suited to directly studying real examples of caldera ring fault fills and surface deposits, to provide an evidence-based model (Wiebe *et al.*, 2021). Then further work, such as models and eruption observations can be applied test the theory and apply it to modern hazard prediction efforts.

1.6 Questions discussed in this thesis

In order to address the poor understanding of the transport system of caldera-forming eruptions, this study aims to address two important questions.

Question 1. How do the processes of caldera slip and magma transport initiate and interact with one another when both occurring across the common surface of the caldera ring fault?

- **Is there a period of very high friction or does no friction occur?**
- **Do these surfaces primarily act as faults or conduits, and therefore should this influence the naming of 'ring faults'?**

Whether caldera ring fault(s) experience friction high enough to produce evidence of frictional melt, or whether caldera fault systems are lower in friction (so instead leave behind evidence of throughgoing pyroclastics) is debate. It is unclear how faulting and transport along ring faults initiate and interact with one another. Different calderas vary in shape and behaviour so there may be variation in the extent of friction, but the basic question of whether overall caldera systematics are capable of producing enough extreme friction to form pseudotachylytes remains applicable to all calderas. A difficulty in this debate is the great similarity in appearance between pseudotachylytes and welded tuffisites (there are lots of descriptive terms suitable for the unit name with the volcanic origin, but in this thesis the term tuffisite is used for clarity) (Passchier and Trouw, 2005). This is a question that will be addressed in this thesis.

The argument supporting high friction suggests that sudden, large slip across a caldera fault, combined with high normal pressures, results in cataclasis followed by the dynamic weakening mechanism of frictional melt, playing a critical role in subsequent collapse dynamics (Spray, 1997; Kokelaar, 2007; Di Toro *et al.*, 2011; Han *et al.*, 2019; Kim *et al.*, 2019). The work of Maddock (1986) and Spray (1997) seeks to theoretically and numerically demonstrate the feasibility of generating pseudotachylytes during caldera collapse (Figure 1.6). Whereas Kim *et al.*, (2019) and Kokelaar (2007) provide field examples of what they interpret to be pseudotachylytes developed along caldera ring faults (Figure 1.8). These examples are shown to be dark, thin units found along the margins of the ring fault intrusions of caldera fault zones in Jansang, Korea and Glencoe, Scotland, respectively.

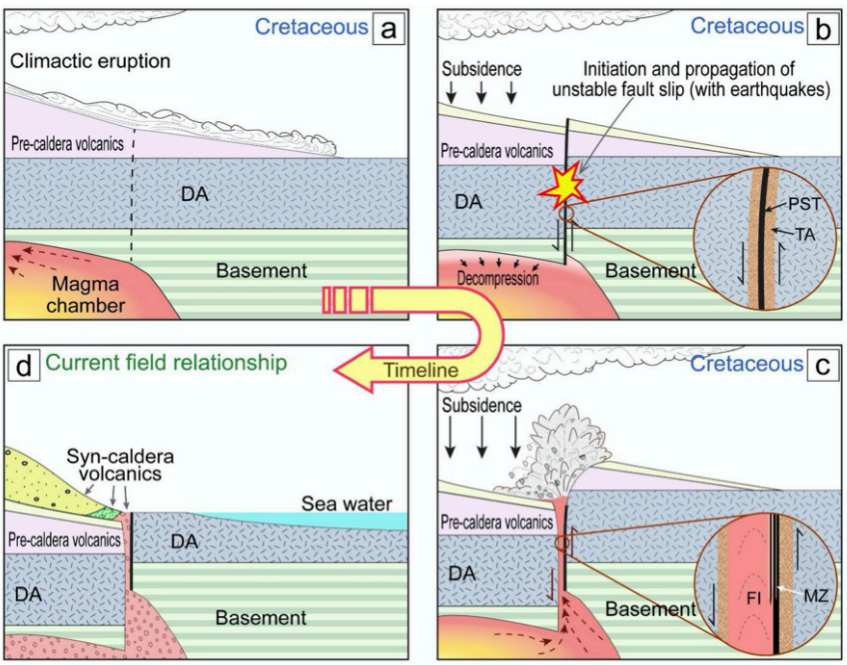

Figure 1.8. *Taken from Kim et al., (2019) to demonstrate the model (founded in the theory of Spray, 1997) which suggests high friction occurs along caldera faults at the initiation of faulting. Note that the fragmentation level is illustrated as being near-surface in panel c.*

The alternate argument is that caldera faults tend to experience low or no friction as a result of fault movement. Instead, any units found along their surfaces which may be interpreted as pseudotachylytes are believed to be densely-welded tuffisites analogous to basal

vitrophyres (e.g. Andrews & Branney, 2011). These form from bypassing fragment transport through the conduits, which have aggregated and welded to develop an obsidian-like welded unit to mark the passing of the vast ignimbrite deposits seen at the surface of many calderas. This argument debates the feasibility of superfaults capable of producing frictional melting at calderas due to questions over the amount of slip (due to incremental and piecemeal collapse mechanisms) and the amount of compressional pressures on the fault surfaces (due to outward dipping fault configuration and the intrusion of volcanic products).

Question 2. At what stage does fragmentation occur during the transport of large masses of magma along ring faults at caldera-forming eruption? Therefore, in what state is magma transported through the crust?

It is unclear for at what point magma fragmentation occurs during its transport throughout a caldera-forming eruption. Pyroclastics (in contrast to the coherent magma within storage reservoirs) form the majority of products erupted at calderas, with large volumes deposited through sustained flows (Brown *et al.,* 2012), yet caldera-specific models often don't explain how or where this change in material state occurs (Wilson *et al.*, 2021). Fragmentation is the process where continuous liquid magma violently breaks into discrete pieces accompanied by gas which occurs due to the conversion of pressure energy into surface and kinematic energy. This process is well understood for single vent simple conduit dynamics because of modelling (Figure 1.9; Gonnermann, 2015). However, due to the greater complexities and much larger sizes of calderas, their fragmentation dynamics are poorly understood.

Recent work has argued for the increasing presence of pyroclastic dykes and the presence of complex, widespread shattering behaviours at calderas caused by extreme pressure changes during eruption and collapse, (Wolff, 1985; Burt and Brown, 1997; Torres-Hernández *et al.*, 2006; Díaz-Bravo and Morán-Zenteno, 2011; van Zalinge, Cashman and Sparks, 2018; Szemerédi *et al.*, 2020; Wiebe *et al.*, 2021). However, pyroclastic dykes are difficult to texturally recognise due to extreme welding of pyroclasts. The feasibility of producing large pyroclastic ring dykes which form the final material through the subsurface is also open to some debate. The outstanding question remains whether or not magma fragmentation occurs either deep or shallow in a caldera fault? This thesis will explore this.

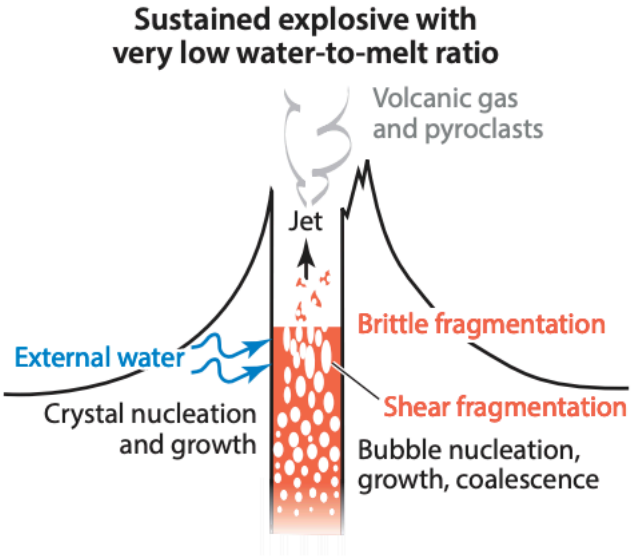

Figure 1.9. *Taken from Gonnermann (2015) to show that the simple process of fragmentation is well understood for single vent eruptions, but that there is little explanation given for how this process occurs for the wide variety of eruption dynamics that occur in nature i.e. what occurs at silicic calderas?*

1.7 Examples of past caldera-forming volcanoes with exposed sub-surface transport systems

Wilson et al., (2021) demonstrates how only 13 supereruptions, which were silicic and caldera-forming, have occurred within the Quaternary (i.e. in the last 2 million years of Earth history), to produce 'fresh' deposits. These examples provide surface deposits of caldera-forming super eruptions which provide evidence of caldera formation being accompanied by large Plinian fall and PDC deposits that denote wholesale fragmentation and production of particles. These surface deposits also provide sufficient samples to allow for geochemical and microstructural analysis which can provide information about the magmas storage conditions. However, these modern deposits are rarely eroded sufficiently to effectively display the important sub-volcanic transport system. Instead, older, more weathered caldera-forming systems that expose their deeper subsurface interiors exist. These provide effective opportunities to study the sub-volcanic transport system using field examples directly (Wiebe *et al.*, 2021). Here the best-studied examples are introduced (figure 1.10).

1.7.1 Ben Nevis caldera

First, Ben Nevis caldera, found in Scotland, is one example of a deeply eroded and variably exposed caldera system formed during the end of the Caledonian Orogeny (Bailey and Maufe, 1916; Burt and Brown, 1997). It has an exposed volcanic pile as well as an intermittently exposed surrounding ring fault displaying fault fill. Previous fieldwork, geochemical and petrographical studies have been conducted into this volcanic system, which has led to the creation of various models aiming to unpick

its history. There exists a thin, fine black aphanitic unit called the Ben Nevis Intrusive Ring Tuff which is believed to be a volcanic unit (Burt and Brown, 1997), however previous authors have debated its origin and name to be a product of frictional melting (Bailey and Maufe, 1960). The question of this unit stems from the importance of friction along caldera superfaults in this complex system.

1.7.2 Slieve Gullion Ring Dyke complex

Second, the Slieve Gullion complex of Northern Ireland (west of the Mourne Mountains, south Country Armagh) is another example of a silicic caldera formed in the Paleogene; 66-56 Ma; Stevenson *et al.*, 2008). The ring complex is deeply eroded so that its sub-surface transport system has become exposed. The porphyritic granophyre and felsite ring intrusion complex has been the subject of research for nearly 100 years resulting in various mechanisms of emplacements for the conduit and its associated deposits in the central Layered Complex. The Porphyritic Felsite and the earlier ring-complex has been a particular focus for researchers aiming to unpick an emplacement model, culminating in the work of Troll *et al.,* (2008) concluding with new evidence supporting the original ring dyke model of Richey and Thomas (Richey, 1932; Richey and Thomas, 1932; Emeleus, 1962; Stevenson *et al.*, 2008; Troll *et al.*, 2008).

1.7.3 Hafnarfjall caldera

Third, in west Iceland is Hafnarfjall caldera, with an exposed ring fault (1.2 km below the original volcanic surface; Franzson, 1978; Gautneb, Gudmundsson and Oskarsson, 1989; Browning and Gudmundsson, 2015) formed at 5 Ma. This has been studied previously using field data and numerical models which Browning and Gudmundsson (2015) used to propose a new model for ring dyke formation applicable to other calderas. This new mechanism suggests that sheets can become deflected into caldera faults hence that some ring dykes do not channel magma directly from magma reservoir margins. This new idea for the understanding of caldera transport systems has particular significance for the timing of volcanic hazards especially on resurgent volcanism.

1.7.4 Jansang caldera

Fourth, the Cretaceous Jansang caldera (K-Ar whole rock age of 67 ± 4 Ma) in Korea was studied by Han *et al.*, (2019) and Kim *et al.*, (2019). Jansang caldera is part of a rhyolitic volcanic complex including pyroclastic deposits and lavas as well as the porphyritic ring intrusions that once fed the caldera eruption and facilitated caldera collapse. At this caldera, there is an entire section of the fault

zone (the wall rocks, the fault intrusions, and the intra-caldera volcanic rocks). Kim *et al.,* (2019) propose the presence of a thin band of black rock to be one of the first examples of a volcano-tectonic pseudotachylyte. Hence, their work argues that frictional melting is an important fault zone process that occurs during caldera collapse.

1.7.5 Glencoe caldera

Finally, the well-studied but incompletely understood Glencoe caldera system in Scotland. This caldera is dealt with in the next Chapter of this thesis and forms the case study for this thesis as a whole.

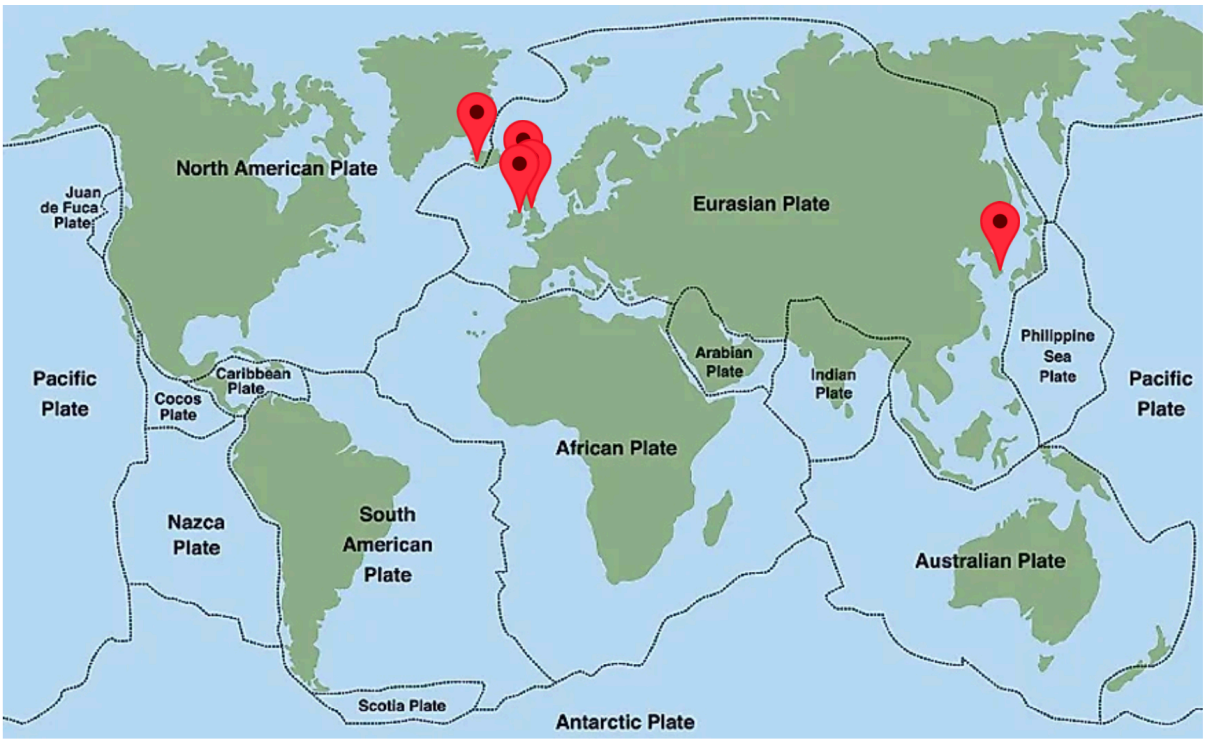

Figure 1.10 *A world tectonic map to give context to the locations given which provide examples of ancient caldera systems which have been eroded sufficiently enough to expose the sub-surface transport system. Adapted from - How Many Tectonic Plates Are There?. [online] WorldAtlas. Available at: <https://www.worldatlas.com/articles/major-tectonic-plates-on-earth.html> [Accessed 28 July 2022].*

Chapter 2: the Glencoe case study

In Chapter 1 I introduce three outstanding questions associated with our understanding of caldera dynamics. In this Chapter I introduce Glencoe volcano specifically and argue that this site can be used as a case study to develop a model for how volcanic material is transported through the crust, next, this model can be applied to other exposed or erupting systems as a test to see if it is widely applicable.

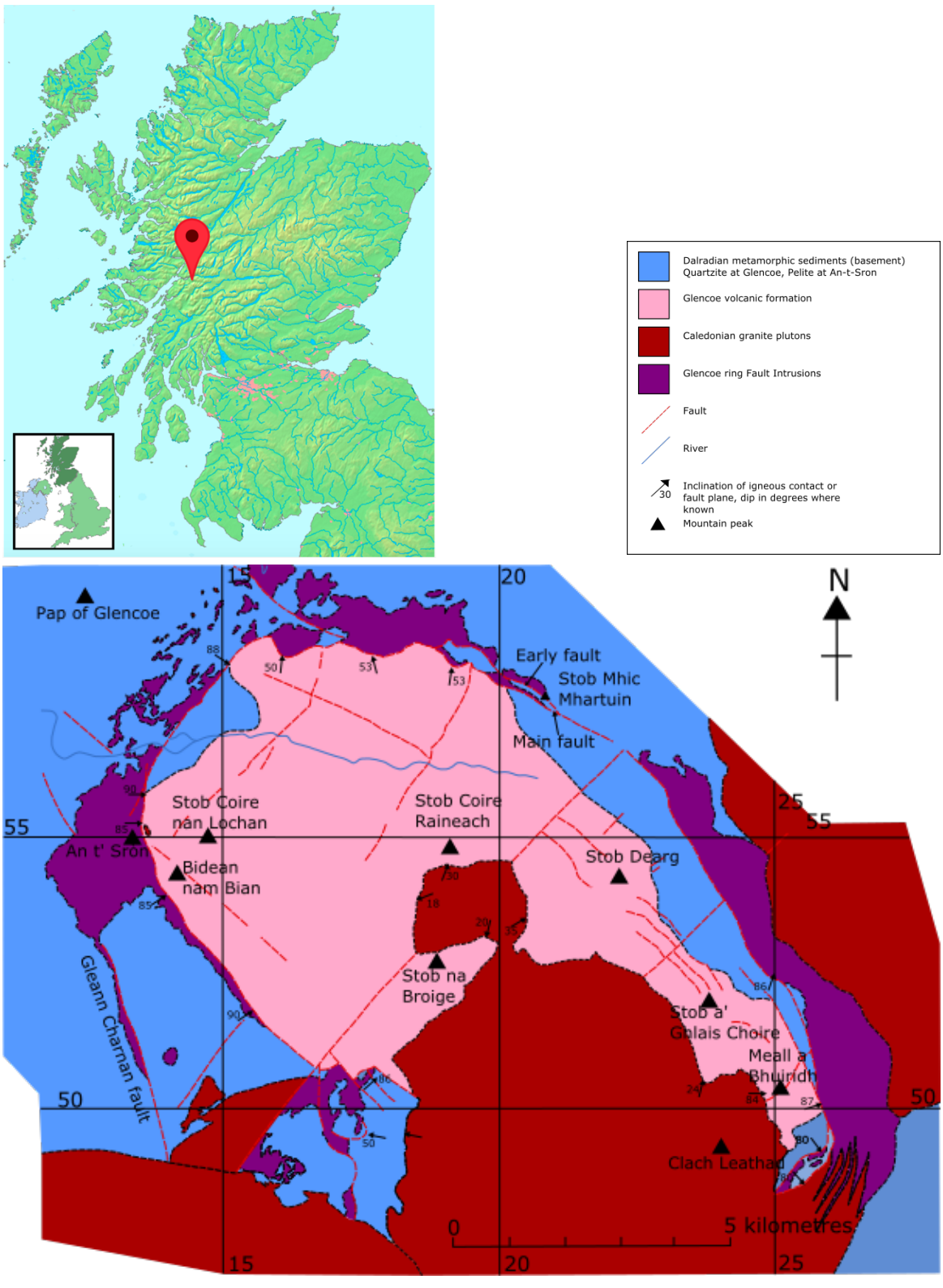

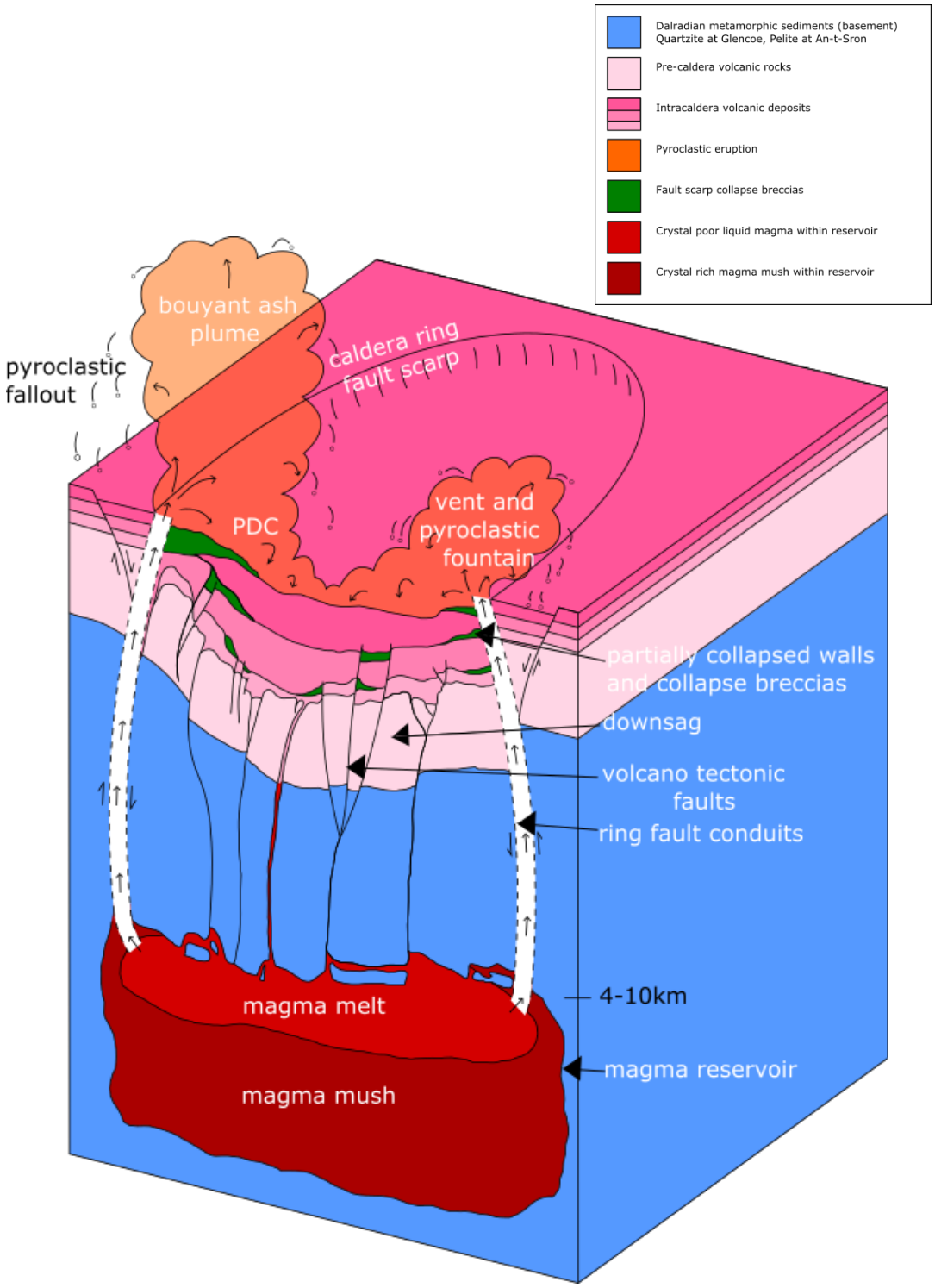

Figure 2.1 *This work is adapted from* (Moore, 1995; Moore and Kokelaar, 1997, 1998; Kokelaar and Moore, 2006; Kokelaar, 2007) *to highlight the detailed understanding of the Glencoe Caldera system as a whole, especially due to the recent and detailed re-mapping of the area by Moore and Kokelaar. (a) A map of the Glencoe area to show what units are exposed (adapted from Kokelaar and Moore, 2006). With an inset map to highlight the location of Glencoe in the context of Scotland and the UK, adapted from ow Many Tectonic Plates Are There?. [online] WorldAtlas. Available at: <https://www.worldatlas.com/articles/major-tectonic-plates-*

on-earth.html> [Accessed 28 July 2022]. (b) A simplified block diagram to show the known dynamics of Glencoe caldera – a reservoir, piecemeal crustal subsidence, and a complex series of surface eruptions and collapse. The sub caldera feeder system is left blank due to unknowns about the processes of this region (adapted from Kokelaar and Moore, 2006).

2.1 Glencoe background

The magmatic province of the Glencoe caldera-volcano complex formed shortly after the Caledonian Orogeny (~435-425 Ma; Moore and Kokelaar, 1997; Kokelaar and Moore, 2006)). An estimated ~85 km^3 of silicic magmatic material (dense rock equivalent, this is an approximate estimate determined by approximate caldera area and subsidence values. This approximation does not differentiate between different eruption or collapse periods, there is not sufficient surface deposit exposure to do so because of preservation and erosion limitations) with calc-alkaline composition was erupted from the Glencoe caldera during its period of collapse (Thirlwall, 1988; Cole *et al*., 2005; Wilson *et al.*, 2021). The key period of caldera-associated volcanism, faulting, and intrusions developed at ~415-421 Ma during the Lower Devonian (Lochkovian stage), and was sustained for 2-3 million years (Kokelaar and Moore, 2006).

Overall, the interplay of magmatism, ring faulting, downsagging and reactivation has culminated to produce the piecemeal caldera structure recognised at Glencoe today (Cole *et al*., 2005; Kennedy *et al.*, 2018). Glencoe is structurally complex and tectonically controlled, it displays a clear example where the controls of pre-existing regional structure and present-time tectonics have influenced piecemeal caldera collapse and the associated magmatic plumbing system. The main succession of the Glencoe Caldera-volcano Complex consists of thick volcanic units intercalated with sedimentary beds and fluvial erosion surfaces. The collective term for the volcanic and sedimentary rocks is the Glencoe volcanic formation (Kokelaar and Moore, 2006). Glencoe preserves a record of changing magmatism starting with early pre-caldera andesitic magmatism, developing to centred caldera volcano rhyolite and andesite magma, finalising with late granitoid pluton emplacement which was uplifted and exhumed. This granitoid plutonism was episodic on a local scale (as opposed to regionally synchronous; Moore and Kokelaar, 1998).

The Glencoe basement rock is composed of intensely deformed metasedimentary rocks which are part of the Dalradian supergroup (Late Precambrian – Cambrian times, 700-500myr; Garnham, 1988), commonly consisting of quartzites and pelites. Compressional tectonics (during the Ordovician, 500-490myr), as well as regional and caldera faulting has resulted in the unit's folded, metamorphosed and fragmented appearance. The breakup of the basement by caldera faulting and the associated intrusions is described in the following Section (2.1.1),

Extrusive and intrusive rocks (basalt/gabbro to rhyolite/granite compositions) were emplaced during volcanism at Glencoe (Garnham 1988). A total of approximately 1.3 km thick intra-caldera volcanic rocks were deposited at Glencoe, this succession was dominated by 7 major silicic ignimbrites whose eruptions are believed to coincide with significant periods of collapse (Kokelaar, 2007). Volcanic deposit thicknesses vary greatly due to the ever-changing structural configuration and vent locations of the caldera, controlled by tectonism. The volcanic rocks are considered to have been derived from more than one centre, due to their bimodal nature (andesite and rhyolite) and thickness variations of units according to area (Garnham, 1988).

Sedimentary units and erosional unconformities are present throughout the volcanic succession due to periods of volcanic quiescence (which may have been up to many tens of thousands of years long) where fluvial systems could dominate. These deposits also change in location and formation throughout history due to the dynamic structure of Glencoe causing changing basin shapes. Signs of alteration within outcrops and samples indicate that hydrothermal activity has been rife throughout the region. Reactivation of faulting and presence of a hydrothermal system is evident through fractures and quartz, epidote, white mica and commonly oxidised pyrite veins (Bailey and Maufe, 1960; Kokelaar, 2007). Additionally, the effects of significant burial and weathering has affected their appearance further.

2.1.1 Caldera faults (and their associated intrusions) at Glencoe

Previous studies of the complex area agree that caldera subsidence at Glencoe was incremental and piecemeal, resulting in the formation of numerous crustal blocks through many non-coherent slip events. Slip was accommodated by numerous cross-cutting faults, grabens (which became basins for successions, the main graben ran NW-SE) and downsag (Roberts, 1974; Branney, 1995; Moore and Kokelaar, 1997, 1998; Muir, 2017). Exposed caldera faults at Glencoe dip steeply. As previously described, tectonics and pre-existing faults played a large control on the collapse structure. There were two clear stages of caldera formation at Glencoe. The first stage consisted of the early evolution of the volcanic system which developed through graben-controlled faulting, well documented by the work of Moore (Moore, 1995; Moore and Kokelaar, 1997, 1998; Kokelaar and Moore, 2006). As the caldera faulting developed, so did Glencoe's piecemeal structure as it became divided by many cross cutting (graben) faults. Later in Glencoe's history the second stage of caldera-formation occurred, whereby there was circum-volcano ring faulting. During this stage there was incremental slip (of up to 1 km total normal displacement along the ring fault, and at least 700 m of piecemeal displacement on structures within the ring fault) and volcanic intrusion along the developing primary ring fault

surfaces, as well as along the piecemeal network that crosscut the system (Moore and Kokelaar, 1998; Kokelaar and Moore, 2006).

The Glencoe ring fault is a near-continuous sub-cylindrical fault structure (14x8km) that bounds the down-faulted caldera block(s). It is poorly exposed, with less than 10% of the total circumference directly visible in the field (Garnham, 1988). The ring fault truncates all the other faults found within its structure. Stob Mhic Mhartuin provides the classic locality where the ring fault has excellent exposure. Despite its ellipse shape, the ring fault structure was once sub-circular but the later intrusion of the large Etive dyke swarm extended the width in the NW-SE direction (Bailey and Maufe, 1960). Furthermore, later varied exposure and obliteration by intrusions (seen to the southeast of figure 2.1a) also makes the structure appear incomplete (Moore and Kokelaar, 1998; Muir, 2017). The ring fault is believed to have emerged after the early stages of incremental caldera collapse which consisted of prolonged subsidence on the earlier NW and NE trending fault systems (Muir, 2017). The ring fault consists of partially linked faults. Throughout the ring-faults development, various different faults became active, reactivated, intruded and linked together at different times, creating a complex history and form. Total subsidence at Glencoe (ring faulting, sagging and regional fault reactivation) was of the order of ~1.4 km (Kokelaar, 2007; Muir, 2017): 650 m can be attributed to ring fault movement, 400 m to downsagging, and 250 m to regional fault displacements (Kennedy *et al.*, 2018). Evidence for flexure (downsag) includes multiple extensional crevasses each hundreds of metres deep and which flare upwards (Moore and Kokelaar, 1997).

The ring fault was exploited by rising magma as a conduit, and now the roughly oval shaped caldera ring fault system is associated with intrusions of gabbros, diorites, tonalites, monzonites and granites – the Glencoe fault intrusions. There are also some smaller associated units (i.e. the red felsite and the flinty crush rock (FCR)). The intrusions are very wide in places (up to 1.5km, figure 2.1a), 419+-5.4Ma in age (Neilson *et al*., 2009). A moderately undeformed ring intrusion and a mostly non-thermally metamorphosed country rock has allowed for the inference that faulting and intrusion occurred simultaneously along the ring fault of Glencoe (Garnham, 1988). Due to piecemeal/broken nature of the central block, successive depocenters which tapped the underlying magma chamber(s) would grow and migrate with time, creating the asymmetrical structure that can be seen today (Kokelaar and Moore, 2006). Therefore, the form and location of each major ignimbrite and the graben changed for each event.

The ring fault stratigraphy generally consists of (1) The Dalradian country rock found on either sides of the ring fault (with varying levels of brecciation and tectonisation) (2) The Flinty Crush Rock (FCR) - a black fine grained, aphanitic band of rock a few centimetres wide found as the first unit lining both the inner and outer sides of the ring fault, marking the transition between fault surface and fault intrusion (this unit is not always present) (3) The red felsite – a porphyritic red-brown coloured

unit found adjacent to the FCR as the outermost intrusion unit (this unit is not always present) (4) The fault intrusion - the darker grey and coarser porphyritic unit of variable composition, found as the central and widest mass of the ring fault fill. The presence and contacts of the FCR and the red felsite lining the contact between the country rock and the fault intrusion is variable (in width and degree of mixing with other units). Throughout this system there is evidence of the hydrothermal activity, burial and weathering that occurred later.

This studies fieldwork focused at the summit of Stob Mhic Mhartuin (706m) (found to the northeast of the map of Glencoe in figure 2.1a), which exposes a northern sector of the Glencoe ring fault. Here, all the units are well exposed, and, there is a clear exposure of the outer ringfault (which is filled with the same stratigraphy) found in the northeastern sector of the caldera. Stob Mhic Mhartuin is chosen as a primary case study location due to this excellent exposure of all units, as well as the work of previous researchers choosing it as a type locality for studies of the Glencoe ring fault.

2.2 Models for fault opening and filling

The FCR is a fine black aphanitic unit rich in quartzite clasts which occurs intermittently along the Glencoe ring faults, in between the country rock and the intrusion units. There are three models which have been proposed for the FCR, the models focus on one key question: did frictional melting occur along the Glencoe ring faults or not?

Clough *et al*., (1909) were the first to recognise, name and interpret the FCR. This is when the frictional melt hypothesis began for the Glencoe FCR, explaining the unit's interpretive name. These researchers proposed the following sequence for the formation of the FCR (Figure 2.2b):

1. Fault initiation due to stress changes associated with underpressure within the magma pressure, causing the crustal roof reservoir to lose its buttressing support.

2. Fault localisation, rupture, and very rapid subsidence of the central caldera block along the caldera ring faults causing strain and frictional heating along the ring fault surfaces, resulting in brecciation and extreme trituration of the faulted country rocks.

3. The rapid build-up of strain and heat on the faulted country rocks causes the country rocks liquidous to become surpassed, resulting in frictional melting to produce a pseudotachylyte (the FCR), which also experienced injection of its still fluid away from its source to create veins and tongues of FCR.

4. Magma wells up around the sinking crustal block and injects upwards along the ring faults to leave behind the adjacent ring intrusions, as these volcanics moved along the new conduit they eroded the fault surface to leave a thin veneer of FCR. The FCR is still in a viscous flow state during intrusion therefore mixing has occurred between the units in places, causing FCR to adopt some feldspar xenocrysts.

5. The fault intrusion fills the conduit at the end of the ring-fault fed eruption, to leave the fault fill seen today. Some simultaneous cooling of the FCR and ring intrusions leaves behind mixed contacts.

This theory proposes that the FCR is a finely ground up and partially fused quartzite and quartzite-schist. Following researchers have supported and developed this theory (Bailey and Maufe, 1916, 1960; Shand, 1916). For example, by justifying a lack of strain on the quartz grains in the FCR to be a result of its intergranular matrix accommodating the shear stresses experienced. Their work suggests that FCR veins are only found in highly dislocated regions with well marked fault planes and crush zones, which makes the possibility of developing enough friction to melt the rocks more feasible. These authors suggest the clear progression from unaffected country rock to increasingly brecciated rock until the final band of FCR shows that this unit is a result of a continuum of stress.

More recently, a sequence of work by authors Kokelaar and Moore (Kokelaar and Moore, 2006; Kokelaar, 2007) involve a re-examination of the frictional hypothesis, to propose a second theory. This newer model is still focused on the importance of frictional melting along caldera ring faults. This is closely linked with the work of Spray (1997). This newer friction model proposes a sequence of events (Figure 2.2c):

1. Fault intitiation due to stress changes associated with underpressure within the magma pressure, causing the crustal roof reservoir to loose its buttressing support. Region xII, found at shallower location along the fault where current exposure is today, cross cuts a hydrothermal system rich in liquid water.

2. Fault localisation, rupture and very rapid subsidence of the central caldera block along the caldera ring faults causing strain and frictional heating along the ring fault surfaces, resulting in brecciation and extreme trituration of the faulted country rocks.

3. At xI the rapid build up of strain and heat on the faulted country rocks causes the country rock's liquidous to become surpassed, resulting in frictional melting to produce a pseudotachylyte (the FCR). At xII the heat build up causes super heating of the hydrothermal system which causes the water rich region to superheat and explode through water expansion

into vapour, causing excavation of the fault to create a cavity. There is also an incipient bend in the ring fault at xII which encourages the creation of a cavity.

4. Frictional melts from xI are transported upwards (possibly for hundreds of metres) through the dilating conduit to xII along the extreme pressure gradient created by the cavity. Upon reaching the excavated chamber they decompress and fragment, forming a foam which blasts onto the conduit sides. At the same time lithic breccias travel up the conduit marking this event at the surface.

5. Following decompressed and fragmented red felsite magmas follow a similar process of transport, blasting, fragementing and coating the cavity. This occurs immediately after the frictional melt movement therefore the two units are heavily mixed due to turbulence in transport and deposition.

6. The fault intrusion fills the conduit at the end of the ring-fault fed eruption, to leave the fault fill seen today. Some simultaneous cooling of the FCR and ring intrusions leaves behind mixed contacts.

This suggests 'superfault' displacements of >0.1-1 cm/s are required to create the pseudotachylytes seen. This theory supports the belief that caldera faults must experience enough friction to produce a frictional melt, but uses the creation of a fault cavity (through hydrothermal blasting and fault bending) to explain signs of fragmentation and the presence of the frictional melt on both sides of the intrusion, something that the original mappers Clough *et al.,* (1909) didn't know.

However, other researchers have proposed that the frictional model is not consistent with the field and microscopic evidence. An alternate model, which suggests friction is not high enough along caldera faults to form and retain a pseudotachylyte, instead suggests the FCR is of a volcanic origin (Reynolds, 1956; Hardie, 1963; Roberts, 1966, 1974; Taubeneck, 1967; Garnham, 1988). These researchers suggest the FCR is a fine grained intrusive tuffisite which travelled through the ring fault conduit as a fluidised system, therefore, a finer grained marginal facies of the ring intrusions which have coalesced to the conduit wall rocks fracked by volcanic gases. The resulting general model proposing a volcanic origin to the FCR is as such (Figure 2.2d):

1. Fault intitiation due to stress changes associated with underpressure within the magma pressure, causing the crustal roof reservoir to loose its buttressing support. Region xII, found at shallower location along the fault where current exposure is today, cross cuts a hydrothermal system rich in liquid water.

2. Fault localisation, rupture and very rapid subsidence of the central caldera block along the caldera ring faults causing strain and frictional heating along the ring fault surfaces, resulting in brecciation and extreme trituration of the faulted country rocks. However, due to the dilational-shear movement along faults, and less extreme displacement velocities, no frictional melt is created.

3. Simultaneous or after step 2, fragmented volcanics intrude along the ring fault, which travel to the surface to produce the sustained pyroclastic eruptions known to occur. However, the energy of the eruption causes fracking (gas pressure driven fracture process, physically analogous to fracking in industrial context) of the conduit walls, resulting in a relatively thin layer of the fine pryoclastics aggregating on to the faults.

4. The eruption continues, tapping increasingly deeper or different zones of the chamber causing the red felsite to travel up the conduit and partially aggregate onto the walls.

5. The fault intrusion fills the conduit at the end of the ring-fault fed eruption, to leave the fault fill seen today showing the progression of the eruption towards increasingly crystal rich magmas. Some simultaneous cooling of the FCR and ring intrusions leaves behind mixed contacts.

Both the frictional melt and the volcanic theories have support from researchers finding similar units at other calderas and relating their origin to frictional melting (e.g. Kim *et al.*, 2019 at Jangsan Caldera, Korea) or volcanics (e.g. Burt and Brown, 1997 at Ben Nevis Caldera, Scotland). This implies that there is no consensus as to the origin of these fault-associated rocks seen at calderas in the rare examples worldwide.

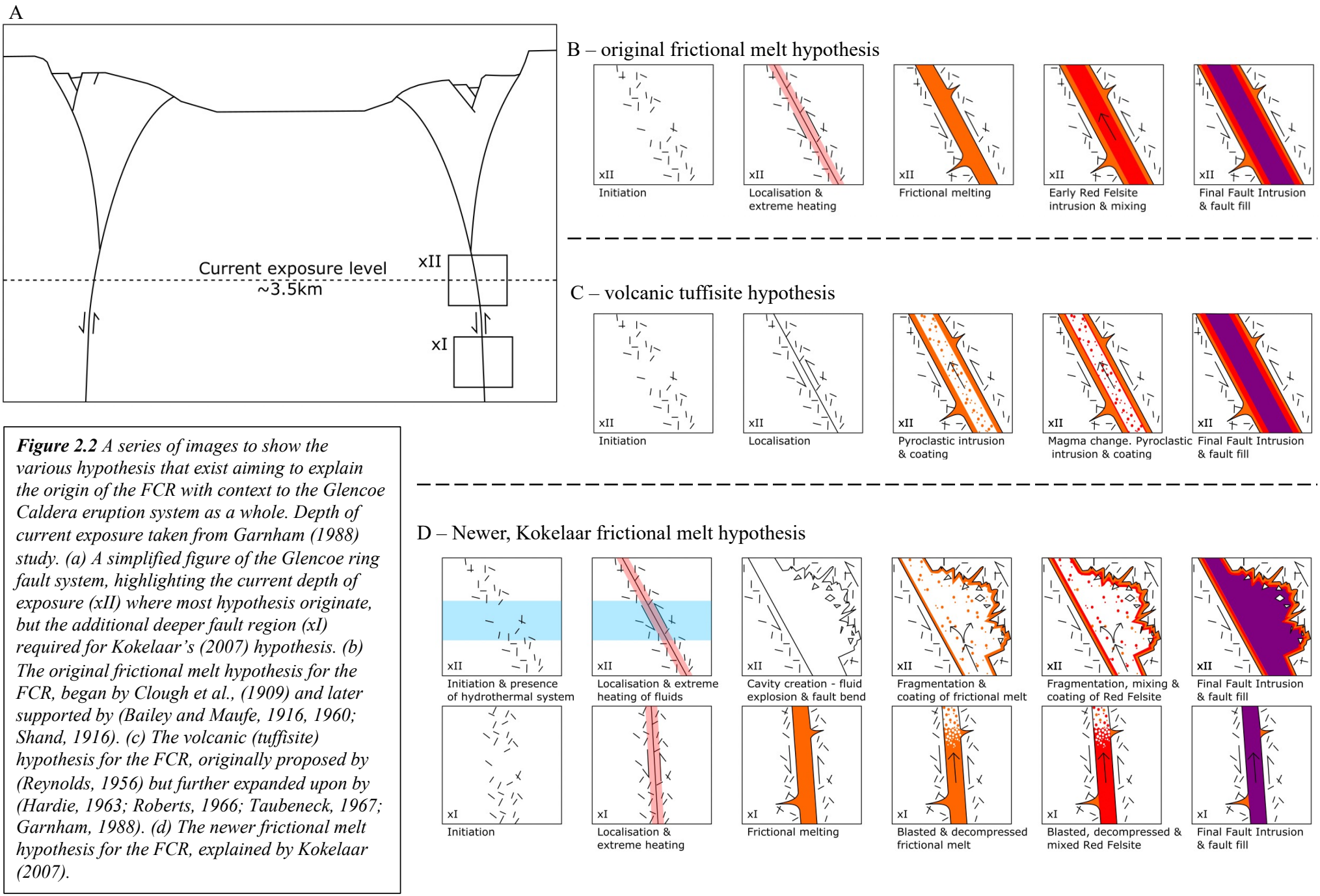

Figure 2.2 *A series of images to show the various hypothesis that exist aiming to explain the origin of the FCR with context to the Glencoe Caldera eruption system as a whole. Depth of current exposure taken from Garnham (1988) study. (a) A simplified figure of the Glencoe ring fault system, highlighting the current depth of exposure (xII) where most hypothesis originate, but the additional deeper fault region (xI) required for Kokelaar's (2007) hypothesis. (b) The original frictional melt hypothesis for the FCR, began by Clough et al., (1909) and later supported by (Bailey and Maufe, 1916, 1960; Shand, 1916). (c) The volcanic (tuffisite) hypothesis for the FCR, originally proposed by (Reynolds, 1956) but further expanded upon by (Hardie, 1963; Roberts, 1966; Taubeneck, 1967; Garnham, 1988). (d) The newer frictional melt hypothesis for the FCR, explained by Kokelaar (2007).*

The origin of the fault intrusion and red felsite at Glencoe is also open for debate. Whether these ring intrusions were emplaced as cohesive magmas or fragmented pyroclasts (which have since become extremely welded) provides insight into the second question proposed about caldera transport systems in Section 1.6. If the intrusions were emplaced at the depths of current exposure levels (~3.5 km, Garnham 1988) this shows that fragmentation is a deep process that may occur somewhat instantaneously during caldera-forming eruptions, and that it is possible for fragmented magma to exist in very wide (1.5 km) intrusions until the very end of the eruption. Roberts (1966) proposed that the ring intrusions represent a frozen fluidised system, using evidence of fragmented crystals as evidence to show the fragmentation of magma has occurred, and the fining of crystals towards conduit margins to represent the sorting that occurs within entrained systems. However, other research into Glencoe has either not addressed this question, or have concluded there to be no evidence of fragmentation of the ring intrusions, implying these were emplaced as cohesive magma flows.

Garnham (1988) uses petrology and geochemistry to demonstrate that the Glencoe ring fault contains a wide array of compositions, therefore showing that its all-encompassing name is a misleading representation of this multi-unit ring fill. The red felsite is a porphyritic intrusion unit found intermittently in between the FCR and the fault intrusion. The unit's redder colour makes it appear distinct from the fault intrusion in the field, however, the significance of the origin causing this change, and hence whether it should be distinguished from the main fault intrusion, is not agreed upon in literature. Prior to the work of Garnham, previous authors had disregarded the red felsite (Reynolds, 1956; Roberts, 1966) or described it as a chilled margin of the ring intrusion (Bailey and Maufe, 1960). However, Garnham's work explaining the reasons why the red felsite can't be so casually associated with the fault intrusion calls for further attention to explain the presence of this ring fault fill unit.

A nuance of the fault filling structure at Glencoe is the presence of a smaller 'outer ringfault' strand visible in the northeastern sector of the caldera (labelled as the 'early fault' at Stob Mhic Mhartuin in figure 2.1). Models of the caldera structure here seek to explain why this second fault strand has opened and become exploited by volcanics, despite the nearby network of intruded ring fault and non-intruded crosscutting faults. Some researchers propose this conduit to be an indicator of two substantial and individual peroids of subsidence (Clough, Maufe and Bailey, 1909; Roberts, 1963, 1966), whereas other query the significance of this structure implying it is just a natural feature of the piecemeal, complex collapse structures seen at Glencoe (Taubeneck, 1967; Garnham, 1988).

2.3 Hypotheses

In conclusion, this study aims to use the case study of Glencoe in order to advance scientific understanding of the subcaldera feeder system. This will allow for improved models of caldera feeder systems to be used in combination with the relatively well understood caldera reservoir and surface eruption processes, in order to aim hazard prediction efforts at currently active caldera systems which pose a huge threat to life. This study will use microscopy and geochemical work directed by fieldwork at Glencoe in order to progress our understanding of these plumbing systems and to provide a model to explain how frictional and volcanological processes develop throughout an eruption along the ring fault feeder conduits. Therefore, in order to aid this outcome, the study clarifies 2 key hypotheses to be addressed with regards to Glencoe, of which outcomes should result in a developed understanding of caldera feeder systems world wide:

> Hypothesis 1 – The FCR is a frictional melt, as stated by the previous researchers Clough, Maufe and Bailey (1909); Bailey and Maufe (1916, 1960); Kokelaar and Moore (2006); Kokelaar (2007). Hence, suggesting that calderas have superfaults which experience significant friction related to subsidence on their surfaces prior to, or simultaneous with, magma transport along their planes.

This hypothesis can be tested using macro- and micro-scale textures which may distinguish features of a frictional melt or volcanic product, therefore clarifying the origin of the FCR. Further geochemical analysis can be used to test the similarities and differences of the FCR to its possible protolith (the country rock) or to the neighbouring ring intrusions which may have originated from the same magmatic reservoir. Finally, theoretical questioning can be applied to all proposed theories for the genesis of the FCR, in order to highlight the strengths and weaknesses of each.

> Hypothesis 2 - The ring intrusions (the FCR if hypothesis 1 is proven wrong, the red felsite, and the fault intrusion) are pyroclastic. These represent the order of volcanic to travel up the conduit, in pyroclastic form. Therefore, suggesting that calderas erupt large volumes of ignimbrites in wide conduits until the very end of their extrusive activity travelling through their ring faults, and that fragmentation occurs below a depth of 3.5km (current level exposure depth estimation taken from Garnham 1988).

The second hypothesis can similarly be tested using macro and microscopical textural analysis, searching for implications of fragmentation within the ring fault units and comparing the evidence to other examples where pyroclastic conduits have been discovered. Further calculations could be used to discuss the feasibility of fragmentation within this depth of the system, however this would struggle to become standalone evidence due to the previously mentioned limitations of numerically modelling large and complex caldera systems.

Chapter 3: Methodology

The aim of this study is to develop a model explaining how caldera ring faults evolve as feeder systems during eruptions at caldera volcanoes. Therefore, the ancient Glencoe caldera was chosen as a suitable test bed for the study, due to the in-places-excellent exposure (for example, at the type locality Stob Mhic Mhartuin further described in section 4.1) of the sub-surface caldera fault/feeder systems at considerable depths (~3.5 km, *Garnham, 1988).* It can be reasonably assumed that the areas of good exposure at Glencoe typify what is poorly exposure or buried elsewhere at the same depths of the system. The exposure at Glencoe informs the development of a direct-evidence based theoretical model in order to improve our limited understanding of the caldera and can be applied to similar more poorly calderas found worldwide.

Please refer to nomenclature Section in the appendix for clarification of terms used.

3.1 Fieldwork

The aim of fieldwork at Glencoe was to sample and understand the ring fault fill unit's appearance and their relationships with one another. This fieldwork aims to supplement the fieldwork of previous studies with new information, hence why Glencoe is a suitable study location as most primary observations have already been made and the wider systems history is well understood. The study will apply a modern understanding of caldera systems upon the ongoing debate about the origin of the flinty crush rock (FCR) and the state of the fault intrusion units at the time of the caldera-forming eruption.

The work of previous authors who have studied Glencoe, particularly Moore and Kokelaar (Moore and Kokelaar, 1997, 1998; Kokelaar and Moore, 2006; Kokelaar, 2007) who conducted a detailed remapping of the area, was used as a guide to focus the fieldwork. It is for this reason that Stob Mhic Mhartuin (Grid reference NN208576) was chosen to be a type locality because it presents excellent exposure of all known units across the ring fault system, including a second outer ring fault. Additional observations were made at An-t-Sron (NN134548) because it is a location where the ring fault cross-cuts different country rock lithologies. The work of previous authors has also been used a guide for terminology of units and processes that exist in the study area, however due to previous differences in uses of these terms between authors a revised terminology has been provided in chapter 2.

Fieldwork methods used included: (1) detailed field descriptions of lithologies; (2) sketches and photograph documentation of key localities; (3) measurements of fault plane orientation, grain sizes, unit widths and extent; (4) geological mapping; and (5) sampling. Where possible when sampling the main fault area, material was sampled that was lithologically equivalent to the primary vertical face that is widely reported in literature, but this specific locality was not directly sampled in order to preserve the outcrop and avoid geovandalism. In total 64 samples and 272 photos were taken in the field, at a total of 20 locations. The OS explorer map 384, the Stob Mhic Mhartuin sketch map produced by Garnham (1988; figure 2.04; page 35), the An-t-Sron sketch map produced by Garnham (1988; figure 5.02; page 125) and the British Geological Survey Glencoe Bedrock geological map provided base maps for physical and geological context when in the field.

3.2 Sample treatment, hand samples, and thin section documentation

In the laboratory, samples were washed by hand to remove dirt and moss. Each sample was extensively photographed in order to allow for a reference glossary of their appearance prior to any later alterations for further laboratory work that might affect this (i.e. polishing). Key samples (Table 1) were cut to produce polished, uncovered thin sections. The units were cut perpendicular to their contacts and banding, in order to show the cross unit relationships. Finally, the polished thin sections were scanned using a flatbed scanner to allow for an enlarged, high-resolution image of the whole slide. This allows for overall trends across the slabs to be observed (e.g. heterogeneities, banding, veining, flow features, gradual unit changes) which therefore meant more unit characteristics were noted.

3.3 Micro-analytical methods: Optical and scanning electron microscopy

Firstly, thin sections were analysed using the Zeiss Axio Scope A1 optical microscope with capabilities for transmitted light, cross polarisation and reflected light, in the Arthur Holmes Earth Sciences building, Durham University. This work allowed for the basic petrology and textural characteristics to be noted. Photos and observations were recorded in both plane polarised light, cross polarised light and reflected light. Due to the very fine-grained texture of many lithologies, particularly the FCR, we additionally used scanning electron microscopy (SEM). 17 carbon coated, polished thin sections (Table 1) of Glencoe ring fault samples (from both Stob Mhic Mhartuin and An-t-sron) were analysed using a Hitachi SU-70 high resolution Analytical Scanning Electron Microscope (SEM) in the G.F. Russell Electron Microscopy Facility, Durham University. We used the SEM back scanning electron detector with a 15 mm working distance, a 15 kV beam. The contrast on SEM images are a function of the atomic number (z) contrast in the sampler, where a brighter

image correlates to a higher z. The SEM was used to observed the fine textures of all units related to the ring fault and their contact relationships. A particular focus was given to the fine scale groundmass/matrix textures, and the shape/contact of any phenocrysts/phenocrysts.

3.4 Geochemistry

Geochemical data is used to allow for the quantitative tests of some hypotheses pertinent to this thesis; in particular, hypotheses associated with the petrogenesis of the fault rocks at Glencoe. We use a combination of energy dispersive X-ray spectroscopy (EDS) on the thin section samples, and existing literature data for the bulk rock chemistry of the units in the region.

3.4.1 Energy Dispersive X-ray Spectroscopy

The G.F. Russell Electron Microcopy Facility is equipped with a 24 Oxford instruments energy dispersive X-ray spectroscopy (EDS) microanalysis system, this allows for the units chemistry to be analysed down to micrometre scale. The micro-analysis system equipped with silicon drift detector was used. The system was operated through Aztec 5.1 micro-analysis software and had a 50 mm detection window. Using this facility, chemical maps of the thin sections were made in order to allow for changes in chemistry (e.g. across banding) to be observed. The same polished and carbon coated thin sections were used as the SEM.

3.4.2 Literature data

Garnham's unpublished thesis (Garnham, 1988) provides geochemical analyses of the Glencoe ring fault fill using x-ray fluorescence (XRF), EDS, and microprobe. The principle analytical methods from Garnham (1988) are summarized here for completeness. Major element analysis (calculated on a dry basis) of the fault intrusion rocks used XRF conducted through a Phillips PW 1212 semi-automated XRF spectrometer at Imperial College London. This used a chromium tub operating at 60kv and 32mA. Mineral analysis of the fault intrusion rocks were produced using a Cambridge Instruments Microscan 5 microprobe fitted with a Link Systems energy dispersive x-ray detector. A specimen current on a Co standard of 4.0nA was used with an accelerating voltage of 15kV for 100 seconds count time. Garnham's analyses were point data from polished and carbon coated thin sections. The microprobe was calibrated using metal oxides, pure meta and end-member minerals. The fault rock units (the breccia, FCR and red felsite) were recorded using EDS x-ray analysis on an SEM at Imperial College London. A JEOL 733 superprobe operating back-scattered electron imaging

mode was used. Small area (1-1000 quare microns) scans of the thin sections using the beam for 200 seconds produced the semi-quantitative bulk rock analyses.

A large majority of the data provided by Garnham (1988) focuses on the varying compositions of the fault intrusions, but chapter 7 of the thesis provides analyses of the units present at Stob Mhic Mhartuin, starting to highlight the trend of compositions seen across the units. In order to present a clearer image of Garnham's results, the major element data from appendix C and appendix E of the Garnham (1988) thesis have been merged here, in order to show all relevant units for this study of the Glencoe ring fault. The units used are the breccia, the FCR, the red felsite (also referred to as rhyolite in literature) and the ring intrusions (gabbros, diorites, monzonites, granites). To supplement the Garnham (1988) work, an average value for the pure Glencoe quartzite has been collated, taken from Hickman and Wright (1983, page 270, table 10, column 3, the quartzite average used a Phillips PW 1212 fully automatic XRF). This data has additionally been presented on a total alkali silica (TAS) diagram in order to highlight the unit classifications given. The data has been re-analysed using a series of calculations in order to highlight the relationships and differences between units, often this re-analysis has focussed on units recorded in or analogous with those at Stob Mhic Mhartuin. These data processing steps are described later in this thesis.

Chapter 4: Results

In this Chapter, the primary results are presented and analysed. The principal field locality Stob Mhic Mhartuin pertinent to this thesis is described, and is compared to An-t-Sron as a subsidiary location to allow for comparison of features across the caldera. Both can be seen located in Figure 2.1a (page 23-24), demarking the localities dealt with in this thesis. Results from this thesis are divided by the study location, method of study, and the unit observed.

The results consist of:

(1) Textural and petrological observations of Stob Mhic Mhartuin (Section 4.1; figure 4.1) units from: the fieldwork including determination of the dominant units and associated lithological descriptions of the Glencoe caldera ring fault rocks; hand sample descriptions; results of optical microscopy investigation; results from the scanning electron microscopy campaign; observations from the semi-quantitative geochemical analysis by energy dispersive X-ray spectroscopy (EDS). These observations have been divided up by unit into Sections 4.1.1 – 4.1.5.

(2) Observations of An-t-Sron that differ from any observations found within the focus locality of Stob Mhic Mhartuin (Section 4.2)

These sections are dealt with in turn.

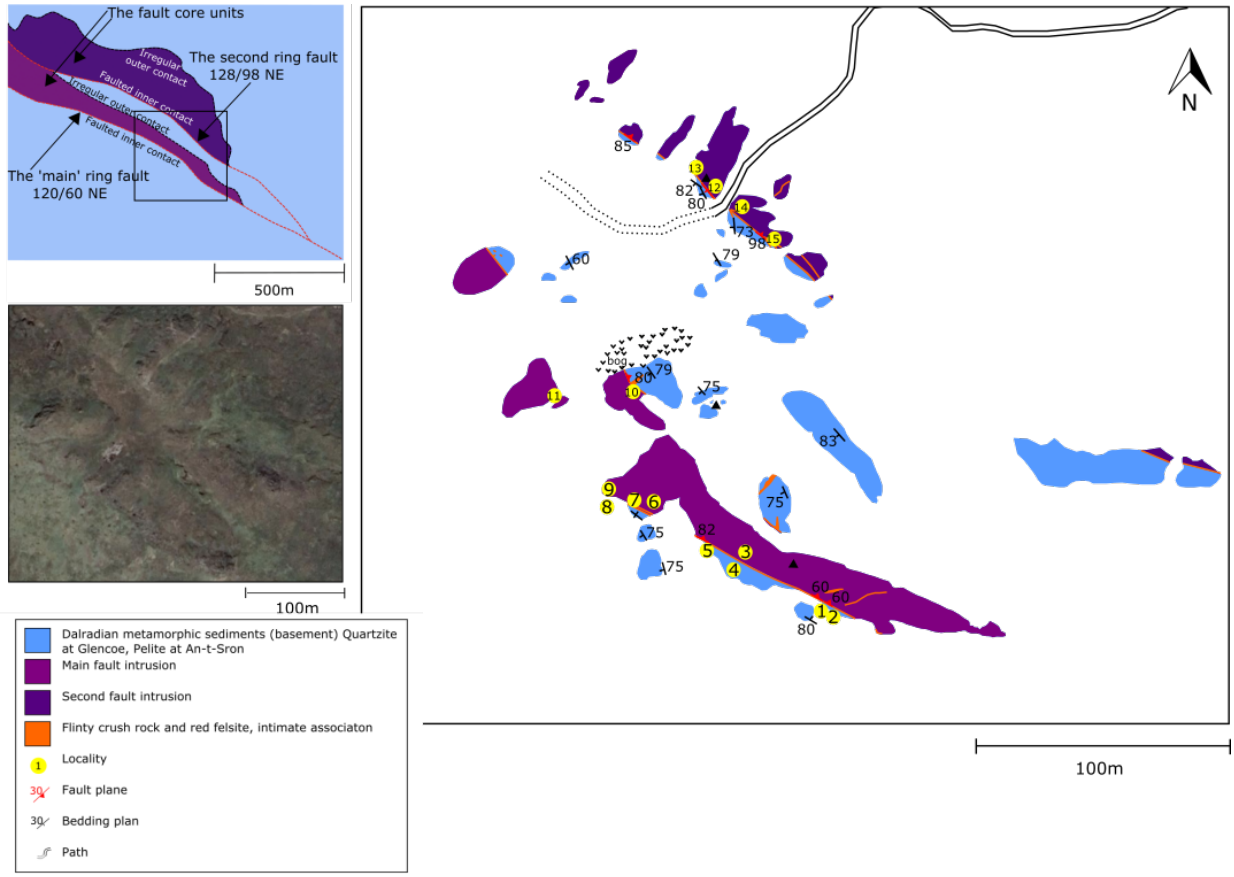

Figure 4.1 *An approximate map of the lithologies found at Stob Mhic Mhartuin, adapted from Garnham 1988 but with additional data from satellite image taken from Google Earth and fieldwork unique to this thesis. Red felsite is not drawn on the map due as it is intimately associated with the FCR. Sample localities are numbered. This figure also shows insets of: a schematic diagram of Stob Mhic Mhartuin to show the geological interpretation of the fieldwork (adapted from Kokelaar 2007) with a box to show where the fieldwork was undertaken; a satellite image to show the surface expression of the area where fieldwork was undertaken; a legend to explain symbols and colours used in the field map.*

4.1 Locality 1: Stob Mhic Mhartuin

At Stob Mhic Mhartuin, the width of the main caldera fault zone is 300 m and it strikes 121/60 NE. The country rock here is a quartzite (Section 4.1.1-4.1.2), which shows evidence of brecciation where the quartzite is exposed near to the ring fault. The fault core is filled with units that can be broadly described in a type stratigraphy (figure 4.2), which from margin to core is: (1) flinty crush rock (FCR; Section 4.1.3); (2) variably coherent bands of red felsite (Section 4.1.4); (3) fault intrusion plutonic rocks (Section 4.1.5). All these 3 units contain inclusions of one another as well as the brecciated quartzite (Section 4.1.2), to varying degrees of concentration. There is a difference in appearance and

inter-relationship of the units along the inner (to the southwest) contacts of the fault core and the more varied, less planar and more veined outer (to the northeast) contact. This difference in appearance of the outer and inner contact of the fault cores is an important feature of Stob Mhic Mhartuin however limited exposure of the outer contact here restricts full analysis of this. Veins of FCR locally cross-cut the quartzite (and occasionally the fault intrusions) at angles oblique to the strike of the marginal contact between the main FCR units and the quartzite. In Figure 4.1, a simplified geological map of the Stob Mhic Mhartuin locality is shown. While this map is based on a map found in Garnham (1988; page 35; Figure 2.04), it has been adapted and updated via fieldwork associated with this thesis. In this section, each lithology is taken in turn and described as it is found in the field, hand sample and through microscopy, in order to provide a full textural and petrological depiction of the units. A key feature of the units at here is the variability and complexity of the appearance and interactions with one another. At Stob Mhic Mhartuin there are two intruded faults that run through the area, these are referred to as the inner or main (due to its connection to the main ring fault) intrusion, and the outer intrusion. The main fault has exposed inner (southwest) and outer (northeast) contacts, whereas the outer fault has only the inner (southwest) contact exposed. The inner contacts of both are referred to as faulted contacts as they lay on the fault surface.

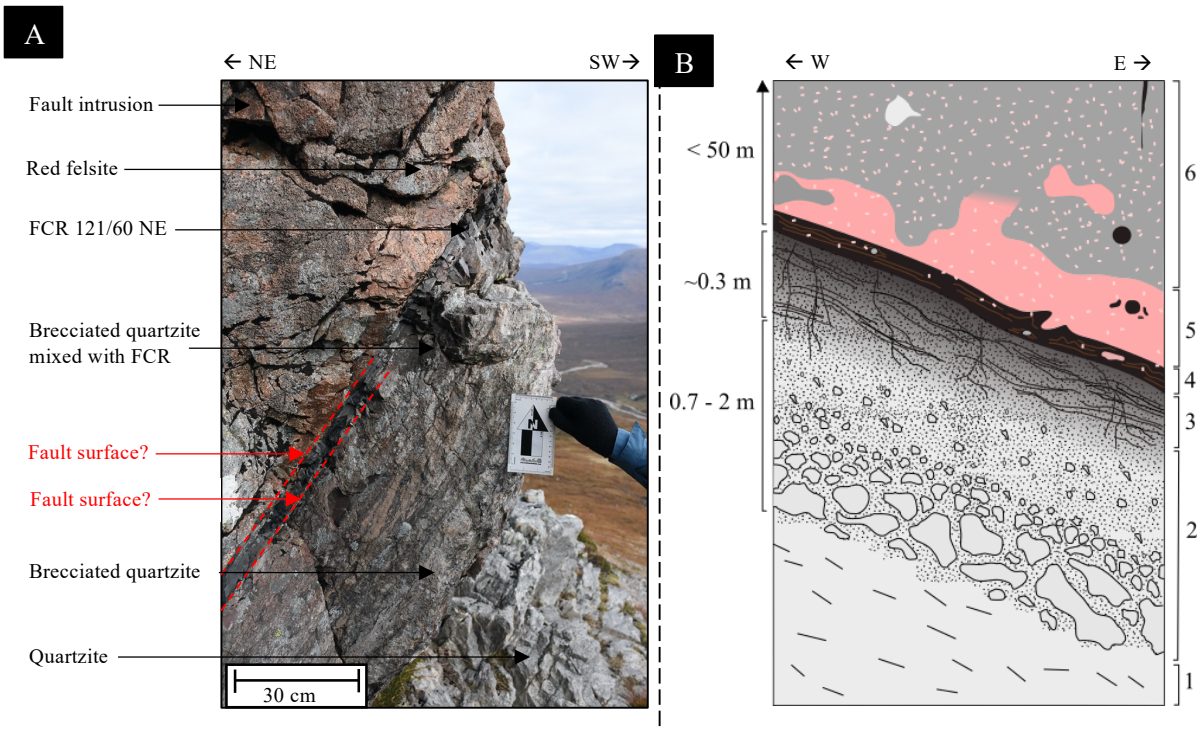

Figure 4.2 *(a) An annotated field image of the type locality 1 at Stob Mhic Mhartuin to show the field relationships between the fault related units.*

(b) A sketch to show a plan view of the field relationships of the main units related to the ring fault along the inner main intrusion contact at Stob Mhic Mhartuin. The other contacts seen are comparable but not the same.

All of these units are known to be part of a ring faulting and venting system, something that this study later discusses. (Note the variable scale). (adapted from McGarvie, 1980; Garnham, 1988)

1. *Flaggy and bedded quartzite of the downfaulted inner block*
2. *Brecciated quartzite*
3. *Brecciated quartzite mixed with FCR in the form of veins and banding*
4. *Banded FCR containing some feldspars, inclusions of red felsite and quartzite*
5. *Red felsite containing broken phenocrysts, inclusions of FCR and fault intrusion*
6. *Main fault intrusion containing larger phenocrysts, inclusions of FCR (as pods and veins), red felsite and lithics*

4.1.1 Quartzite

The quartzite is bright white-grey (or occasionally pink) and weathering-resistant (flaggy; figure 4.3a). It is composed of interlocking quartz with rare mica and mafic minerals, with <70 cm pure-quartz lenses. The quartzite is massive but with occasional, poorly-developed foliation (figure 4.3a), as well as fractures in planes that align with nearby faulting. Optical microscopy and SEM confirms the relative homogeneity of the quartzite microstructure with 100-2000 µm polygonal quartz crystals comprising >90 vol.% of the sample (figure 4.3b). In some areas there are signs of strain (deformation lamella, tuttle lamella, undulose extinction) and recrystallisation. Micas (namely biotite and mica) <0.25 mm tend to be found in the interstices between quartz crystals (<5-10 vol.%). Opaques (for the purpose of this thesis all optically opaque non silicate minerals are referred to as opaques unless otherwise classified through texture or chemical study) are also found trapped between quartz crystals with irregular shapes (<5 vol.%). The unit also contains a variable, minor amount of orthoclase feldspar, which on rare occasions replaces the quartz to occupy up to ~40% of the unit, causing a pink sample colour (figure 4.3c. In these occurrences the texture of feldspars imply they are possibly an alteration product, and they are also commonly coated by minor amounts of albite feldspar (figure 4.3d). Within approximately 10 m proximity of the caldera faults cutting through the quartzite at Stob Mhic Mhartuin, the country rock becomes gradually broken down into progressively finer clasts forming a brecciated quartzite (Section 4.1.2).

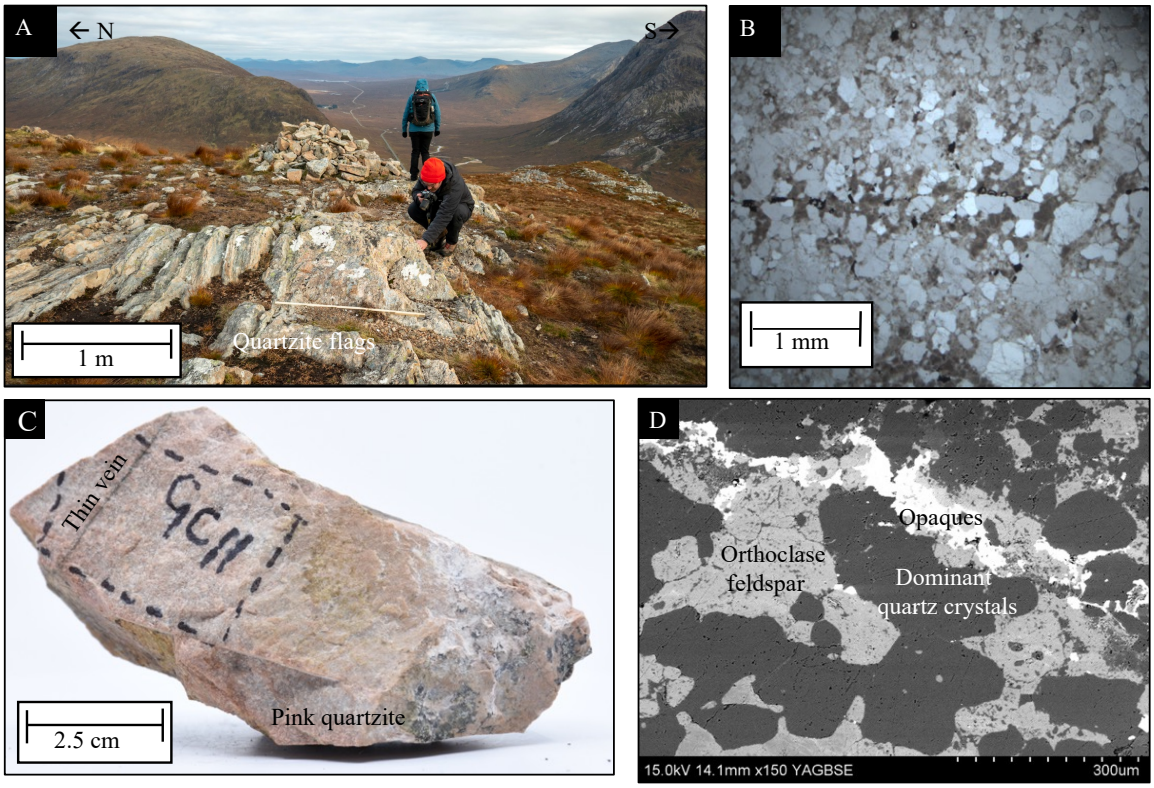

Figure 4.3a-d *Images to show the nature of the quartzite in field, hand sample, optical microscopy and SEM. (a) Steeply dipping (c.70-75°) quartzites against the outer margin of the inner intrusion. A pink colour has developed here due to the presence of oxidised feldspars (just north of locality 10). Photo taken by Dave McGarvie. (b) An optical microscope image of an unbrecciated quartzite rich with oxidised feldspars creating a pink colour, this is a more finescale quartzite example (locality 4). (c) Hand sample (locality 4) of pink coloured quartzite taken with a fine possible FCR vein cross cutting one end (d) An SEM image of an unbrecciated quartzite (quartz is the darker grey colour) rich with oxidized feldspars (lighter grey colour) creating a pink colour. Veins of quartz cut across the feldspar crystals implying they may have formed through the hydrothermal alteration of quartz (locality 4).*

4.1.2 Brecciated quartzite

Far from the caldera faults, the quartzite is not brecciated (Section 4.1.1), however, within 2-10 m of the southwest side of the main fault (Figure 4.1-4.2), brecciation is characterised by (1) smaller quartz grainsize relative to the far-field (figure 4.4); (2) cataclastic textures such as veinlets of fine grained material; (3) some incorporation of the flinty crush rock lithology (see Section 4.1.3) in grain interstices, which is most prevalent proximal to the caldera fault. Additionally, discrete veins of flinty crush rock cross cut textures in the brecciated quartzite in veins sub-parallel to and sourced from the fault margin (figure 5.6b-c). At the fault margin and within 0.3 m (figure 4.4; 4.6a), the brecciated quartzite appears hybridised with the flinty crush rock. On the north side of the caldera fault, the

brecciated quartzite is only ~7 cm thick and the contact between brecciated quartzite and flinty crush rock is gradual.

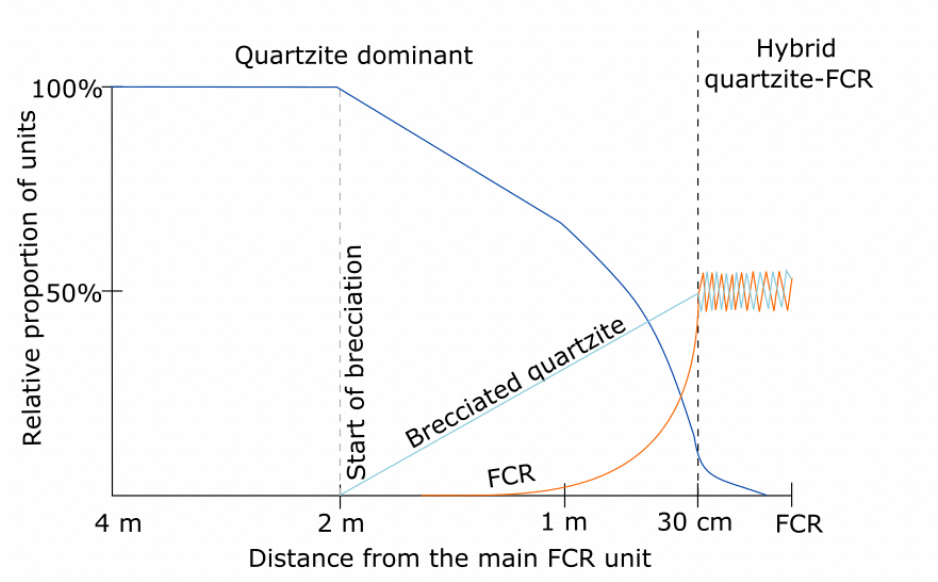

Figure 4.4 *A schematic graph to show the relative degree of brecciation, and volumes of each unit (quartzite, brecciated quartzite, and FCR) present along the gradual contact between quartzite and FCR. This contact is variable and chaotic but this is a general summary. Mixing of FCR into the breccia occurs in the form of fine stringers and some banding which appears to fluidised close to the contact. The graph terminates at the contact of pure FCR (to the right) which is sharp.*

Microscopy reveals that there are 3 key parts to this sub-unit: large polymineralic <8 cm quartzite clasts (4.6d), smaller <1.5 mm monomineralic clasts, and a fine (<0.2 mm) matrix. The organisation of domains of these parts changes close to the fault as the polymineralic clasts are absent. There are no additional signs of internal strain within brecciated clasts than seen within the quartzite. The matrix contains predominantly quartz, as well as occasional alkali feldspar and albite felspar as shown on EDS. Some opaques (<25 µm) are found within the unit, often in clusters, and they are variably rich in calcium, titanium, magnesium, phosphorous, sodium and iron. The fine fractures which actively breakup quartz crystals are rich in orthoclase and titanomagnetites.

The contact of the brecciated quartzite with the FCR lays on the faulted contact of the main (121/60 NE) and outer (129/98 NE) intrusions, as well as the outer (non-faulted) contact of the main intrusion (158/80 NE, but variable due to irregular shape). The faulted, inner intrusion contacts are sharp and distinct (such as locality 1). Often the faulted contacts are planar but this is occasionally affected by swirling and veining between the units. Crosscutting irregular and anastomosing veins (up to 5 cm wide) and matrices of FCR and brecciated quartzite create a network through the rock (figure 4.6b-c, e-f). This irregularity is more common along the non-faulted outer intrusion contacts (figure 4.6h).

Along the contact with FCR there is a lot of veining, best displayed in sample 29, where FCR protrudes into the quartzite. The change in unit from a coherent quartzite, to a brecciated quartzite, a microbreccia, a hybrid rock and finally the FCR shows a progressive decrease in grainsize (figure 4.4). Near to the contact with FCR the geochemical composition (figure 4.5) of the breccia matrix starts to become less homogenous, contain a wider variety of elements and resemble that of the FCR's and starts to develop some subtle banding similar to that of the FCR. The FCR matrix that veins into and suspends clasts of quartzite is slightly richer in potassium and aluminium than within the main FCR unit. Therefore, there remains a fairly sharp geochemical change between the contain with the main FCR unit. Near (within a few millimetres) to the contact with brecciated quartzite and within the veins protruding into the brecciated quartzite, the FCR is particularly rich in opaques and quartz clasts (figure 4.6e).

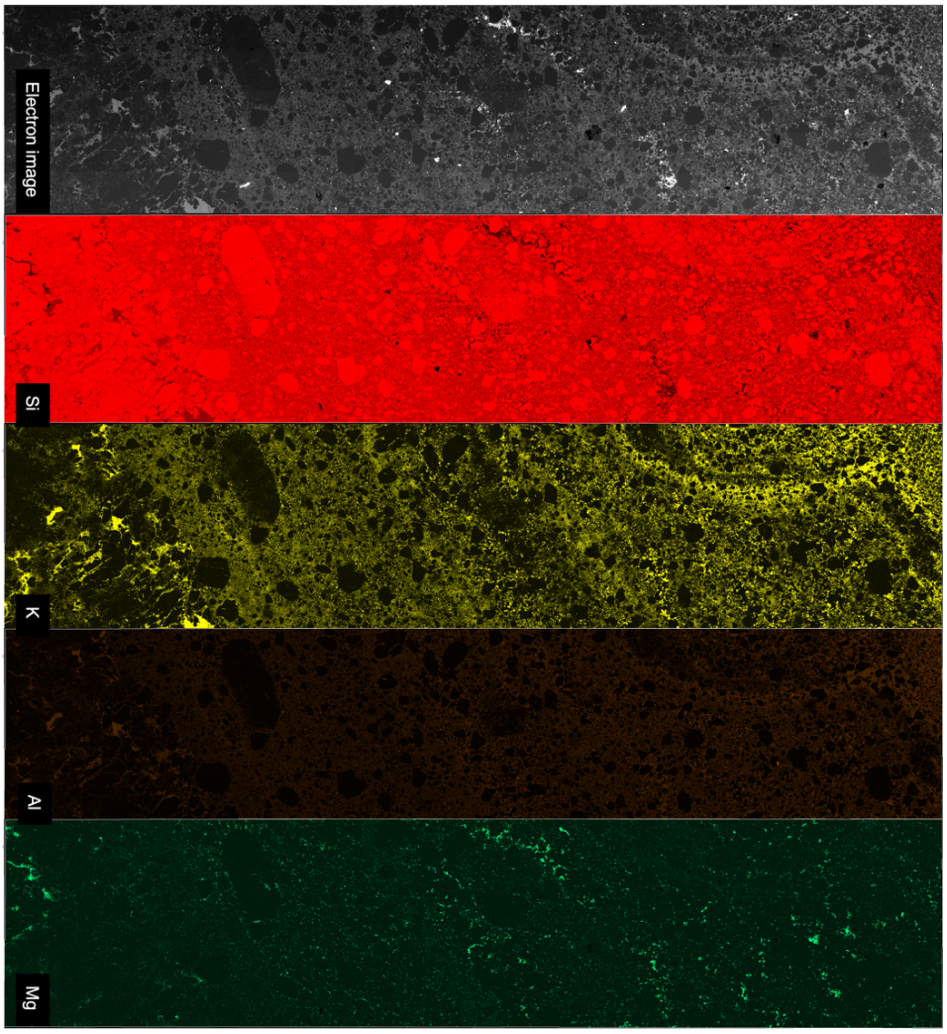

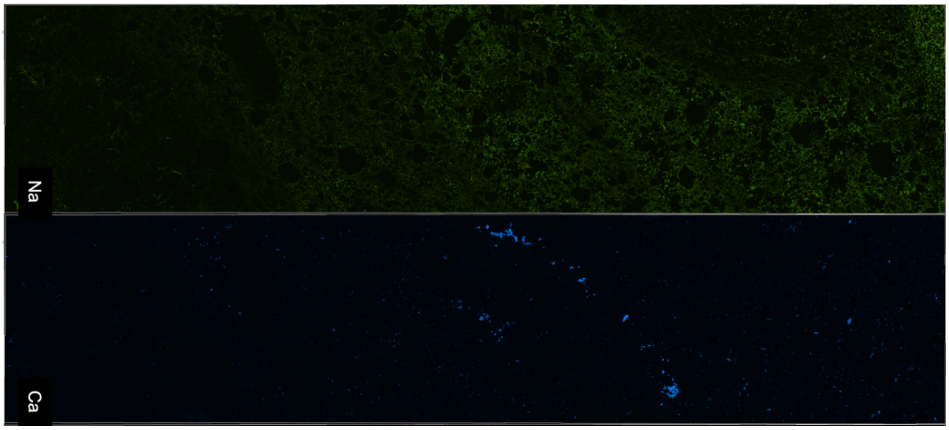

Figure 4.5 *An example of the contact between the quartzite (left hand side) and FCR (right hand side), which shows how most elements other than silica are introduced within the FCR that aren't within the quartzite. This also shows the banding of the FCR which is mostly controlled by potassium, and some aluminum and sodium, typical of volcanic glasses (unlike the mafic-felsic bands controlled by Fe and Mg expected for frictional melts).*

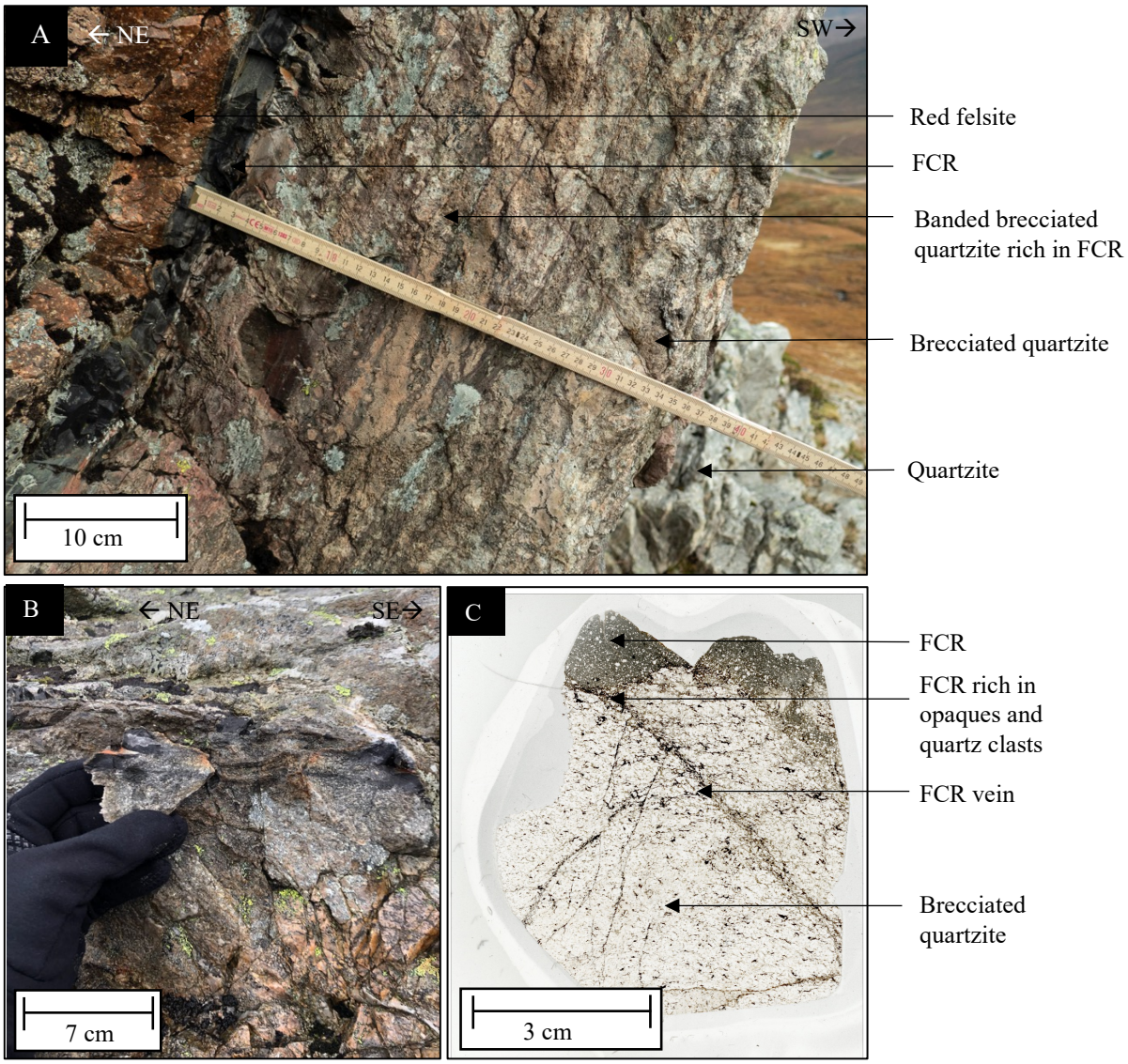

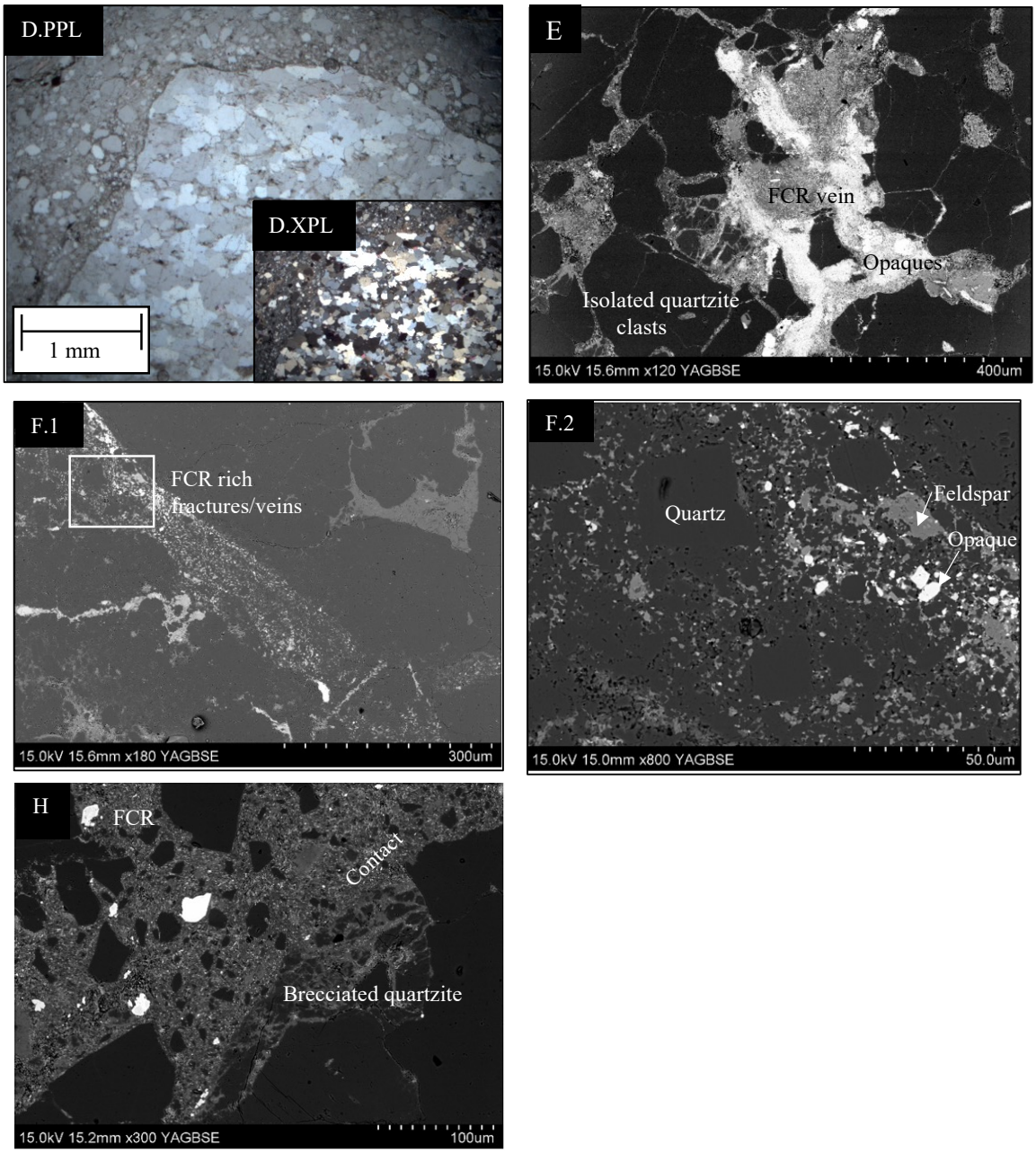

Figure 4.6a-j *An array of images highlighting the nature of the brecciated quartzite, it's contact with the FCR and veins of the FCR crosscutting the subunit. (a) A field image of the contact of the quartzite with the main fault and FCR, taken at the classic type locality (1). Red felsite – FCR - 25 cm of banded brecciated quartzite mixed with FCR in a fluidized structure - progressively less brecciated quartzite can all be seen in order towards the southwest. Photo taken by Dave McGarvie. (b) A field image showing the projection of FCR veins into the brecciated quartzite along the second fault (locality 15), the veins splay at multiple angles but they are mostly parallel to the fault. (c) A scan of a thin section of the sample shown in 4.6d (locality 15, second fault) showing the veining of FCR into the brecciated quartzite and how the structure contains many oblique and anastomosing veins that become very thin and break up quartzite clasts. (d) An optical microscope image of the edge of a large polymineralic quartz clast surrounded by a network of monomineralic quartz clasts and some fine matrix, in plain polarised light (PPL) and cross polarized light (XPL). Taken from the main fault contact (locality 5).*

(e) An SEM image of a vein which extends from the FCR which consists of brecciated quartzite clasts and a matrix rich in fine opaques, feldspars and quartz. Taken from locality 15 along the second fault. (f.1) An SEM image of a vein which extends from the FCR into the brecciated quartzite which consists of brecciated quartzite clasts and a matrix rich in fine opaques, feldspars and quartz. Taken from locality 10 along the intrusions outer non-faulted contact. (f.2) A higher magnification image of the vein material shown in figure 4.6h (h) An SEM image of the contact found at locality 15, along the second intrusion contact. The contact is clear and sharp, and some banding in the FCR along the contact is visible. There is a sudden introduction of paler feldspar rich material in the matrix, and a sudden change in the size of quartz.

4.1.3 Flinty crush rock (FCR)

The FCR lies along the contacts of the two ring intrusions of Stob Mhic Mhartuin, as bands (planar and non-planar), pods and sigmoidal infillings (Garnham, 1988). The FCR along the main fault is the most uniform, planar (121/60 NE) and the thinnest (2 – 3 cm). The outer intrusion FCR also lies on a fault and is quite planar (128/98 NE), whereas the outer main intrusion FCR sits on a very irregular (non-fault) plane (roughly 158/80 NE), both units are however blacker and have very variable thicknesses (1 – 14cm, and 1 – 5cm, respectively). Microscopy, particularly SEM, is an important tool for unpicking the nature of the FCR due to its very fine grained texture. The FCR is surprisingly variable under the microscope when compared to the homogenous seeming aphanitic black rock seen in sample. Key variations exist in the groundmass texture, banding and phenocryst appearance.

The FCR is a fine black-brown aphanitic rock. Garnham (1988) made the observation that the finest grained units are blacker and banded. Approximately 55% of the FCR's volume is occupied by a very fine silicic groundmass which gives the rock its dark colour. SEM is important to reveal the nature of this groundmass which consists of equal parts of a lighter coloured (when using SEM, therefore with a higher atomic number) orthoclase feldspar component and darker flecks of quartz material (approx. =<10 um in size). These two components form anhedral, irregular shapes and often develop a wormy myrmekite intergrowth graphic texture (figure 4.7g). The groundmass contains some extremely fine crystals creating a speckled appearance, consisting of many anhedral opaques (often ilmenite bearing titanomagnetites, <1 – 5 μm), many rounded to angular quartz (<= 5 μm) which sometimes interlock with the groundmass and have a very variable concentration (figure 4.7h), uncommon albite feldspar laths which are mostly euhedral, and, low and variable concentrations of calcium bearing pyroxene fibres or clusters (their presence is associated with larger quartz xenocrysts < 25 μm). The FCR contains pores within its groundmass, especially around large phenocrysts. The groundmass is in places covered by fine green chlorite fibres, a feature of later alteration not focused on in this thesis.

The unit is crosscut by fine lighter brown bands (figure 4.7e-f), which are the most striking and the most uniform along the main intrusion inner contact FCR (where the 'type locality' is found). The bands are of varied thicknesses (<<1 – 9 mm) and will clump in places. In places bands become non-parallel, contorted, tapered or, form wings and diversions around FCR phenocrysts. Banding along the outer main intrusion contact is very contorted whereas along the second intrusion it is very rare. Optically, the bands seem to be defined by the colour of the groundmass which is explained using SEM to be a feature of multiple varying characteristics which change across different bands: (1) changing volume, texture (anhedral crystals to wormy intergrowths to fine < 5 μm crystals) and coarseness of the quartz groundmass component (2) change in the volume and type of reactionary behaviour of quartz xenocrysts (3) change in the number of very fine (< 5 μm) opaques within the groundmass (4) resemblance to the red felsite (including presence of feldspars) (5) very subtle changes in the volume, size and shape of quartz xenocrysts. Some of the FCR bands bare a lot of similarity to the red felsite, due to their similar groundmass and feldspars. Fine fractures filled with haematite, opaques and mica will sometimes align to the banding present. With EDS geochemical maps the banding is also recognisable. Potassium is the key element controlling the occurrence of banding. Sodium, aluminium and magnesium also experience some variability according to the unit's banding. These changes are controlled by the amount of orthoclase, albite and quartz in the groundmass (as flecks or as small phenocrysts sat within the groundmass). Magnesium is mostly seen as fine coatings of phenocrysts, whose occurrence clusters along planes that align to the banding, and this feature becomes more common near to the contact with the red felsite. In places titanomagnetites also faintly cluster along bands.

The FCR is littered (80-90% of the total phenocryst volume, which is 45% of the sample) by vitreous (~1 μm - 1 mm) quartz xenocrysts, particularly near to the quartzite contact. The quartz is anhedral with signs of breakage and rounding. There are occasions where the xenocrysts lose their clastic appearance due to highly irregular shapes. The edges of the xenocrysts may be fractured or rounded, or, show irregular interaction with the quartz groundmass component. Evidence that the quartz are xenocrysts (originating from the adjacent brecciated quartzite) includes their sintered texture matching the protolith, their faint signs of strain matching the protolith, and their reactions with the groundmass they sit within (figure 4.7j). Reactionary behaviour of quartz includes rare embayment's (which contain coarse groundmass particularly rich in orthoclase, and albite feldspar crystal growths; figure 4.7i), irregular borders of clasts, a 2 – 3 μm halo of groundmass material with a ruffled/wormy shape (believed to be a poorly developed myrmekite intergrowth), and, a coating of fibrous pyroxenes which extend from the crystal edge (which are limited in size by the width of the myrmekitic halo present). Reaction rims and embayments are not always present and are sometimes poorly developed. Some quartz contains fish-scale-like fractures which may resembles cristobalite (this requires further

research) and occasionally inclusions. Larger (up to 2 mm) polymineralic quartzite lithics are also common, apart from their larger size their characteristics remain the same. There are also places within the FCR where quartz xenoliths are tightly packed and surrounded by quartz rich groundmass which results in them appearing like large single lithic clasts at low magnifications. The FCR and the quartzite have an intimate association shown by their mixture of clasts resulting in a xenolith rich FCR and the veins of FCR within the quartzite.

Opaques (particularly titanomagnetites) are a common phenocryst phase within the FCR, but they are rarely larger than 0.5 mm so retain only 5% of the phenocrystal volume. The smaller components elongate and align to create a poorly shear during flow banded texture in places. They often form irregular and interstitial shapes. Larger opaque phenocrysts display widmanstätten pattern on their surface which shows they are titanomagnetite's which have experienced solid state exsolution of ilmenite. They are occasionally embayed (in which case calcium bearing pyroxenes grow within the embayed zones; figure 4.7k) and sometimes contain fine inclusions. As seen in geochemical maps, the groundmass coating embayed titanomagnetites are rich in magnesium, calcium, sodium and aluminium, yet depleted in potassium.

Amphiboles and biotites (<=5% phenocryst volume each) are mostly <1.5mm (but seen to reach 5 mm) and often occur in clusters. Their crystal habits are recognizable but often rounded or fractured. In-situ fragmentation is present. Micas are regularly slightly kinked and aligned to the unit's banding. Opaques (rich in titanium and calcium) also commonly coat these phenocrysts and chlorite commonly pseudomorphs them.

Sparse (<5% phenocrysts vol.) fragmented feldspar (both plagioclase and alkali) crystals (<2 mm) with similar appearances to those in the red felsite are set within the FCR, these are particularly high in quantity near to the contact with the red felsite and they sometimes align to the banding within the unit. Albite feldspars are particularly common, and they tend to be overgrown by an albite rich component of groundmass. These relatively large phenocrysts are often intensely embayed and altered often by sericite (figure 4.7l).

The outer FCR band found along the main fault intrusion is slightly blacker in colour and it is often completely hybridized with adjacent brecciated quartzite, so it is richer in quartzite xenoliths that are often larger and elongate (up to 3.5 cm). Here, the banding is less planar and becomes more intense closer to the contact with the red felsite. The FCR along the second intrusion is much blacker, more opaque, more homogenous, massive and generally simpler/less variable, this clear difference is most noticeable microscopically. Banding is rare and the groundmass occupies a larger volume (70-80%) of the rock. The groundmass has a different texture under high magnification (figure 4.7m), it appears

a lot more clastic, consisting of a network of very fine (~1 um) quartz, opaque and a few mica grains, as well as regular pores. There are fewer phenocrysts that are finer (<5 – 400 μm), unsorted and not-aligned. There is also less mineral variability as most phenocrysts are quartz or opaques. Quartz xenocrysts here have no reactionary behaviours.

The FCR injects veins and thinner 'stringers' into the adjacent quartzite, red felsite and fault intrusion (such as locality 15). These are quite common with variable thicknesses (up to 5 cm) and angles. Often along the inner faulted contact the veins injecting into adjacent rocks develop a near parallel angle to the fault/intrusion.

The FCR and the adjacent red felsite have an intimate association (figure 4.7a-d). The contact between the units is often, but not always, sharp, and interrupted by feldspars from the red felsite protruding into the FCR (figure 4.7a,o-p). In some of these cases, the phenocryst which crosses the border displays slightly different characteristics on either side of the contact, such as being less weathered (so displaying a better habit) on the FCR side (locality 8) or having a phenocryst coating on the red felsite side (locality 10). The contact is not always planar, the units regularly show mixed contacts, interfingering, hybridisation (to produce a non-banded, brown, quartz and feldspar rich poorly porphyritic rock, figure 4.7e), inclusion of red felsite phenocrysts within the FCR and pods of material containing the other unit (figure 4.7c-d). The array of mixed contacts, of which there are 6 types, are meticulously described by Garnham (1988). FCR banding often conforms to the plane of the contact, but in places it is truncated by the red felsite (figure 4.7f-n). Isolated lenses of red felsite are often found within the FCR (up to 20 cm in length), particularly along the second intrusion (Locality 1 for example). Garnham (1988) highlights that both FCR and red felsite are found at all ring fault outcrops except where the Devonian metasediments and volcanic units have become downfaulted against Dalradian metasediments (in these places, neither unit is observed). There are few places along faulted contacts where due to the turbulent mixing relationships of the red felsite and the fault intrusion, the latter directly contacts with the FCR, in these cases the contact is similar. The intimate associated is also displayed by the similarity between the two units, especially noticeable when comparing their groundmass at high magnifications and when FCR bands are truncated by the red felsite to show the similarity with the lighter coloured bands. The geochemical composition of the FCR and red felsite groundmass shown in geochemical maps is very similar, due to both units containing the same groundmass components, however the groundmass texture does change (figure 4.7o-p). Overall, the red felsite groundmass is richer in aluminium, sodium, potassium and magnesium, yet slightly poorer in silica – this has occurred because of a decrease in quartz but increase in feldspar. However, the FCR groundmass becomes gradually richer in magnesium towards their contact, due to mixing. The concentration of titanium, associated with titanomagnetites, remains constant.

Overall, observations of the FCR show that it is a fine grained silicic unit which is closely associated with quartzite in the manner of mechanical mixing of quartzite xenoliths with have reacted within the groundmass. The unit also has an intimate association with the red felsite due to a similarity in nature and the occurrence of quite extreme mixing in places.

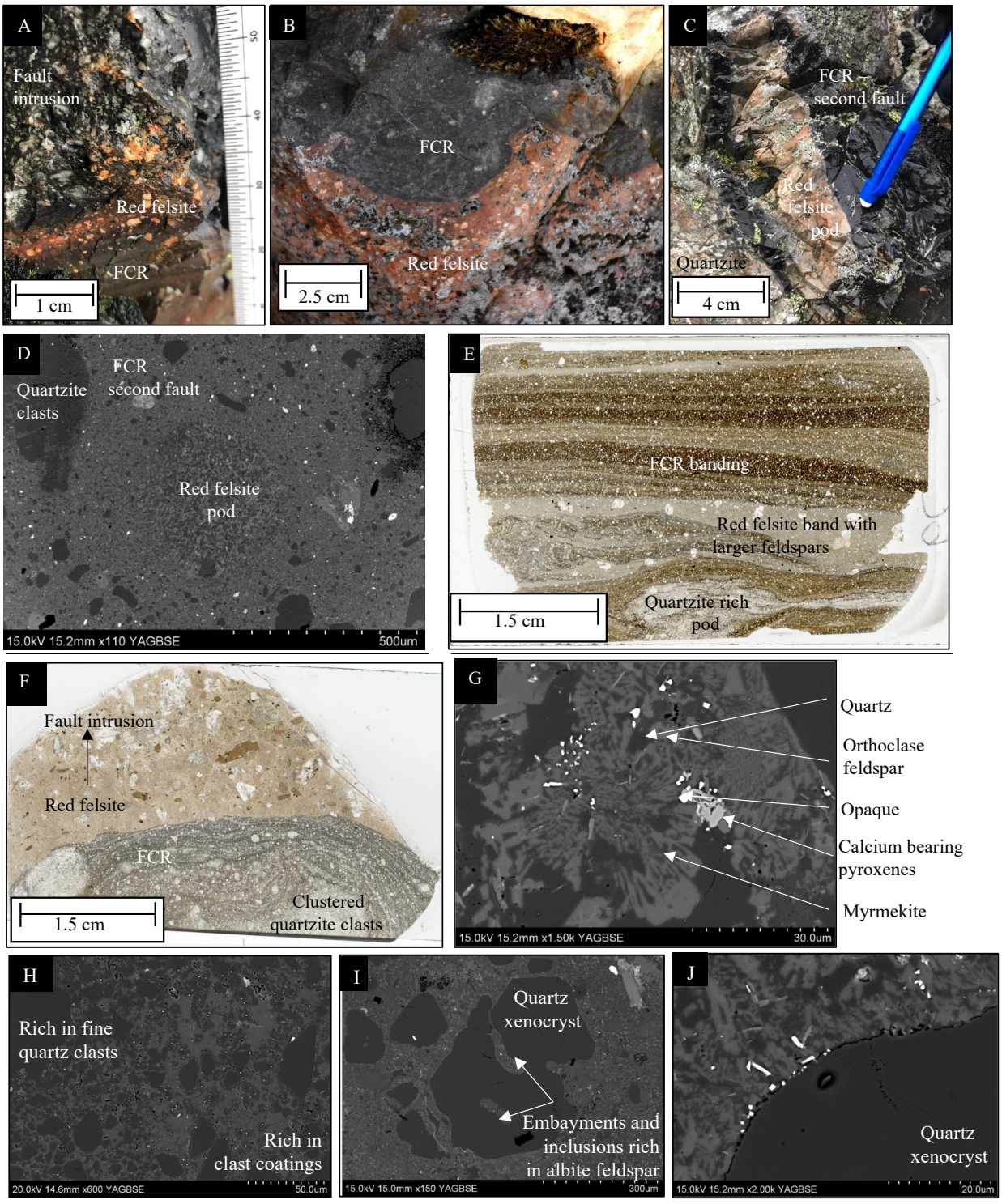

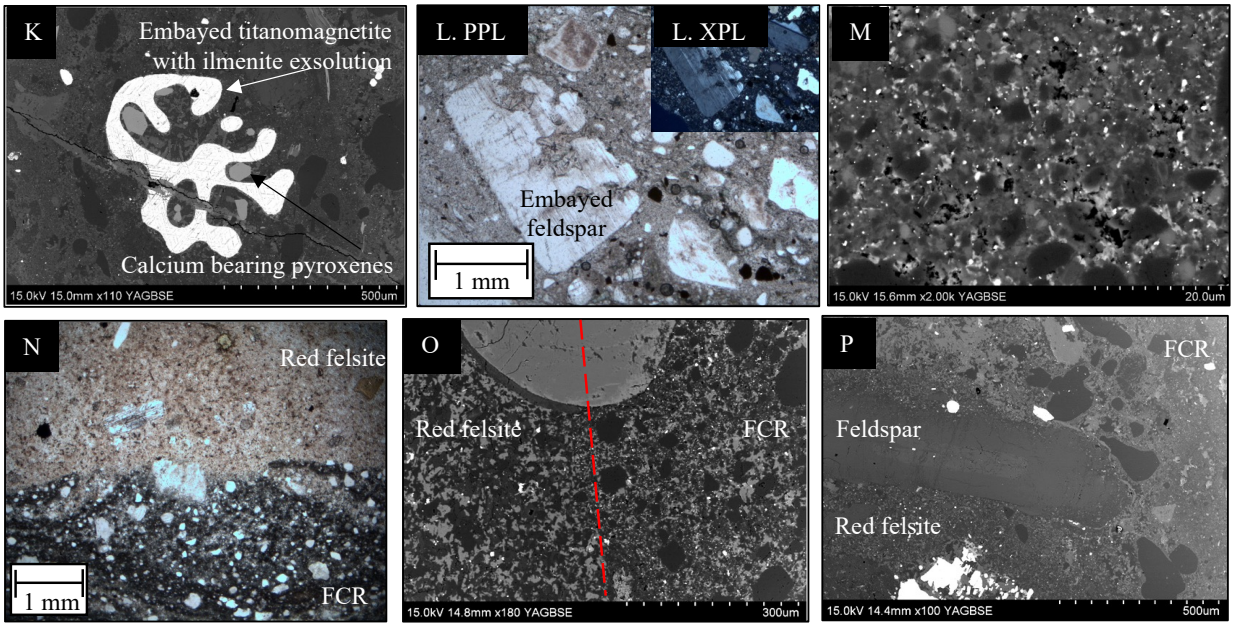

Figure 4.7a-p *An array of images highlighting the nature of the FCR and its relationship with the red felsite.* (a) *A field photo of the gradual contact between the banded FCR and the red felsite, as well as the very turbulently mixed contact between the red felsite and the fault intrusion. The FCR has feldspar phenocrysts which are adopted from the red felsite. This is found along the type locality at the faulted inner contact of the main intrusion, at locality 2. This highlights the planar bands of the FCR along the main fault.* (b) *A field photo to show an example of a sharp contact between the FCR and the red felsite which displays some liquid immiscibility. This image also highlights the more contorted FCR bands along the outer contact.* (c) *A field photo of a lens of red felsite found within the FCR. This is found along the second intrusion at locality 12.* (d) *An SEM image to show a pod of groundmass (found within the second intrusion FCR) that closely resembles the red felsite, which appears like a clast at lower magnifications. Taken from locality 15.* (e) *A thin section of the FCR found along the type locality of the inner main intrusion contact (locality 9). This unit is dark brown, banded, contains feldspar phenocrysts adopted from the red felsite, contains quartzite lithics and has a thick band which closely resembles the red felsite.* (f) *A thin section of the FCR to show an example of contorted banding, large clusters of quartzite lithics, and a darker example of the unit.* (g) *An SEM image of the myrmekite texture found in the FCR groundmass formed by the wormy intergrowth of quartz (darker colour) and orthoclase feldspar (lighter colour), giving the rock a graphic texture and implying slow cooling. Also present are the fine opaque and pyroxene crystals within the FCR groundmass, that are lower in atomic number than the main silicic groundmass therefore much lighter in colour with the SEM. From locality 2 along the inner main fault intrusion contact.* (h) *An SEM image of the FCR groundmass textures which displays banding. In one band the quartzite component of the groundmass appears as fine clasts, in the band on the right hand side the groundmass quartz contributes to the reaction rims around quartz xenocrysts composed of myrmekite and pyroxene fibres.* (i) *An SEM image to show the most extreme example of embayment seen within quartz xenoliths of the FCR. Taken from the FCR along the inner main intrusion contact (locality 2).* (j) *An SEM image to show the dark irregular, reactionary edge of quartz clasts within the FCR. This also shows the tendency of fine more mafic pyroxene fibres to coat quartz clasts. Taken from the FCR along the inner main intrusion contact (locality 2).*

(k) *An SEM image of an opaque phenocryst which is a very irregular shape, filled with embayment's and pyroxenes that have grown within them. This opaque also displays the widmanstätten pattern – typical of a titanomagnetite which has exsolved ilmenite. The groundmass surrounding this opaque is also a different shade. This is taken from the FCR along the inner main intrusion contact (locality 2).* (l) *An optical microscope image of a heavily resorbed feldspar phenocryst within the FCR (found along the inner main intrusion contact locality 2). Most feldspars in the FCR are resorbed. Taken in (a) plane polarised light and (b) cross polarised light.* (m) *An SEM image of the clastic appearance of the fine groundmass components of the FCR along the second intrusion (locality 15). Still composed of very fine (=<5um) quartz, feldspar, opaques, pores and pyroxenes.* (n) *An optical microscope image of the truncation of FCR banding by red felsite which exposes the similarity between the light bands and the red felsite.* (o) *An SEM image to show the subtle changes in unit between the red felsite (left) and FCR (right). The coating of the large phenocryst at the top of the image is not present on the FCR side. (p) An example of where the red felsite – FCR contact is clearer, and also cross cut by a large red felsite feldspar phenocryst.*

4.1.4 Red felsite

The red felsite occurs in large discontinuous lenticular zones (several metres) or enclaves (<5 cm) irregularly along the ring fault in close association (often commonly laying in between) to the FCR and the fault intrusion. Sometimes it is not present for distances of up to 10m along the fault. Occasionally the red felsite is recognized away from the FCR, such as in pods south of the FCR along the main fault contact and as dykes within the quartzite (described well by Garnham 1988). There limited exposure along the outer contact of the intrusions which restricts observations of the red felsite.

The red felsite is red-brown coloured medium grained glomeroporphyrite. The unit's appearance varies slightly caused by changes in the concentration of phenocrysts (causing it to become aphyric in places) and the matrix colour. The groundmass is very fine grained and occupies ~70% of the unit, this volume decreases with proximity to the centre of the intrusion. The groundmass (similarly to the FCR) consists of flecks of quartz, albite feldspar and orthoclase feldspar (figure 4.8a). The texture of these fine components is coarser, more subhedral and less wormy than seen within the FCR, with no direct examples of well formed myrmekite. Fine splinters of pyroxene (<= 10 μm) and albite feldspar (<= 20 μm) laths create a slightly crystalline, splintered texture to the groundmass. The unit is littered by fine specks of opaques (<<5 μm) as well as smaller volumes of quartz (~ 5 μm), amphibole, biotite, feldspar and chlorite minerals which are anhedral. The groundmass opaques and quartz are lower concentration than seen in the FCR groundmass. The groundmass also contains fine pores, mostly lining the edge of phenocrysts. Garnham (1988) presents evidence for a spherulitic texture seen within

the red felsite which aligns to the FCR's flow bands, this is not seen in this study but this may be a result of limited sample numbers.

The red felsite contains old and altered (including chlorite alteration) phenocrysts which are broken and resorbed (figure 4.8e,g). There is also large crystal size variation (<1 – 5 mm). The unit is rich in crystal aggregates which contain multiple minerals where contacts between the individual crystals seem sutured, strained or crushed. Crystals, predominantly feldspars, also often grow together to create a glomeroporphyritic texture. There are usually no signs of alignment amongst the crystals.

Albite feldspar, as well as smaller amounts of orthoclase, dominates the red felsite (>70% of total crystal content), they are occasionally tabular and are the largest crystals present (up to 5mm). Often their tabular habits are very fractured, rounded and embayed. Crystal breakage becomes clear when their twinning is truncated. Lamellae twinning is most common. Alteration, including sericite**,** is present within the feldspars, this in places becomes so extreme it can be difficult to distinguish the phenocryst from the groundmass. Orthoclase feldspars are often overgrown by the albite feldspar component of the groundmass and sometimes internally altered into albite (figure 4.8f). Occasionally feldspars are coated by a darker (in SEM) material which sometimes develops a wormy texture implying that it may be a form of myrmekite. Feldspars also often form glomerocrysts.

Opaques (10-15% of the crystal volume present) are fine (< 1mm) and tend to occur with a bimodal size distribution, either as very fine groundmass components <<10 μm, or as larger more clastic features (0.25-1 mm). Larger opaques are recognised to be titanomagnetites which display the same widmanstätten texture as seen in the FCR of ilmenite exsolution. These opaques are associated with hexagonal pyroxene crystal growths occurring within embayments or inclusions.

5-10 vol. % of the phenocrysts are quartz (figure 4.8c), up to 1mm in size. They are rounded, mostly unstrained and tend to be found in clumps. Sintered textures are seen on their surfaces, suggesting at least some are quartz xenocrysts from the quartzite, despite less evidence for extreme reactions with the surrounding groundmass. Some larger xenocrysts are embayed and some occasionally are surrounded by groundmass with a slightly wormy, graphic myrmekitic texture, but this graphic texture is much less common than within the FCR.

Biotite and amphibole are present (~5-10% total crystal volume each) up to 1.5 mm in size (figure 4.8d). They are often fractured and kinked, yet their habits are still recognisable. Amphiboles are occasionally fractured in situ along their cleavage planes. They occasionally possess inclusions and are often overgrown by the feldspar component of the groundmass. Both are commonly pseudomorphed by later chlorite alteration.

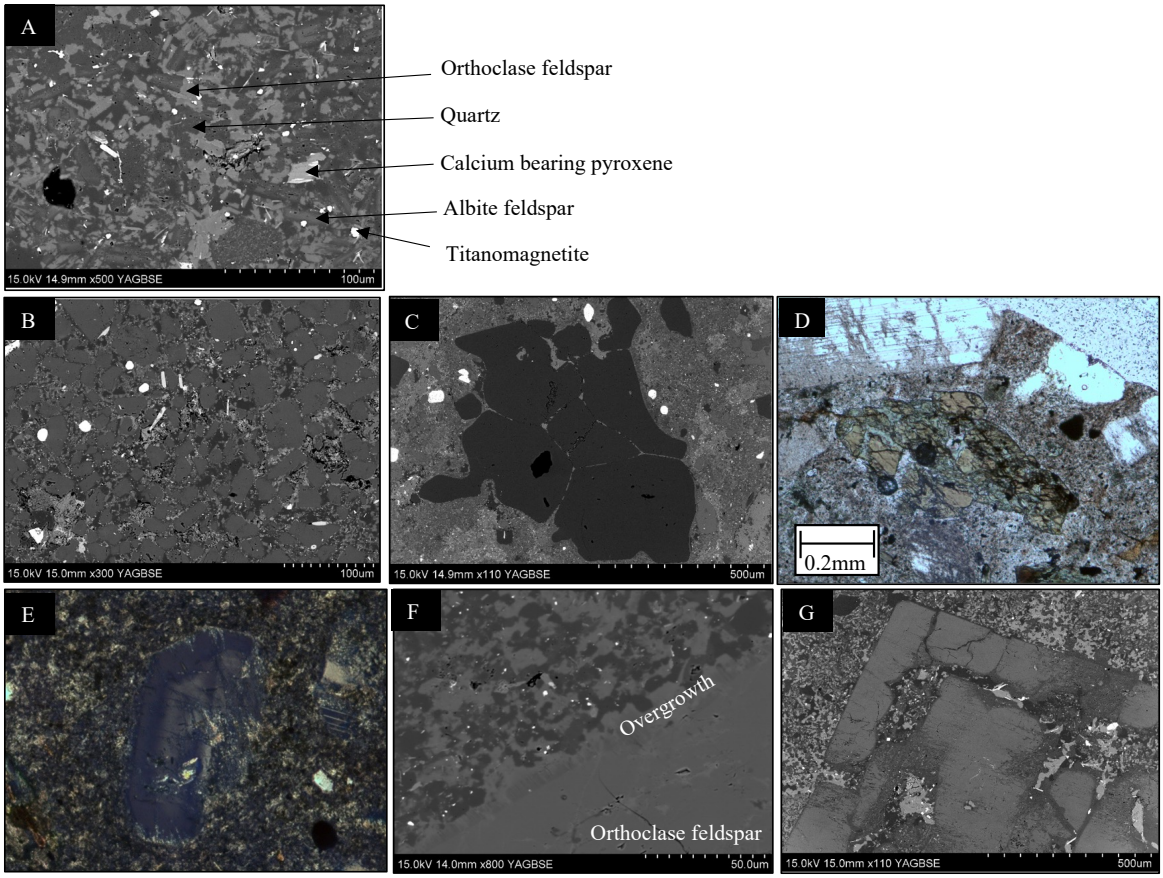

Figure 4.8a-g *Images of the red felsite to highlight its texture and mineralogy.*
(a) SEM image to portray the nature of the red felsite groundmass which contains quartz, two types of feldspar components, pores, opaques and pyroxenes. In figure (b) the intermediatory shade groundmass feldspar has formed crystals. These are taken from (a) at locality 10 and (b) at locality 8. (b) An SEM image of a finger of FCR within the red felsite, showing its crystal rich groundmass texture. The different texture of the FCR finger, which is rich in fine (50 um - 1 mm) feldspar crystals. From locality 2. (c) An SEM image of the very irregular and embayed shapes of quartz. From locality 2. (d) An optical microscope image of an amphibole crystal which has been partly pseudomorphed by chlorite and has experienced in situ fracturing, whereby the once subhedral crystal habit can be recognised. (e) An optical microscope image of a broken feldspar crystal, evident due to the cross cutting of its oscillatory zoning. This is common throughout the red felsite. Found at locality 7.(g) An SEM image of the overgrowth of a feldspar phenocryst interacting with the feldspar component of the groundmass. From sample found at locality 8. (h) An SEM image of the internal resorption of a feldspar phenocryst which occurs commonly in the red felsite. Found at locality 8.

The red felsite contains isolated pods (up to 4cm) and veins (up to 2mm wide) of FCR (figure 4.9b-c). The pods have varied shapes of which their interfingered edges and contorted edges imply liquid mixing has occurred. The pods maintain the same characteristics as FCR and often contain red felsite phenocrysts. Often, hybridisation (figure 4.9e) occurs with the FCR to produce an intermediate brown, slightly banded, quartz rich poorly porphyritic unit in places. A finger of FCR material protruding

into the red felsite is recognised to have crystalised further than the regular FCR, causing it to be rich in uniform and fine (<50 um) cubic feldspar crystals which have crystalised from the groundmass (figure 4.8b).

The second fault is a slightly simpler unit, because it contains less (still very broken) phenocrysts of which are nearly all (>80%) feldspars.

The contact between the red felsite and fault intrusion is very irregular (figure 4.9a,d): in places it is very uniform and planar aligning to the main fault, but often it is very heavily mixed and contorted. Heavy mixing has resulted in each unit containing pods of the other. The contact resembles a fused boundary (figure 4.9g). The two units have very similar appearances (figure 4.9d, f-g, figure 4.10), their key difference is phenocryst volume (greater in the fault intrusion), phenocryst breakage (greater in the red felsite) and groundmass colour (darker in the fault intrusion). Therefore, when using microscopy these differences may not be noticeable which makes the contact very ambiguous, highlighting their likeness.

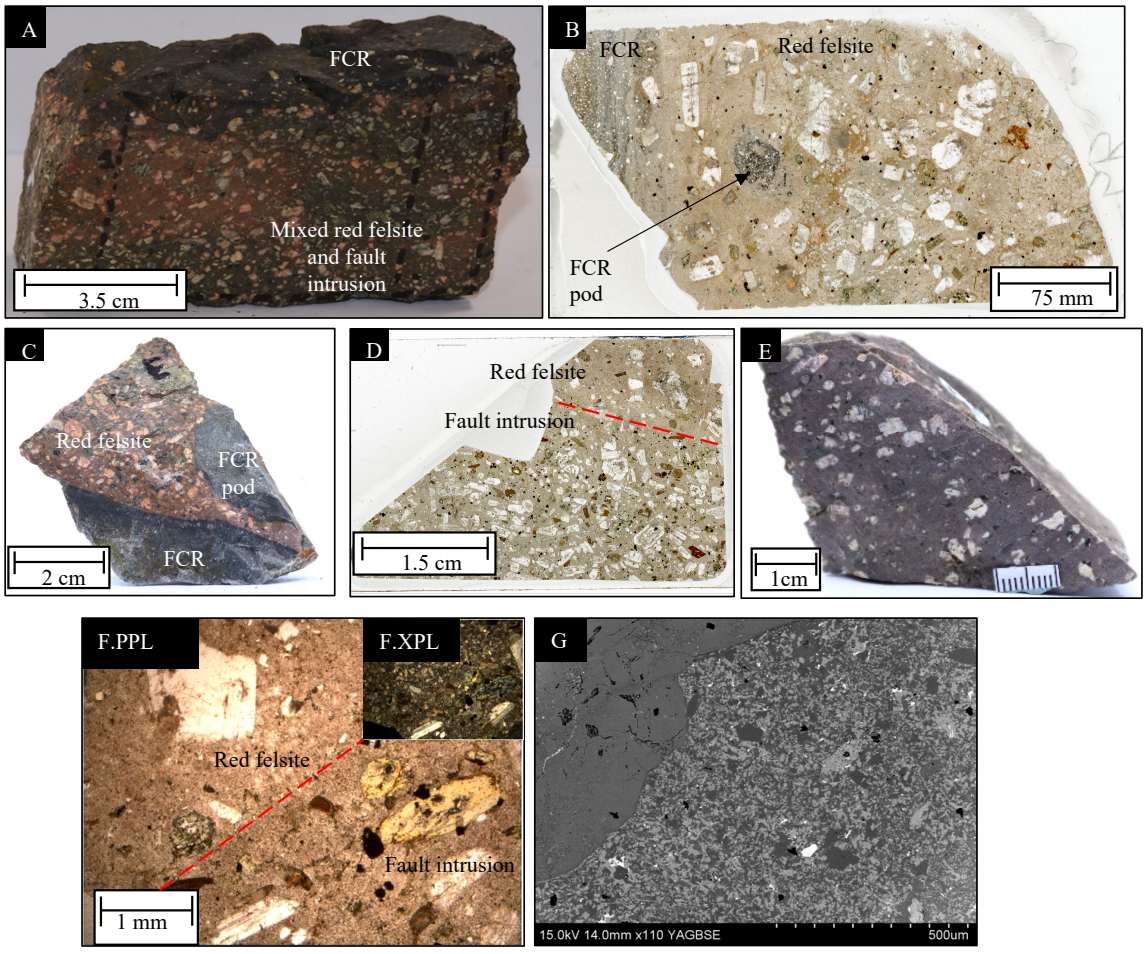

.

Figure 4.9a-g *Images of the red felsite's contact relationships with the adjacent red felsite and fault intrusion including the units inclusions of FCR pods and its contact with the fault intrusion.*
(a) An example of a sample showing the heavy mixing that occurs between the red felsite and the fault intrusion. (b) A thin section of the gradual contact between the FCR and the red felsite. The FCR has adopted some feldspar phenocrysts from mixing with the red felsite, and the red felsite contains a pod of FCR material. This is found along at the inner contact of the main intrusion, at locality 8. (c) A sample showing the inclusion of a pod of FCR within the red felsite, and the sharper contact between the two units. (d) A thin section from locality 2 showing an example of a more planar and sharp contact between the red felsite and fault intrusion. This is difficult to spot due to the similarity between the two units. (e) A sample to show the extreme mixing of the red felsite and FCR to produce a hybrid rock. (m) An optical image of the contact between the red felsite and the fault intrusion (taken from locality 2). The contact is clear due to the change in colour and phenocrysts. (n) An SEM image of the contact between the red felsite and the fault intrusion (locality 2). Here the contact is very difficult to spot as the magnification is high so the change in phenocryst volume cant be seen and the greyscale prevents colour change indicators. The best indicator of the unit change is the slight increase in fine feldspar laths within the groundmass of the fault intrusion (found on the right hand side of the images).

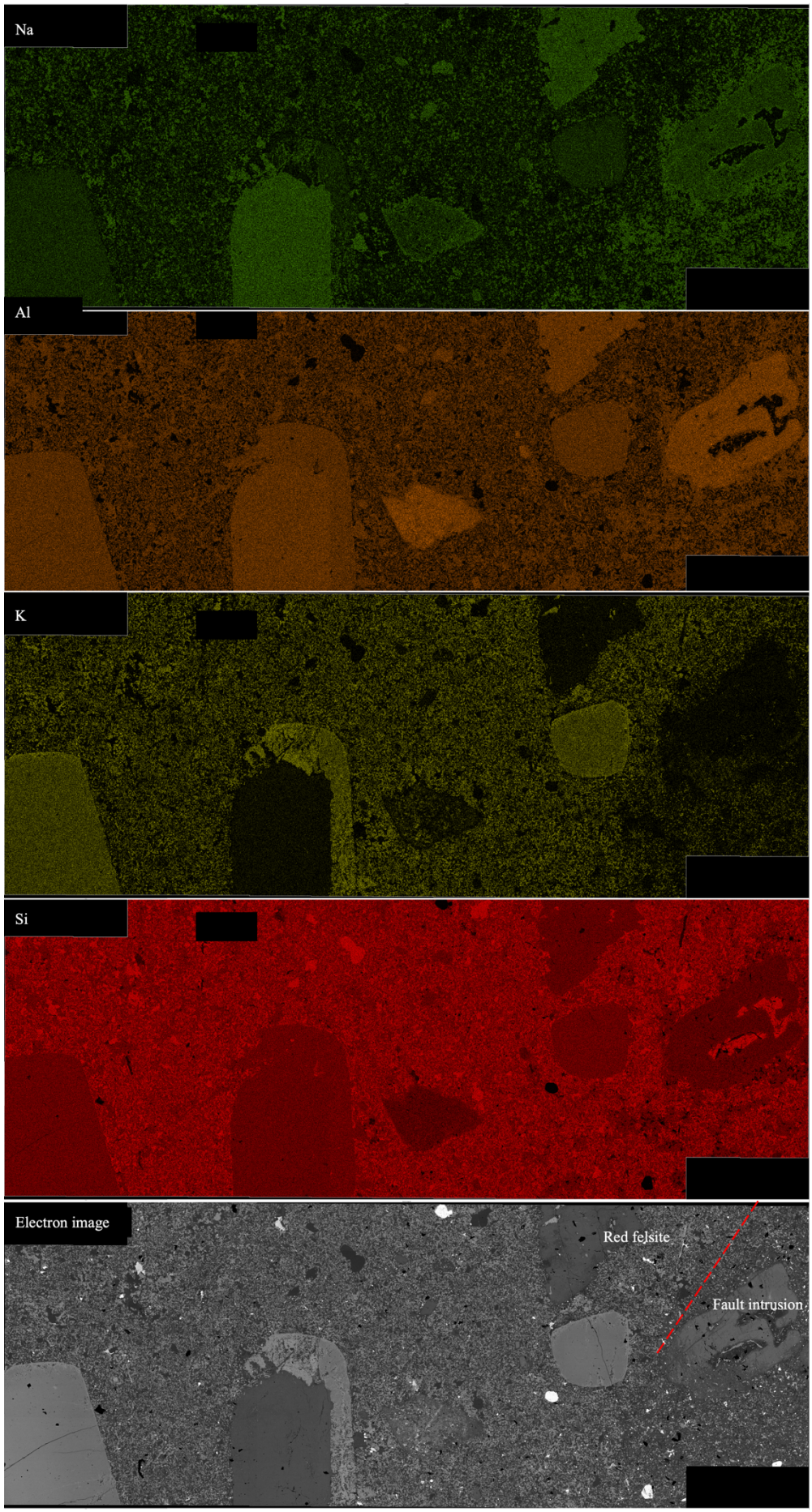
Na
Al
K
Si
Electron image
Red felsite
Fault intrusion

Figure 4.10 *An EDS chemical map to show the contact between the fault intrusion (RHS) and red felsite (LHS). The change is subtle at this scale and when using electron imagery but the increased presence of albite in the groundmass (mostly in the fine crystal form) of the fault intrusion creates the most noticeable change as it causes a darker colour and texture change with the electron image, a relative loss of potassium and increase in sodium.*

4.1.5 Fault intrusion

The fault intrusion fills the two faults that run across through Stob Mhic Mhartuin (figure 4.1). The fault intrusion is a grey glomeroporphyritic diorite-monzonite (McGarvie, 1980; Garnham, 1988) of medium-coarse crystal size (figure 4.11b, e). The groundmass is fine grained, dark grey and occupies ~40% of the rocks volume. The groundmass closely resembles that of the FCR and red felsite, consisting of fine components of quartz, albite feldspar and orthoclase feldspar, sometimes resembling myrmekite (figure 4.11f). There are fine (< 0.25 mm) albite feldspar crystals, pyroxene fibres, anhedral opaques and quartz. The proportion of fine feldspar laths are much higher in this unit than the other fault fill units. Pores are present within the groundmass, but they occupy a much smaller volume than within the red felsite.

Phenocrysts of the fault intrusion have variable sizes (1 – 10 mm) and shapes, are all fairly weathered/altered and sometimes oxidised. The crystals vary are anhedral to euhedral depending on the degree of crystal breakage. Occasionally the phenocrysts are aligned to create a flow texture within the porphyrite. Glomerocrysts are very common in the fault intrusion, consisting of feldspar crystals that have grown together. There are however a lot less aggregates in the fault intrusion than in the red felsite. The crystal rich fault intrusion displays a similar spectrum of phenocrysts as seen in the red felsite, with the exception that it's crystals are generally coarser (up to 10 mm), have better habits, and there is a greater volume of the less common mineral phases. The unit is quite variable in crystal content and colour, including occasional aphyric patches and occasional redder patches where the unit appears oxidised and resembles the red felsite. Chlorite alteration is present throughout.

The dominating (50-80% of the phenocryst volume) phenocryst phases are coarse (up to 10 mm), euhedral and sometimes fractured phenocrysts of alkali and plagioclase feldspar. Albite is the most common feldspar, and is slightly more common than seen within the red felsite. Feldspars are very often embayed, where pyroxene shards and coarse groundmass grows, They are also commonly altered, mostly by sericite. Within the embayment's of feldspars, crystalline groundmass fibres will often grow to become quite coarse. Albite feldspar overgrowths commonly coats the crystals. Feldspars are also commonly coated by a quartz rich, non-solid textured material which may be the same as the myrmekite coatings seen in the red felsite, but this is unclear.

The unit is rich (5-20% phenocryst vol.) in fine opaques (<1.5 mm, mostly titanomagnetites and calcium bearing opaques), these are slightly larger and more common than seen in the red felsite. There is a variation in sizes and shapes (from fractured/rounded and clastic, to irregular and interstitial). They are sometimes embayed or contain inclusions, and often pyroxenes are found growing within. Again, opaque surfaces also display the widmanstätten exsolution pattern of ilmenite within titanomagnetites, with very few exceptions showing other surface textures.

Biotites and amphiboles, commonly pseudomorphed by chlorite, occupy up to 5-10% and 5-15% (respectively) of the phenocryst volume in the fault intrusion. They occur up to 6 mm in size and often display recognisable habits that are however commonly fractured, sometimes embayed and occasionally kinked. They tend to occur in clusters. Amphiboles that have been fractured in situ are found both in the fault intrusion and the red felsite. These minerals commonly have overgrowths formed by the groundmass. Muscovite and pyrite also occupy a small volume (1%) of the phenocryst body, often <=4 mm.

Quartz is present at variable quantities 0-10%. Phenocrysts of quartz often resemble those also seen in the red felsite and the FCR: rounded, sintered, unstrained, and relatively small (<1 mm). This implies that some are also quartzite xenocrysts. These sometimes have very irregular anhedral shapes and are often overgrown by groundmass material.

The fault intrusion often contains large xenoliths (1cm - 3 m) of quartzite (figure 4.11a) and granite from nearby plutons. Quartzite lithics have brecciated edges where finer quartz xenocrysts break off to form the small xenocrysts within the unit. Strikingly clear when using the SEM is the large reactionary rims of these quartzite xenoliths (figure 4.11g-h). These clasts have halos of up to ~150 um which consist of myrmekite intergrowths of quartz and orthoclase feldspar. The xenoliths also have some small embayment's.

The fault intrusion is intruded by veins of the FCR (figure 4.11c-d). These veins tend to be quite planar, fine (<3 mm) and less anastomosing than those seen within the quartzite. The vein has characteristics of the FCR with the exception of being relatively poor in quartz clasts. Thin section of this sample highlights a similarity between the FCR and fault intrusion groundmass because it is very difficult to recognise amongst the unit it cuts through. Garnham (1988) observed that veins within the main intrusion seem to push phenocrysts aside, suggesting the rock wasn't brittle at the time of intrusion.

The second fault intrusion (further to the north of Stob Mhic Mhartuin, figure 4.1) is similar in appearance to the type example, however it does have some clear differences. The unit contains less phenocrysts (30-10% rock vol.), smaller phenocrysts (of which have more evidence of crystal breakage), more alignment of lithics and a more even size distribution of the phenocryst phase. Feldspars remain dominant, however chloritized biotites and amphiboles also become more common (~20% phenocryst vol. each). There are more FCR veins found within the second fault intrusion, which is closely associated to the more fractured nature of this unit.

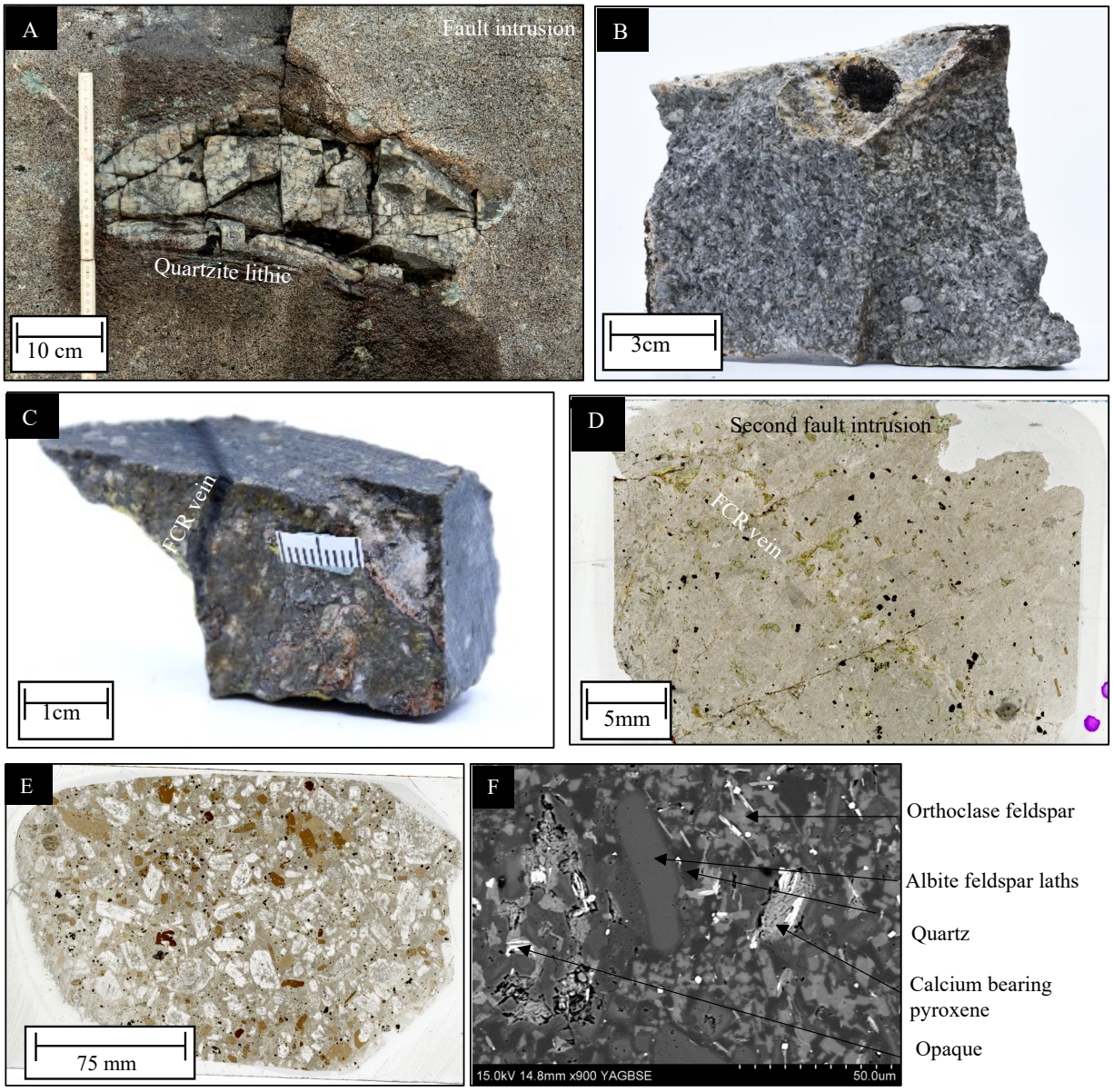

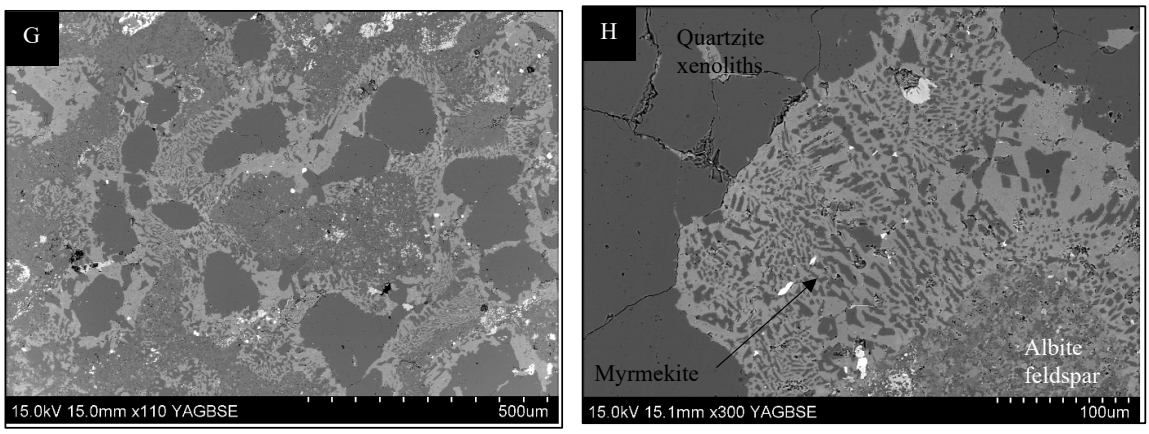

Figure 4.11 *images to show the nature of the fault intrusion at Stob Mhic Mhartuin*
(a) A field photo of the main fault intrusion with a quartzite xenolith, with evidence of original bedding. Taken at locality 6. Photo taken by Dave McGarvie. (b) A sample of (from locality 9) the main fault intrusion – a grey glomeroporphyritic rock rich in feldspars. (c) A sample (from locality 12) of the second fault intrusion containing a FCR vein which is difficult to spot amongst the fault intrusion and poor in quartz compared to the main FCR unit. This also displays a phenocryst poor example of this second intrusion. (d) A thin section (from locality 12) of the second fault intrusion containing a FCR vein. This also displays a phenocryst poor example of this second intrusion. (e) A thin section of (from locality 9) the main fault intrusion – a grey glomeroporphyritic rock rich in feldspars.(f) An image to show the contents of the fault intrusion (locality 2) groundmass at two magnifications. This is composed of quartz, albite and some orthoclase, opaque specks, and pyroxene shards. (g) SEM image of the thick myrmekite coating of quartzite xenoliths within the fault intrusion (from locality 13). (h) SEM image of the thick myrmekite coating of quartzite xenoliths within the fault intrusion (from locality 13).

4.2 Locality 2: An-t-stron

An-t-sron (figure 4.12a)is located at (NN134548) to the north west, anti-clockwise around the caldera ring fault from Stob Mhic Mhartuin (see Figure 2.1a page 23). Much of the general broad-scale features of this locality are like those described at Stob Mhic Mhartuin, but with some key differences. Namely, (1) the country rock is a more mafic pelite, which is much less rich in quartz (2) the FCR has the same appearance and composition, with the exception that there aren't quartzite lithics mixed into the unit, it does however adopt lithic clasts of the wall rock (3) more chlorite alteration has affected the appearance of units here (figure 4.12b) (4) there are more examples of veins of FCR, and the contacts of these veins appear quite brecciated and brittle (5) the fault intrusion is slightly different here (different phase distribution, lighter colour, more quartz and plagioclase), the difference in fault intrusions around the ring fault is well described by Garnham (1988) (6) the fault intrusion contains pelitic xenoliths here.

Figure 4.124a-b *images of An-t-Sron, (a) A field image of the outcrop of An-t-Sron showing the two main gullys that are clear at the top of the horizon which outline the ring fault and some outcrops closer in the image which consist of a pelite (further to the east), FCR, red felsite and fault intrusion rocks (further to the west). (b) A thin section image taken from a sample at An-t-Sron where FCR vein cross cuts and brecciated the schist. The units here are quite heavily chloritized.*

Chapter 5: Geochemistry

In this Chapter we use data from Garnham (1988) and Hickman and Wright (1983) collected via X-ray fluorescence spectroscopy (XRF) of whole-rock samples and Energy Dispersive X-ray Spectroscopy (EDS) for samples of the dominant lithologies discussed in Chapter 4. Figure 5.1 shows that the Glencoe magmatic suite straddles the alkaline-to-subalkaline trend.

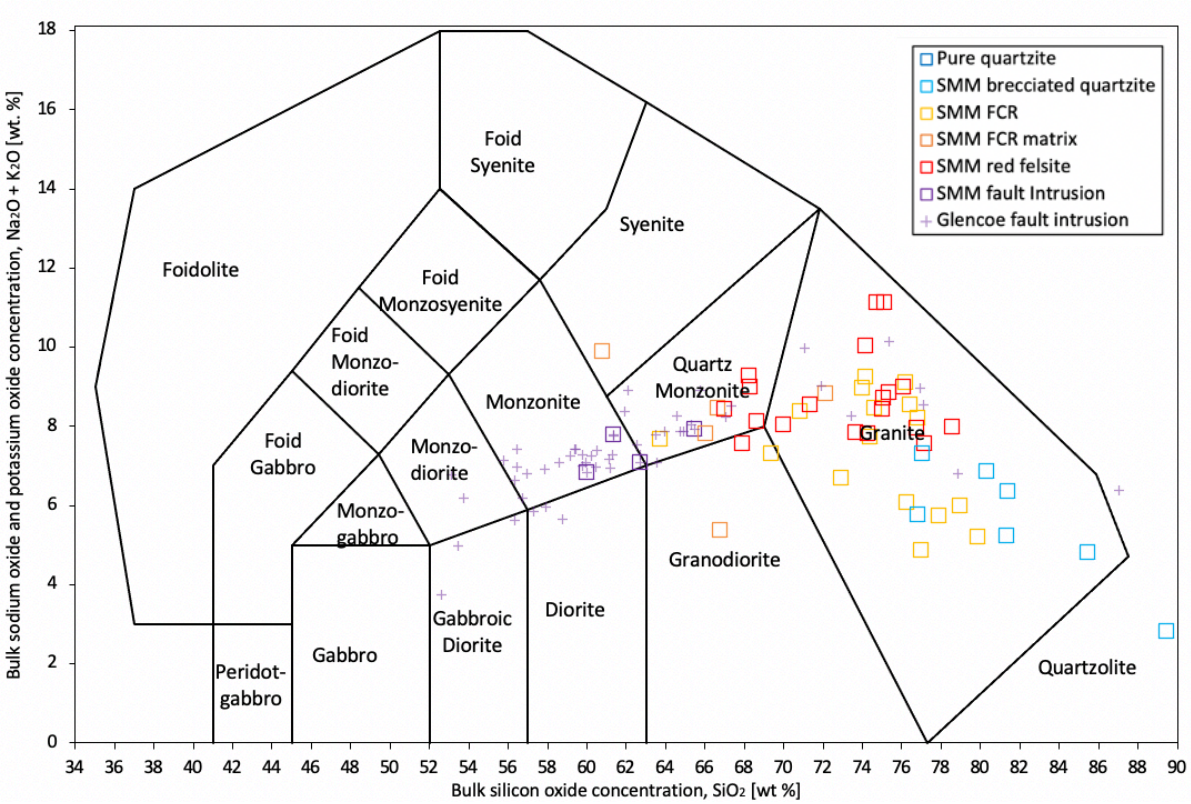

Figure 5.1 *A total alkali silica diagram to display the geochemical composition of Glencoe caldera rocks, with a particular focus on Stob Mhic Mhartuin. Results taken from (Hickman and Wright, 1983; Garnham, 1988)*

5.1 Mechanical mingling of FCR melt with quartzite

The geochemical data can be used to test if the brecciated quartzite and FCR lie on a continuum that can be explained by mechanical incorporation of quartzite clasts in the FCR matrix. To test this, we define two possible FCR end-members: (1) the mean value of the FCR measurement suite; and (2) the value with the lowest SiO2 concentration. The quartzite end member is taken from REF. The concentration C_i of any element in a mixture of the FCR matrix and pure quartzite (100% silica) is

$$C_i = C_{FCR}\theta + C_Q(1-\theta) \qquad Eq.1$$

where: subscript FCR indicates the FCR matrix end member, subscript Q indicates a pure silica end member, θ represents the fraction of the silicic end-member in the mixed magma.

The measured samples of FCR, quartzite breccia, and quartzite show broad agreement with the mechanical mixing model (figure 5.2). Remaining deviation may be due to chemical variability in the quartzite not accounted for here. Nevertheless, we conclude that mechanical mixing models are consistent with the geochemical evidence as well as the textural and field evidence (Section 4).

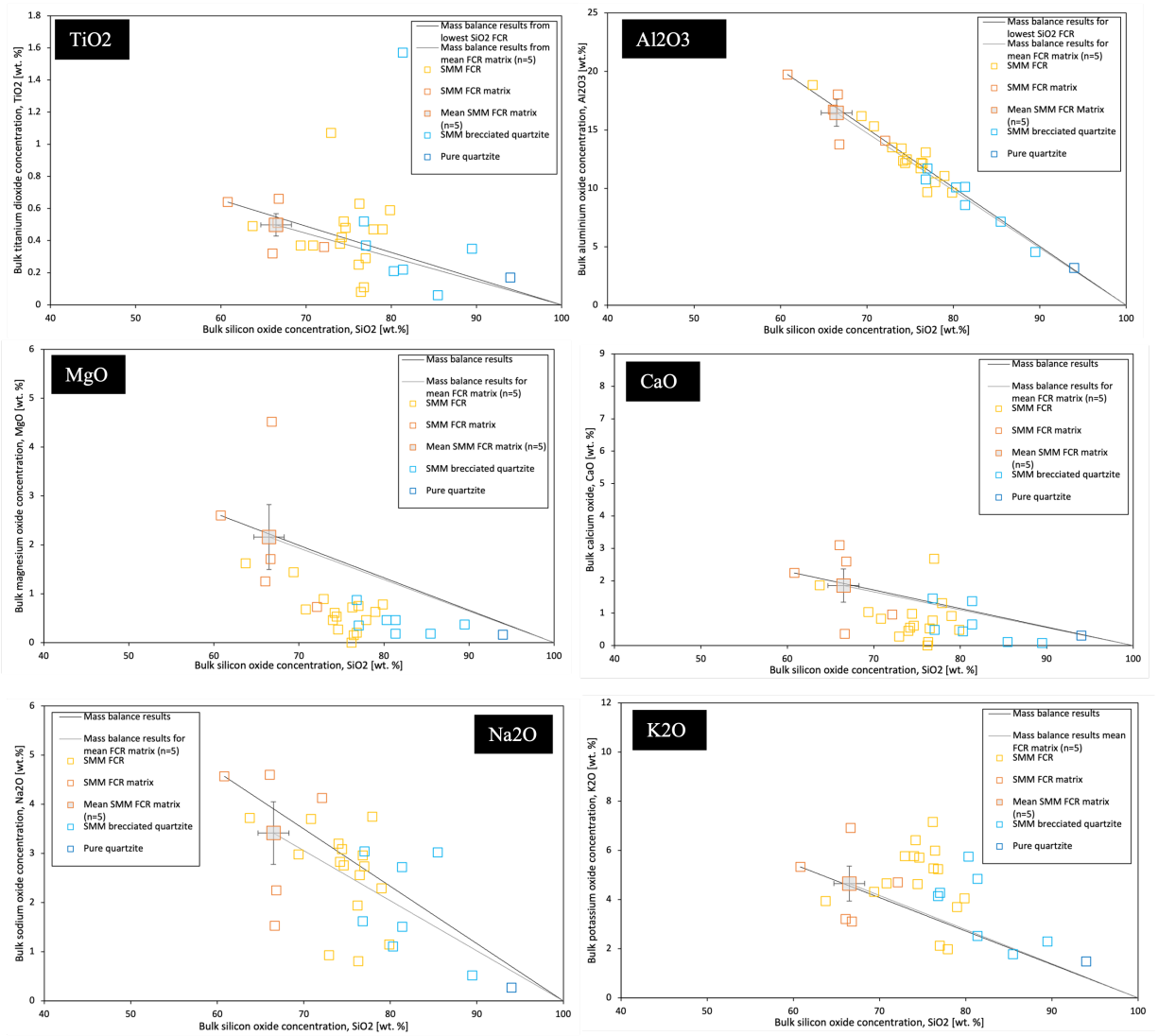

Figure 5.2a-f *Harker diagrams to compare the calculated trendline of mixing FCR matrix with pure quartzite to the samples recorded by Garnham (1988) which show a relationship between the FCR, breccia and quartzite.*

These calculations were performed to whether mechanical mixing explains the geochemical relationship between FCR, breccia and quartzite.

5.2. The petrogenesis of the FCR

The geochemical data can also be manipulated to test the similarity of the FCR to the intrusion units, thereby whether these are likely genetically related. In multiple ways the matrix of the FCR is compared to the matrix of the fault intrusion, for Stob Mhic Mhartuin and another location, to assess whether these behave in the same way.

Firstly, the composition of the phenocryst body within the fault intrusion for an array of Stob Mhic Mhartuin samples is calculated using individual mineral analyses (Table 3.1; appendix A; appendix D, Garnham 1988). This phenocryst composition is mathematically subducted from the whole unit composition (Appendix C, Garnham 1988), proportional to the phenocryst volume present (Table 3.1, Garnham 1988), in order to produce values for the geochemical composition for the fault intrusion matrix. This fault intrusion matrix composition is compared to the FCR matrix (Appendix E, Garnham 1988) in order to test their similarity, presented on an array of Harker Diagrams (figure 5.3).

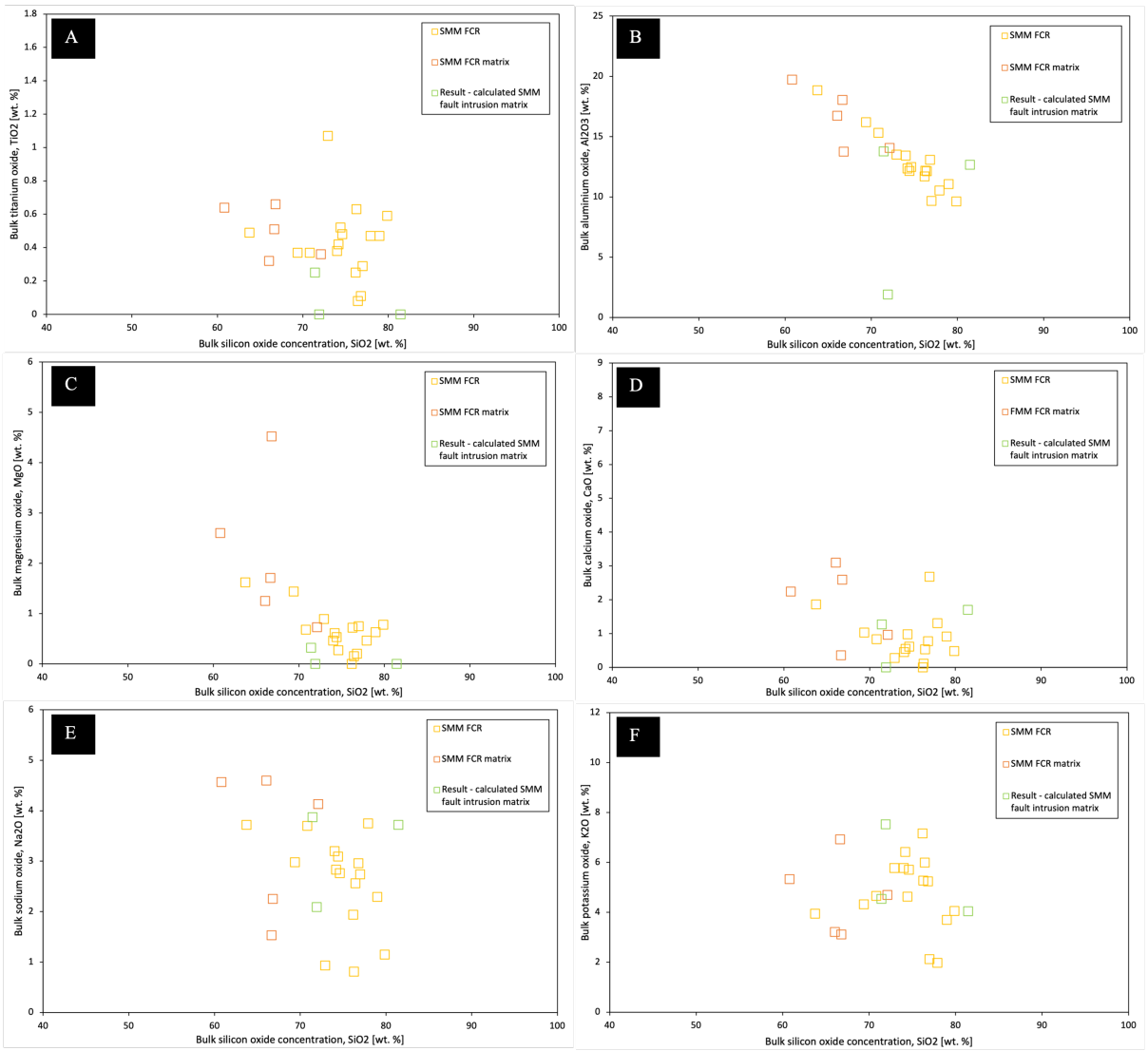

Figure 5.3a-f *Harker diagrams to compare the calculated fault intrusion matrices representative of those at Stob Mhic Mhartuin to the FCR. These calculations were performed to test the similarity of the FCR and fault intrusion matrices at the study location.*

Secondly, the similarity of the two matrices is compared by adding the composition of the FCR groundmass to the composition of the fault intrusion phenocryst body, in order to replicate the fault intrusion unit (figure 5.4). The concentration, C_i, of any element in a mixture of the FCR matrix and fault intrusion phenocrysts is:

$$C_i = C_{FCR}\theta + C_{FI}(1-\theta) \qquad Eq.2$$

where: subscript FCR indicates the *FCR* matrix end member, subscript *FI* indicates a fault intrusion phenocryst end member, represents the fraction of the matrix end member in the magma.

Due to limitations in sample recordings available, this uses fault intrusion compositions that are representative of the units present at Stob Mhic Mhartuin, but they are not direct recordings of the rocks there. This is done so that it is directly comparable to the FCR recordings which are taken at Stob Mhic Mhartuin.

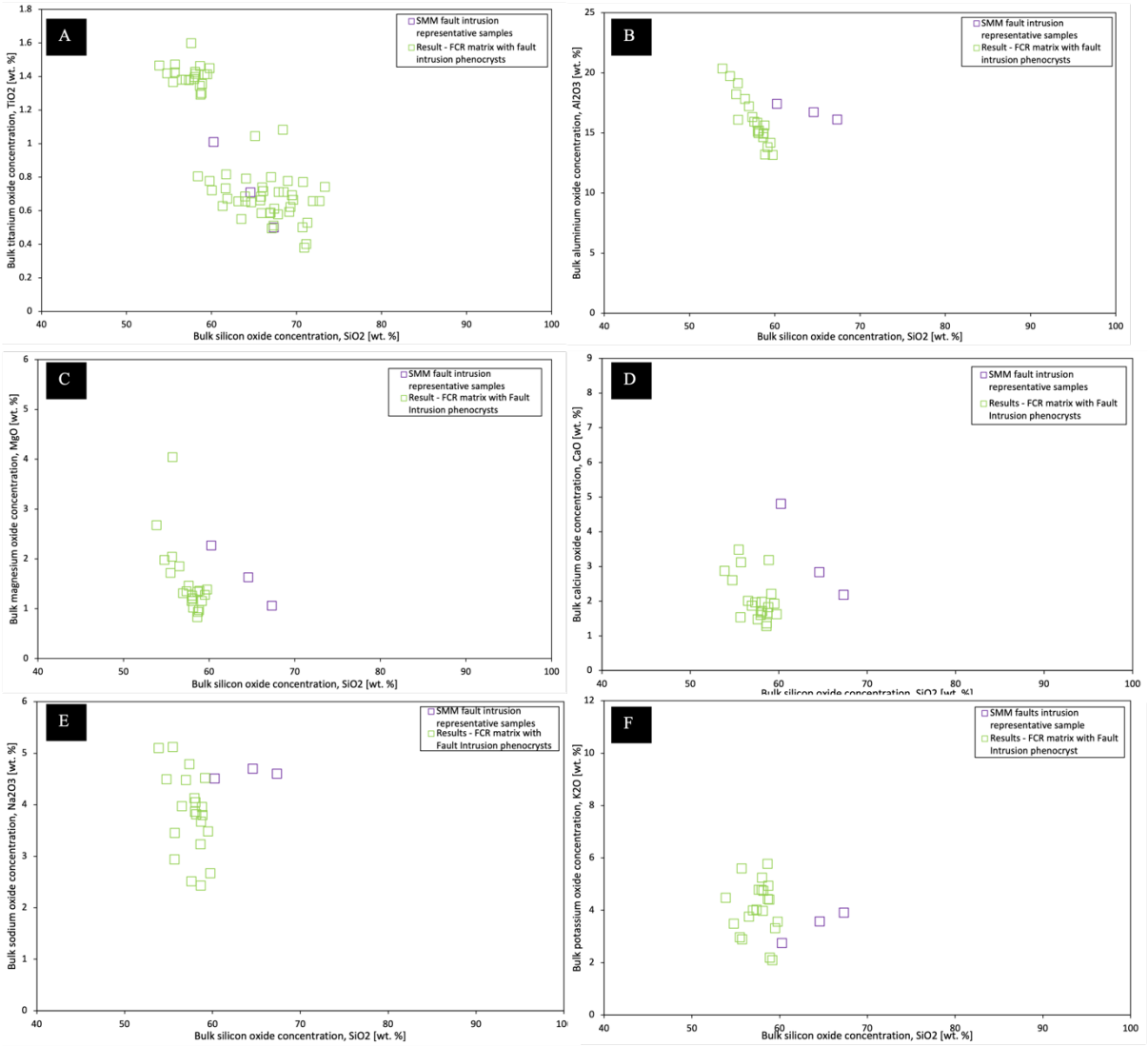

Figure 5.4a-f *Harker diagrams to compare the calculated FCR matrix mixed with fault intrusion phenocrysts, to the real fault intrusion values representative of Stob Mhic Mhartuin. These calculations were performed to test the similarity of the FCR and fault intrusion matrices at the study location.*

Due to limitations in samples available, this process is repeated for the fault fill rocks of Cam Ghleann where all the appropriate data is available for FCR and fault intrusion, in order to remove uncertainty (figure 5.5).

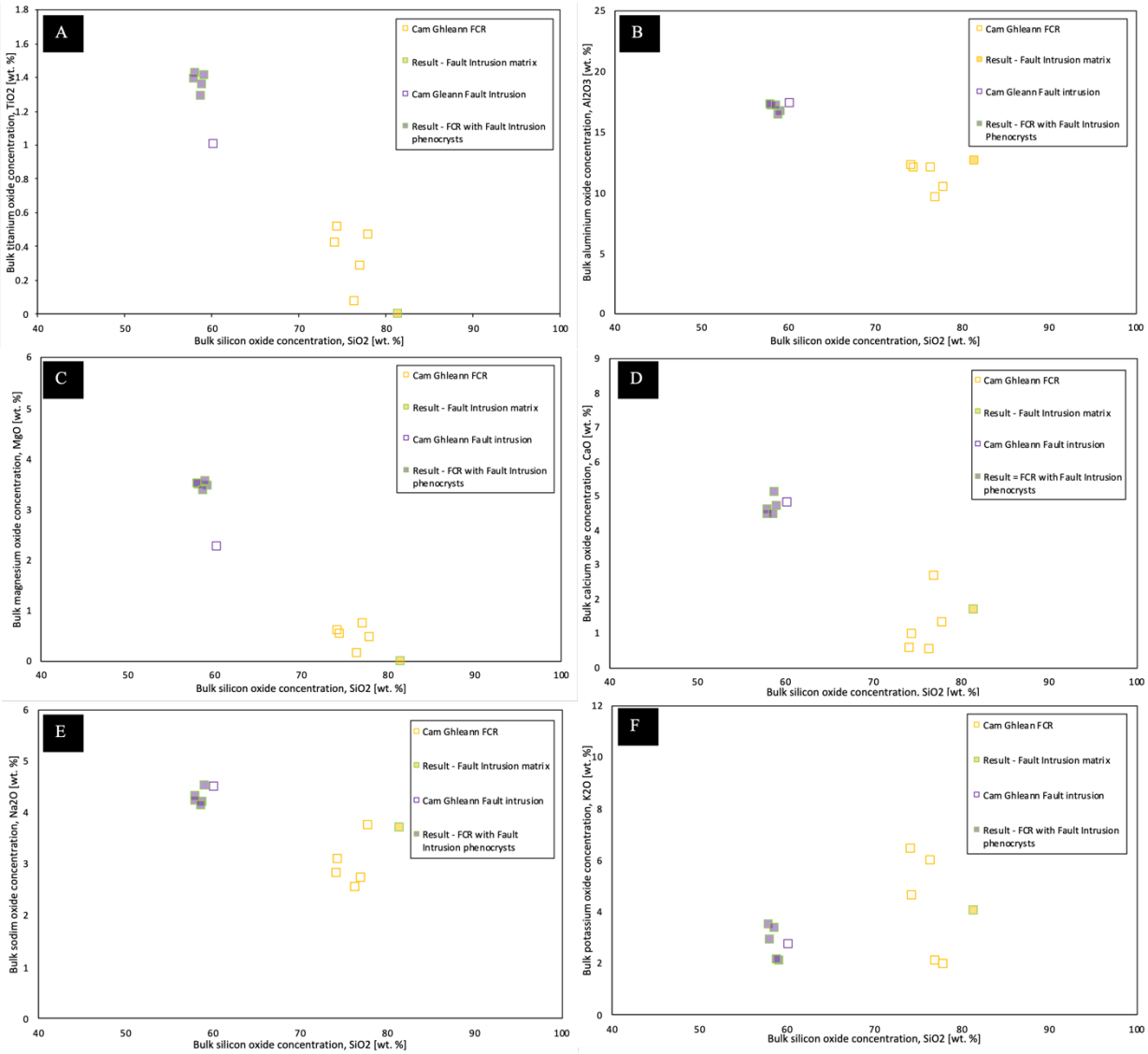

Figure 5.5a-f *Harker diagrams to compare the calculated FCR matrix plus fault intrusion phenocrysts, to the real fault intrusion values of Cam Ghleann. These calculations were performed to test the similarity of the FCR and fault intrusion matrices at a location where the available geochemical data is abundant.*

The recorded compositions of the phenocryst rich fault intrusion and the phenocryst poor (removing the presence of brecciated quartzite clasts) FCR shows similarity in the behaviour of the two unit's matrices. Replacing the matrix of one rock with the others has little effect on the units overall composition.

Whilst there is some similarity in the simulated rocks, there is a lack of accuracy in places. This variation from the trend can be attributed to: inaccuracy of measurements using old techniques;

measurements of Stob Mhic Mhartuin not having a full data set therefore requiring recordings of the same unit elsewhere; and, variability within natural rocks.
Overall, it is clear that there is a relationship in the geochemistry of the two rocks, which implies a genetic relationship/similar origin. It is very unlikely that frictional melting (hypothesis 1 stated in chapter 2) of the quartzite country rock would produce a rock with a matrix so similar in composition to the unrelated intrusions by coincidence.

Therefore, the results of chapter 5.1 and 5.2 suggest that the FCR is a unit composed of the fault intrusion matrix which has become removed and erupted earlier, and has mechanically mixed with brecciated quartzite to become silica rich. This fits well with wider knowledge of magma reservoirs, as this would suggest that the FCR is a melt extraction of liquid magma from a predominantly magma mush storage region. And knowledge of (pyroclastic) eruptions as it is common that lithic rich tuffs would form along conduit edges due to brecciation and mixing of the faulted wall rock. As well as expected variability in the results produced due to data collection and natural variability in rocks, this idea fits well with the knowledge of magma evolution. The fault intrusion is less silicic and richer in plagioclase than its preceding units (the red felsite and FCR), therefore this matches the idea it is a less evolved magma mush which was tapped later in the eruption. This is further expanded in the discussion.

Chapter 6: Discussion

This study has focused on the interpretation of the Glencoe ring fault rocks including a re-evaluation of available whole-rock geochemistry data (Chapter 5). Here, this study discusses and interprets all evidence together in order to answer hypothesis 1 and 2 set in Chapter 2. The end result of this section is a preferred model for the sequence of sub-surface events during the Glencoe eruption that is consistent with the available evidence.

6.1 A summary of novel or important observations from this study with regards to the hypothesis set in Chapter 2

The key findings from this study include (c.f. Chapter 5):

- *Variability:* the nature of the Glencoe ring fault fill units is that they are very complex and variable.
- *Fracturing, comminution and brecciation:* The outer contact of the main ring fault is less regular and planar than the inner contact. The evidence for brittle failure of the quartzite is pervasive over a long distance at the inner main intrusion contact, showing comminution through frictional sliding and grain size reduction. The brecciation distance is much shorter for the other contacts between intrusion and wall rock.
- *Mineralogy:* The FCR contains some bands which have the same appearance as the red felsite. The FCR, the red felsite, and the fault intrusion all have a similar groundmass mineralogy (quartz, feldspar, opaques) which varies mostly due to crystallinity and albite feldspar. Sampled veins of FCR within the fault intrusion do not possess banding or phenocrysts, notably there is a lack of quartz xenoliths.
- *Quartz xenoliths:* The FCR (fig. 4.7f, i), the red felsite and the fault intrusion (fig. 4.11a, b) all contain quartzite xenoliths, which are identified by their sintered surfaces and reactionary boundaries interacting with the groundmass; the FCR contains the largest proportion of these. Quartzite xenoliths within the FCR regularly contain reaction rims composed of a halo of myrmekite, a halo of pyroxene fibres, embayments, anhedral shapes, and/or, inclusions. Some quartz are embayed in all cases. Some larger quartzite xenoliths within the fault intrusion contain thick halos of myrmekite.
- *Myrmetkite:* The FCR, the red felsite, and the fault intrusion all contain myrmekite textures which are variably well developed and are found within the groundmass or coating a xenolith/phenocryst.

- *Slow cooling:* The FCR, the red felsite and the fault intrusion all contain titanomagnetites with a widmanstätten pattern on their surface which shows they experienced lamellar ilmenite exsolution which is commonly associated with rocks of intrusive bodies that experience intensive sub-solidus re-equilibriation on slow cooling (Tan *et al.*, 2016). Feldspars, quartz and biotite all show signs of overgrowths due to interaction with the groundmass material variably in the FCR, the red felsite and the fault intrusion.
- *No direct evidence of welding:* There is a lack of welding, glass and devitrification textures within the FCR, the red felsite and the fault intrusion, with the key exception of the intense flow banding (caused by shear) within the FCR. The red felsite and the fault intrusion both contain broken crystals and crystal aggregates. The FCR, the red felsite and the fault intrusion all present textures which imply they behaved as fluids at the time of mixing. The contacts between these units are all variable and contain crossover of fingers or phenocrysts. The contacts between these units can be difficult to define without the use of optical colour.
- *Mingling:* The FCR contains pods of red felsite (fig. 4.7c, d). The red felsite contains pods of FCR (fig. 4.9b, c) and fault intrusion (fig. 4.9a). The fault intrusion contains pods of red felsite. The FCR contains clasts which are derived from the red felsite (fig 4.7e; 4.9b, e). In places the FCR appears completely hybridised with either the brecciated quartzite or red felsite (fig. 4.9e). There are veins of FCR within the quartzite (fig. 4.6b, c) and the fault intrusion (fig. 4.11c, d). Quartzite xenoliths are found within the FCR, red felsite and fault intrusion (fig. 4.7f, i; 4.11a, g-h). The geochemical composition of the FCR and the fault intrusion is similar. They can numerically replace one another in mixtures containing other phenocrysts/xenoliths and still produce similar rock compositions (fig. 5.3; 5.4; 5.5). The trend in relationship of the breccia which links the composition of the FCR and the quartzite can be explained by the mechanical mixing of FCR with brecciated quartzite clasts (fig. 5.2).
- *Heterogeneities from locality to locality:* There is a difference in characteristics of the FCR and the fault intrusion of the outer ring fault, where they both tend to be simpler and more homogenous, there is also more fracturing and veining. The FCR groundmass also appears to be more clastic. The FCR is similar in appearance and composition in An-t-Sron despite the distance between localities and the difference in composition of country rock (quartzite for Stob Mhic Mhartuin, pelite for An-t-Sron). The FCR is less silicic than the quartzite but more silicic than the intrusion rocks at Stob Mhic Mhartuin.

In what follows in this Chapter, the observations summarised above are drawn upon first, to test hypotheses, and second, to underpin a unified model for the emplacement of these rocks during eruption. Underlying the complexity and variability at Glencoe there must be order and process.

6.2 Testing hypothesis 1 – "The FCR is a frictional melt, as stated by the previous researchers Clough, Maufe and Bailey (1909); Bailey and Maufe (1916, 1960); Kokelaar and Moore (2006); Kokelaar (2007)."

6.2.1 Support for hypothesis 1

The frictional melting hypotheses for the origin of the Glencoe FCR is favoured by many authors who have studied Glencoe (Clough *et al.,* 1909 Bailey and Maufe, 1916, 1960; Kokelaar and Moore, 2006; Kokelaar, 2007). Notably, Kokelaar (2007) supported the frictional melt hypothesis with theoretical additions in order to explain certain features, such as the idea the FCR has been blasted upwards into a fault cavity (Figures 2.2b & 2.2c) and suggested it provides evidence for the presence of caldera 'superfaults' (Spray, 1997).

Support for the frictional melt theories can be found both texturally and mineralogically. The FCR has characteristics closely resembling a typical pseudotachylyte – it is a dark, fine, cohesive, aphanitic rock. The quartz rich nature of the rock, as well as its heavily mixed relationship with the quartzite, implies that these rocks are closely related, something that would be expected if the quartzite was a protolith for the frictional melt. Furthermore, the reaction textures of the quartz clasts that litter the unit show embayments, reaction rims and irregular shapes, implying that these clasts have undergone some physiochemical change which suits the rapid, high strain, high temperature, melting that occurs within frictional melts. It is also noted through fieldwork by authors supporting this theory that where the ring fault juxtaposes volcanic or sedimentary rocks on its inside contact against Dalradian metasedimentary rocks on the outside, neither the FCR nor the red felsite is present (Garnham, 1988). This pattern implies a genetic relationship between the fault's wall rock and the occurrence of these units (despite the relationship of the red felsite to the wall rock being unexplained). Additional to field and textural features, the geochemical graphs shown in Figure 5.1 and figure 5.2 highlight the trending similarity between the quartzite, brecciated quartzite and FCR. This further indicates a close relationship between the units, which may be interpreted to show a non-equilibrium frictional melting trend. Along with the difference in geochemistry of the FCR to the adjacent intrusions, all these features of the FCR have been used as support for the frictional melt hypotheses.

The superfault hypothesis for the FCR is also supported in work outside of Glencoe. The idea originates from the work of Spray (1997) who provides a mathematical explanation for why they believe frictional melting along caldera ring faults is possible and likely. Han *et al.*, (2019) developed this idea with more mathematical and experimental explanation, concluding that frictional melts are an important part of the caldera collapse processes. Also, along with Kim *et al.*, (2019) they provide

a new field example of what they believe to be a caldera fault pseudotachylyte. This work finds a unit closely resembling the Glencoe FCR in Jansang Caldera, Korea. Their work uses textural characteristics of the unit as well as its geochemical similarity to the wall rock to conclude that this unit is a pseudotachylyte which was formed coevally or near coevally to the adjacent ring intrusions, therefore supporting the superfault theory of Spray (1997) and Kokelaar (2007).

6.2.2 Problems with hypothesis 1

Despite the evidence for the frictional melt hypothesis, both for authors studying Glencoe (Clough, Maufe and Bailey, 1909; Bailey and Maufe, 1916, 1960; Kokelaar and Moore, 2006; Kokelaar, 2007), those looking at other field examples (Kim *et al.*, 2019) or those considering caldera dynamics more generally (Spray, 1997; Han *et al.*, 2019), this study has revealed a wide range of flaws in applying this hypothesis to Glencoe. Since research of the Glencoe ring faults, there have been numerous advances in the scientific understanding of calderas and frictional melts. Here, this new knowledge is applied to the frictional melt hypothesis, to explain several new theoretical flaws in the model.

All explanations of frictional melting along caldera superfaults (Clough, Maufe and Bailey, 1909; Bailey and Maufe, 1916, 1960; Spray 1997; Kokelaar and Moore, 2006; Kokelaar, 2007; Han *et al.,* 2019) rely on the fundamental idea that caldera ring faults experience very large displacements (≥100 m) occurring during a single-slip event at seismogenic velocities (>0.1 m/s). However, the recent work of Kokelaar and Moore (Moore and Kokelaar, 1997, 1998; Kokelaar and Moore, 2006) at Glencoe has shown that (a) significant collapse at Glencoe did not occur along the caldera ring faults (i.e. through graben-controlled slip and through ductile downsag instead) (b) collapse was piecemeal by nature, occurring along multiple crustal blocks and faults (c) collapse occurred incrementally (figure 1.4 page 15, 6.1). Additionally, there is also growing evidence for examples outside of Glencoe for the slow, stick-slip nature of caldera collapse. For example, Gudmundsson *et al*., (2016) provides evidence of the recent caldera collapse of Bárdabunga volcano (Iceland) which experienced maximum fault displacements of only 1.4 cm/day. Therefore, this study uses this knowledge of Glencoe slip dynamics to highlight that friction caused by collapse was distributed over space (across many faults and grabens) and time (through slow or incremental slip). Hence, this contradicts the idea of sudden catastrophic caldera slip events, which suggests the likelihood of friction building enough to melt a rock is unlikely. Furthermore, in such a system where friction is distributed across many faults, it would be unusual for no frictional melting to occur along the other (non-intruded) faults in the piecemeal caldera.

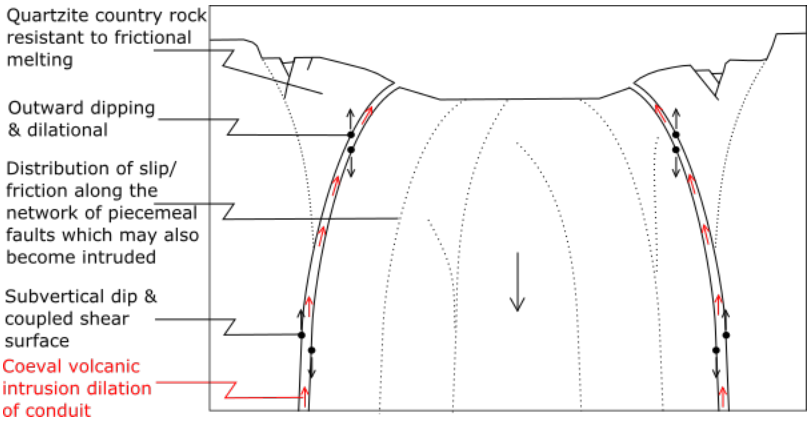

Figure 6.1: *A schematic diagram to show the theoretical problems with the frictional model for producing the FCR, due to dilation of the fault surface (due to the outward dipping ring faults and the intrusion of volcanics), the piecemeal slip structure distributing the friction across multiple fault surfaces, the incremental slip structure not allowing friction to build as high and the present of a quartzite country rock (at Stob Mhic Mhartuin) that is resistant to frictional melting.*

Recent work has led to the consensus that caldera ring faults dip outwards or near-vertically at depth (which is supported by measurements of the Glencoe ring fault planes in the field) (Kennedy *et al*., 2004; Cole *et al*., 2005; Acocella, 2007). Application of this structural configuration to caldera collapse suggests that slip motion is inherently dilational or at low normal stress under simple-shear (backed by the work of Holohan (2015) who states that the presence of brecciation of the host rock at the dyke margin of Glencoe is evidence of faults form in simple shear) (figure 6.1). Therefore, the Glencoe ring faults fundamentally lack the normal stress or horizontal compressional pressure that is required to build heat through friction in order to produce a pseudotachylyte (instead their motion creates a void).

Further developments in the understanding of calderas show that they are likely to form through reservoir under-pressure which triggers the downwards movement along ring faults (Roche, Druitt and Merle, 2000; Torres-Hernández *et al.*, 2006; Acocella, 2007; Stix and Kobayashi, 2008; Cashman and Giordano, 2014; Geyer and Martí-, 2014; Browning and Gudmundsson, 2015; Kennedy *et al.*, 2018; Geshi *et al.*, 2021). It is also believed that volcanism at Glencoe pre-dated ring fault collapse, with evidence that the ring fault intrusions were emplaced prior to and simultaneously with ring fault slip (Garnham 1988; Moore and Kokelaar, 1997, 1998; Kokelaar and Moore, 2006). This understanding for the sequence of events shows further evidence that the ring faults behaved as conduits (which are inherently dilational due to the widening created by magmatic products) prior to significant slip, again meaning that when slip does occur there is not enough normal pressure (hence friction) between their un-coupled surfaces to produce a pseudotachylyte.

New research by Di Toro and colleagues (Goldsby and Tullis, 2002; Di Toro *et al*., 2004; Di Toro *et al.*, 2011) has shown the inability of quartzite to form a frictional melt. This is due to an alternate dynamic weakening mechanism that occurs due to the formation of thin layers of silica gels on fault surfaces, which progressively reduces the frictional resistance (extrapolated to zero friction at slip rates of ~1 m/s) with increasing slip velocities. Since this work, subsequent authors (Lee *et al*., 2017) have tried to prove the ability of quartzite to melt, their work has managed to frictionally melt quartzite, but this has only been achieved through very specific laboratory context with extremely high slip rates, normal stresses and subsequent temperatures, which is unrealistic for Glencoe. The country rock at Stob Mhic Mhartuin and a significant portion of the Glencoe ring fault where FCR is present is quartzite, therefore applying this new knowledge of pseudotachylytes further highlights the problems with natural occurrences of country rock frictional melting at Glencoe to produce the FCR. Using the new model of Kokelaar (2007) it might be argued that the frictional melt protolith came from elsewhere with a less silicic country rock. However, this alternate suggestion remains a weakness in the superfault hypothesis because it would suggest an unknown, unseen protolith.

Understanding of pseudotachylytes has improved significantly since the origin of the frictional melting hypothesis. Pseudotachylytes are known to occur up to thicknesses of 10 cm, however this is very uncommon, as 75% of them have thicknesses ≤2.5 cm (Sibson and Toy, 2006). The FCR in comparison has widths of 2–14 cm lining both sides of the intrusion, therefore the total cumulative width of the FCR along one fault is much greater than even the most extreme known cases of pseudotachylytes. Furthermore, if the FCR is a frictional melt it must be assumed that this is not the total width of the melt that was once present, as the passing of sustained and high energy volcanic material travelling through the ring fault conduit would erode this unit down. Psuedotachylytes of such sizes are unknown even with modern day advances in research, hence it is questioned that these dilational to shear regime faults with a quartzite protolith is where such extremities would be found.
The textural characteristic of the FCR also does not align with modern day knowledge of pseudotachylytes, a frictional melt would expect to have: some crystal alignment; no gradual zones of cataclasis; strong signs of strain within the clasts (such as undulose extinction), and a uniform clast distribution with no anomalously large clasts. None of these characteristics are seen. Signs of spherulites and glass may also be expected for pseudotachylytes but the lack of these are not used as evidence against the frictional melt theory as it is unlikely these would survive considering the age and levels of alteration of the unit.

A key issue with the model is a lack of consideration for spatial-temporal sequencing of events along caldera ring faults, something that is now better understood. As well previously described issues, there is not a clear explanation for the presence of FCR veins within the fault intrusion. Without complex

dynamics of when each unit may be solidified and when a frictional melt may still maintain energy to inject into a nearby unit, there is no plausible reasoning behind this.

A striking problem with the frictional interpretation of the FCR is its petrology with respect to finding a protolith. Additional to the new work of Di Toro highlighting the inability of quartz to frictionally melt (Goldsby and Tullis, 2002; Di Toro *et al*., 2004; Di Toro *et al.*, 2011), the geochemical studies of Garnham (1988; figure 5.1, 5.2) show that the FCR is not the same composition of the quartzite. Whilst frictional melts do not always produce identical compositions to their host (because the melting is out of equilibrium) they are usually very similar (Magloughlin and Spray, 1992), especially with the case of a quartzite which has such little elemental variation (near 100% SiO2). Therefore, it is difficult to explain the frictional melting of the quartzite to produce the FCR, or anything other than a near 100% SiO2 composition unit, as the unit would be composed of elements that must originate from elsewhere. This problem is highlighted in EDS compositional maps of the contact between the FCR and the quartzite (figure 4.5 page 46), as there is a sudden introduction of elements (aluminium, potassium, sodium, as well as smaller concentrations of titanium, calcium, iron) within the FCR that do not exist within, therefore cannot have originated from, the quartzite. As well as the weakness with identifying an alternate unknown frictional melt protolith, another difficulty arises as the FCR maintains a similar appearance and composition throughout the originally ~8 km diameter ring fault (Garnham, 1988) despite changes in wall rock composition. Therefore no unit present at Glencoe can be proposed to occur across this widespread region, or, that would be capable of travelling the great distances across caldera when melted. Additional to providing no suitable protolith, the Kokelaar (2007) hypothesis becomes very complex, creating a sequence of events improbable to occur in nature so commonly across this one large ring fault as well as at other calderas worldwide. There are also some ideas in the complex story which might be questioned, such as: is ~3.5 km depth (current level exposure for Stob Mhic Mhartuin; Garnham, 1988) too deep for the presence of an aquifer? Is ~3.5 km depth too deep for water to be able to suddenly flash into steam to excavate a cavity? Would the presence of a water rich environment reduce the likelihood of frictional melting due to reduction in normal stress and pore fluid pressurisation as an alternate dynamic weakening mechanism?

This study finds that the frictional hypothesis suggested by Clough *et al.,* (1909) and Bailey and Maufe (1916, 1960) as well as the newer adaption by Kokelaar and Moore (2006) and Kokelaar (2007), has been shown to be theoretically implausible due modern improvements in knowledge of both calderas and pseudotachylytes. There are fundamental spatial-temporal and petrographic issues with the model, as it does not (1) consider the low normal stress and friction along the fault surfaces as a result of dilational (due to fault motions and intrusion), distributed and incremental slip (2) provide a suitable protolith for frictional melting (3) explain the unlikely withs, textures and distributions of the FCR as a pseudotachylyte. Due to a wide array of theoretical, geochemical and

textural problems the FCR cannot be a frictional melt, consequently, this study rejects hypothesis 1 introduced in chapter 2 of this thesis, and does not find any evidence that the Glencoe caldera ring fault experienced high enough slip velocities and consequential frictional melting to be considered a superfault (Spray, 1997).

6.3 Hypothesis 2 - The ring intrusions (the FCR if hypothesis 1 is proven wrong, the red felsite, and the fault intrusion) are pyroclastic. These represent the order of volcanics to travel up the conduit, in pyroclastic form. Therefore suggesting that calderas erupt large volumes of ignimbrites in wide conduits until the very end of their extrusive activity travelling through their ring faults, and that fragmentation occurs below a depth of 3.5km (current level exposure depth estimation taken from Garnham 1988).

Following the conclusion to reject hypothesis 1, this section now deals with the 3 main ring fault fill units found at Stob Mhic Mhartuin (the FCR, the red felsite, and the fault intrusion) in order to assess their accordance with hypothesis 2. The reason for this process is that hypothesis 2 is not an established theory, henceforth it needs elucidating in a different manner.

6.3.1 The FCR

In order to provide an alternate model to explain the emplacement of the FCR, this study investigates the possibility that the FCR is a welded product of primary magma fragmentation (often called a fragmented tuffisite), an idea originally proposed by Reynolds (1956) then later supported by Roberts (1966), Taubeneck (1967), and Garnham (1988).

The fragmented volcanic FCR hypothesis aligns with both the spatial and temporal understanding of overall caldera dynamics. As described in chapter 1, ring vents are known produce large volumes of sustained pyroclastics during a caldera-forming eruption *(Branney and Kokelaar, 2003; Brown et al.*,2012; Devenish, 2013; Costa *et al*., 2018). At Glencoe there are known deposits of intra-caldera volcanic rocks of approximately 1.3 km thickness (Kokelaar and Moore, 2006) (this means a minimum volume of 85 km^3 of volcanics was produced at Glencoe, for context, this is much larger than the 1.8ka caldera-forming eruption at the Taupo Volcanic Zone, one of the biggest quaternary caldera volcanoes, which produced only 35 km^3 products (Wilson *et al.*, 2009)). Without this model their voluminous and long-lived transport through the subsurface would otherwise not be accounted for in the exposed system seen today. Due to the high energy of such explosive eruptions it is expected that the majority of ash would travel to the surface, however it is likely that small volumes of ash would aggregate and stick onto the fragmented conduit sides. This model therefore explains the

likelihood that most products would not stick to conduit edges due to the shear energy of eruption, resulting in a relatively small FCR compared to the volume of ignimbrites deposited at the surface.

Calderas are fed by zoned reservoirs of crystal magma mushes and liquid magma (Bachmann and Bergantz, 2008; Parmigiani et al.,2014; Bachmann and Huber, 2016; Wilson *et al*., 2021). This similarly fits the volcanic hypothesis for the FCR because the ring fault fill therefore displays the progressive tapping of deeper, more crystal rich magmas as the Glencoe eruption evolved over time. Therefore, the outermost fill unit, the FCR, marks the crystal poor magma which is preferentially erupted at the start of a volcanic eruption to produce the large ignimbrites and fall deposits found at the surface. Whereas the central fault intrusion fill represents the final products entrained into the conduit during an eruption, due to its more crystal rich content making it resistant to movement. Overall, this hypothesis accounts for the long-term progression of events that occurs during caldera-forming eruptions and allows for all stages that occur (faulting, explosive voluminous ignimbrite eruptions, later tapping of deeper magmas) within the ring fault transport system to be represented in the fill and structure.

The appearance of the FCR matches the lithic rich tuffs that are expected to occur along the edges of pyroclastic conduits due to vent erosion (Díaz-Bravo and Morán-Zenteno, 2011; Szemerédi *et al.*, 2020). Vent erosion is an iterative process in the eruption of ignimbrites, explaining why subsurface lithic fragments taken from the conduit walls are such a large component in surface pyroclastic deposits (Wilson, *et al.,* 1980). The fracking of conduit walls by highly explosive gas and ash which then subsequently aggregates to the walls is a process known to occur in the subsurface volcanic transport system (Wadsworth *et al.*, 2020). The sheared brecciated quartzite present at the contacts of the ring fault intrusion at Glencoe occurs as a consequence of the shear stresses exerted on the wall rocks during the explosive fragmentation process of the entrained system onto the heated wall rocks (Wiebe *et al.*, 2021). The existence of this microbreccia along the outer intrusion contact at Stob Mhic Mhartuin, where brittle deformation cannot occur due to brittle stresses as the down fault block falls away from it, shows that such signs of brittle strain are a result of the gas fracking process (Roberts, 1966). As well as the presence of lithic rich FCR and sheared quartzite microbreccias, the fracturing of wall rock caused by the high energy pyroclastic eruption also explains the asymmetrical wall rock contacts seen at Glencoe.

The process of fracturing is driven by gas pyroclast mixture overpressure which opens tensile fractures in the country rock. This natural may be understood as physically analogous to fracking processes in an industrial context. It is by this same natural fracking process that FCR veins seen projecting into the quartzite. The quartzite fragmented entrained into the fluidised FCR have become rounded by attrition. The outer intrusion contact studied at Glencoe is highly irregular compared to

the planar inner contact seen at Stob Mhic Mhartuin. This can be explained by the outward dip of ring faults at calderas such as Glencoe. The high energy pyroclastics travelling through the conduits would travel vertically, therefore repeatedly hitting the outer side of the vent to create an askew thalweg. This causes asymmetrical erosion and widening with irregular brecciation of this side.

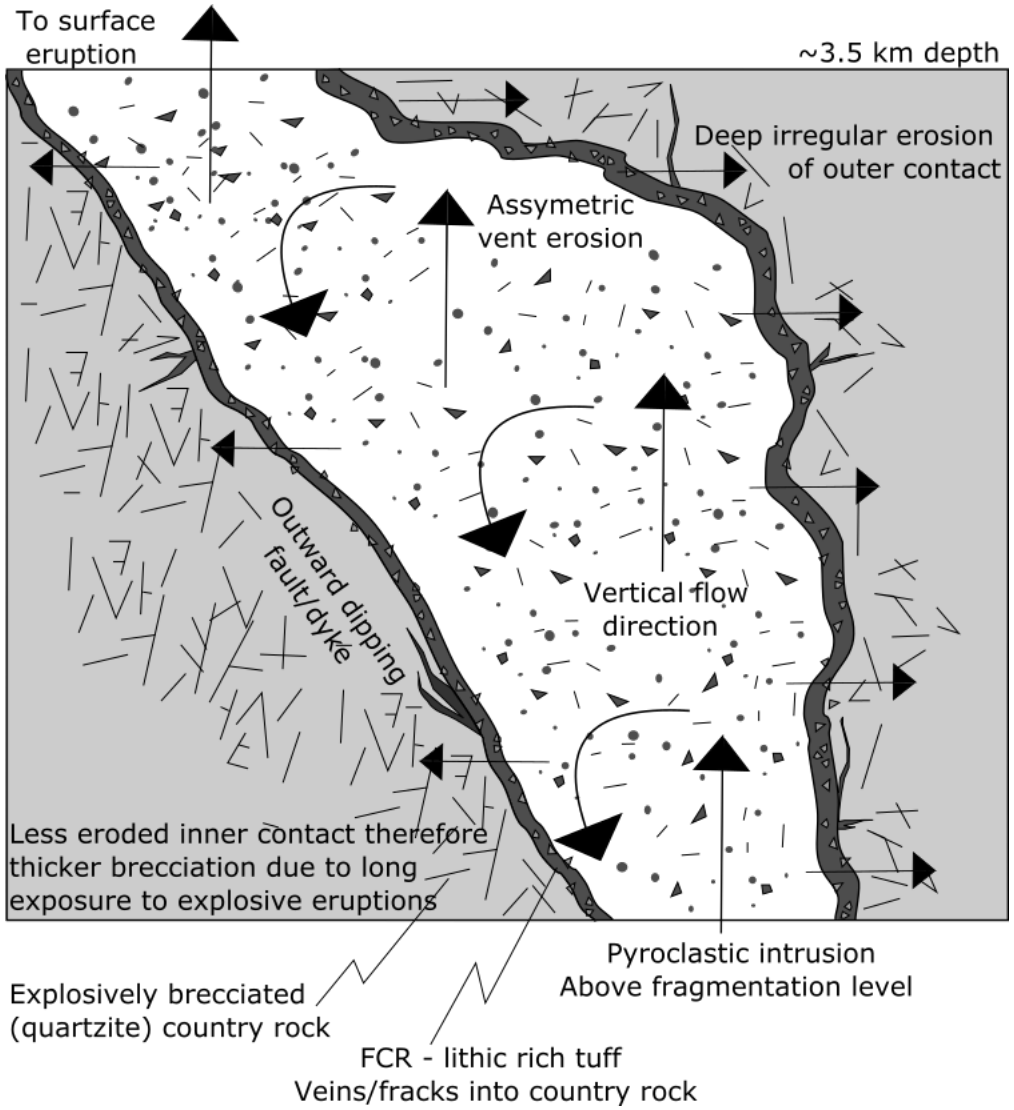

Figure 6.2 *A schematic diagram of a ring fault dyke which has been explosively intruded by fragmented magma resulting in the fragmentation of wall rock and the creation of a lithic rich tuff due to the deposition of some pyroclastics on the conduit wall which have mixed with the brecciated wall rock. Adapted from* (Kokelaar, 2007)

The reactionary behaviour (such as myrmekite, pyroxene splinters and crystal embayments) (figure 4.7 G-J) regularly displayed by quartzite xenoliths within the FCR provide another indicator that the quartz has been mechanically added to the matrix henceforth is reacting to the change in chemistry and temperature. This has been further investigated to find an explanation for this characteristic. The texture can be explained through a haplogranite ternary diagram. This graph shows that the FCR matrix is relatively undersaturated in silica. Consequently, the mechanical addition of silica rich

quartzite (described to be a result of volcanic fracking and erosion above) would inevitably cause the resorption of material into the groundmass. Furthermore, some resorption textures are also seen within the ring intrusions, which is also supports that this cannot be an indicator of a non-volcanic origin. The reaction rims of the fault intrusion xenoliths pictured in 4.11g-h are much bigger due to the even more mafic composition of the unit.

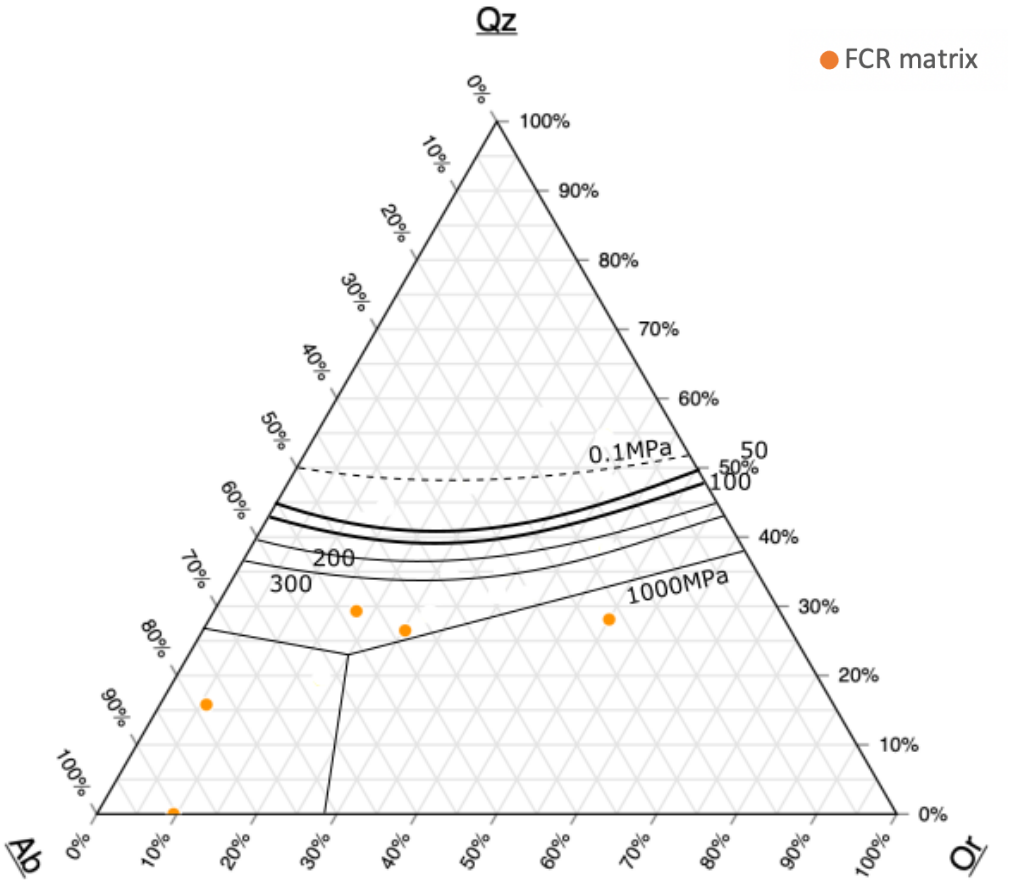

Figure 6.3 *A ternary haplogranite plot which demonstrates the silica undersaturation of FCR matrix, therefore explaining the reaction structures seen surrounding silica rich quartz xenoliths that have become mechanically added to the matrix.* (Blundy and Cashman, 2008).

Key evidence indicating that the FCR is a volcanic product which travelled the ring fault alongside the red felsite and the fault intrusion is found when addressing their geochemical compositions which imply the units are related. Firstly, the graphs shown in figure 5.3 negates that the trendline seen between the FCR, breccia and pure quartzite is produced due to the melting of quartzite, and instead shows that this trend is a result of mechanical mixing of breccia clasts and FCR clasts. This mechanical mixing of brecciated quartzite and the volcanic FCR provides evidence of the conduit fracking and erosion described previously. Moreover, figures 5.4, 5.5, and 5.6 all provide evidence suggesting that the groundmass of the FCR and the fault intrusion are similar enough to suggest they are related (with some variation allowed for natural variation in rocks, variation in magma

compositions throughout an eruption and uncertainties from the old data collection techniques). Therefore, the mathematical mixing equations done in chapter 5 are used to suggest that there are two key geochemical trends occurring across the Glencoe ring fault rocks:

1. That liquid magma (therefore the groundmass) is extracted from the reservoir with progressively increasing volumes of additional phenocrysts taken from the settled, more rigid magma mush, creating an increasingly more mafic composition. This increasingly mafic composition is shown between the less crystalline FCR to the more crystalline and less silicic fault intrusion. This trendline fits what we know about evolution occurring in magma reservoirs as it is expected that more mafic minerals will crystallise first, therefore there will be more of them in this semi-solidified magma.

2. That FCR progressively mixes with the brecciated quartzite (which has become brecciated through volcanic fracking/wall erosion processes as well as possibly some effects of faulting) to create a lithic rich tuffisite lining the volcanic conduit which becomes increasingly more silicic in composition due to the mechanical addition of quartz (Wilson, Sparks and Walker, 1980; Díaz-Bravo and Morán-Zenteno, 2011; Szemerédi *et al.*, 2020).

These two behaviours which explain the geochemical trends within the fault related rocks at Glencoe, these are described in figure 6.3a-d.

Figure 6.4a-d *An array of harker diagrams (Al2O3, TiO2, MgO, CaO vs. SiO2) which show the two key geochemical trends seen within the fault rocks of Glencoe, which are described through inset figures to show their wider geological meaning.*
Trend 1) The breccia zone of mechanically mixed FCR and quartzite lies along the mixing line of the average FCR value with 100% SiO2. This shows that the trend seen of the breccia, which connects the FCR and the quartzite, is a result of mechanical mixing introducing ~30-70% of quartz into FCR.
Trend 2) A second mixing line is seen, which lies at a different angle showing its independent behaviour. This is the link between FCR and the fault intrusions. The fault intrusions have a wide range of compositions, but the mixing line shown correlates is specific to the compositions of the monzonite-diorite fault intrusion and FCR at Stob Mhic Mhartuin. This mixing line represents the gradual removal of melt from the crystal mush, in order to produce the crystal poor end member of FCR.
Geological meaning) The FCR represents magma melt which has been removed from the reservoir which, at Stob Mhic Mhartuin, has later become deposited and mechanically mixed with the quartzite breccia.

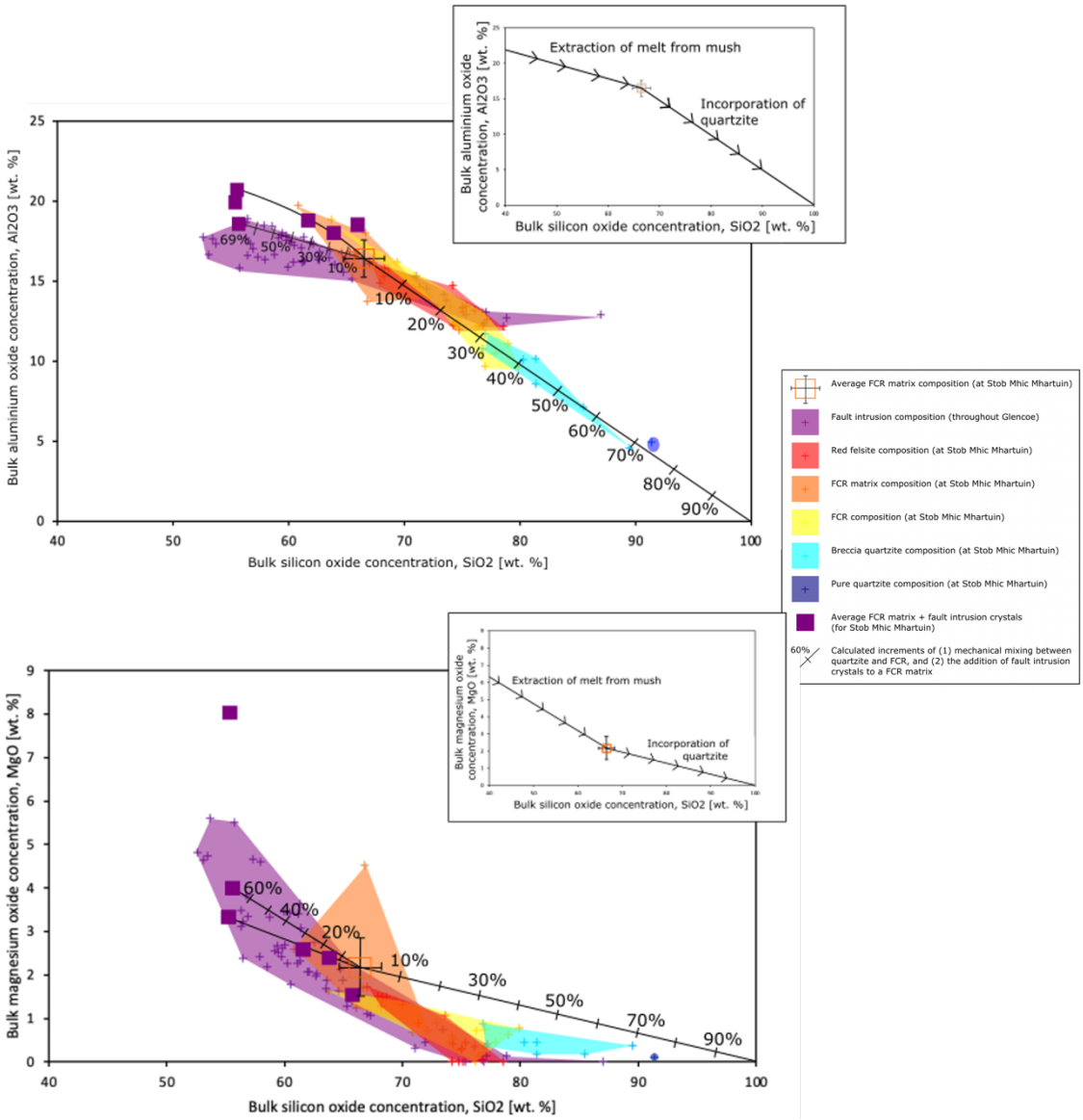
Bulk aluminium oxide concentration, Al2O3 [wt. %]
Bulk silicon oxide concentration, SiO2 [wt. %]
Extraction of melt from mush
Incorporation of quartzite
69%
50%
30%
10%
10%
20%
30%
40%
50%
60%
70%
80%
90%
Bulk magnesium oxide concentration, MgO [wt. %]
Bulk silicon oxide concentration, SiO2 [wt. %]
Extraction of melt from mush
Incorporation of quartzite
60%
40%
20%
10%
30%
50%
70%
90%
Average FCR matrix composition (at Stob Mhic Mhartuin)
Fault intrusion composition (throughout Glencoe)
Red felsite composition (at Stob Mhic Mhartuin)
FCR matrix composition (at Stob Mhic Mhartuin)
FCR composition (at Stob Mhic Mhartuin)
Breccia quartzite composition (at Stob Mhic Mhartuin)
Pure quartzite composition (at Stob Mhic Mhartuin)
Average FCR matrix + fault intrusion crystals (for Stob Mhic Mhartuin)
60%
Calculated increments of (1) mechanical mixing between quartzite and FCR, and (2) the addition of fault intrusion crystals to a FCR matrix

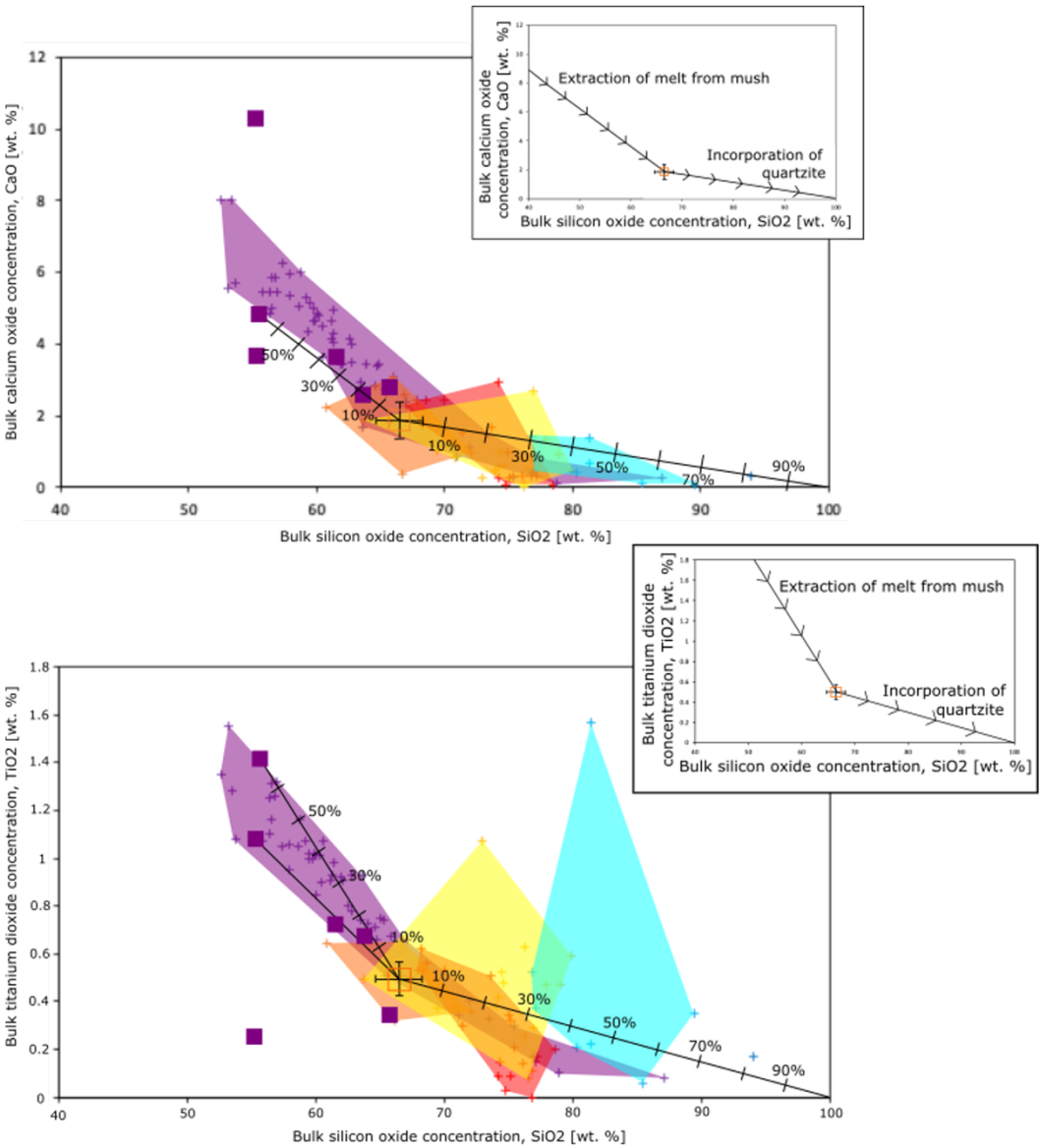

Further geochemical validation of the volcanic FCR theory is found using EDS chemical maps. Banding seen within the FCR is chemically controlled by the varied concentration of potassium and sodium. This characteristic is consistent with known volcanic glasses which have devitrified to form silica rich phases. Furthermore, the major elements present in the FCR (silica, aluminum and potassium) are all major constituents of volcanic glass which aligns to the supported hypothesis. The similarity of the FCR to the adjacent intrusions can be tested through EDS chemical maps which show that whilst there are some changes in composition across contacts, these are non-abrupt, and generally the units consist of the same elements just at varying concentrations. Again, differences in composition between the FCR and intrusions is largely controlled by the variation in phenocryst and quartzite xenolith volume and phase. The genetic relationship between the FCR and intrusions is shown by their possession of similar groundmass, shown through geochemical graphs, EDS maps, textural and petrological classifications.

The groundmasses of the FCR, the red felsite and the fault intrusion are extremely similar. They consist of the same 4 components - quartz, albite feldspar, potassium feldspar and opaques. The concentration and shape of each of these components vary between units. Such as the fault intrusion and red felsite groundmass appears more coarse and crystalline, with a greater proportion of albite feldspar. Whereas the FCR groundmass texture is wormier in appearance, regularly developing into myrmekite intergrowths between the quartz and feldspar phases. The microscopic similarity between the units is made abundantly clear when assessing the thin section GC22 which exposes a FCR vein cutting through the fault intrusion, because it is very difficult to even spot where the vein occurs.

The opaques found across the various fault related units also provide a key indicator that the FCR is volcanic. The FCR, red felsite and fault intrusion all contain similar volumes of the same titanomagnetite, recognisable by its distinct widmanstätten surface patterns showing the exsolution of ilmenite. The presence of this unique and identifiable mineral across the FCR, red felsite and fault intrusion, whereas the quartzite contains none, is an indicator of a shared origin between the fault fill units. The similar volume of these ilmenite bearing titanomagnetites within the FCR and the intrusions also shows that this cannot be due to mixing between units. As well as using the widmanstätten pattern to show the similarity between the fault fill units, it can also indicate that the unit cooled slowly (Tan *et al.*, 2016). This opaque is also associated with oxidation of units, which in the intrusive volcanic context could imply the presence of fragmentation of units due to this process allowing the increased surface area of units to interact with less reducing environments (Tan *et al.*, 2016). Finally, the FCR often has a vanguard of opaques along its contact with the quartzite, especially along veins, this aligns to the suggestion that the FCR fragmented because it allows increased surface area which is able to interact with the less reducing environment within the conduit (opposed to the magma reservoir). Therefore, the first FCR material would have the most opportunity to become oxidised by mixing with the new, surrounding environment. The repeated presence of myrmekite textures throughout the FCR (as well as the red felsite and fault intrusion) within the groundmass and coating crystals, particularly quartzite xenoliths, provides further support for a volcanic origin for the FCR. This graphic texture is a typical indicator of a magmatic origin, which occurs due to the intergrowths developing between the quartz and feldspar minerals.

The volcanic explanation for the FCR also makes it much easier to explain the heavily mixed relationship between the FCR, red felsite and fault intrusion where each unit is found with inclusions of one another. During the sequential or co-eruption of volcanics during activity it is likely the different materials ejected would interact and mixed with one another within the conduit. The variable presence of the FCR, as well as the red felsite, along the ring fault is explained because is common

that throughout an eruption the dynamic changes between various vent openings and various levels of explosivity/erosion will result in places where the FCR is not deposited or is greatly eroded.

At Ben Nevis a unit closely resembling the FCR, was named the Ben Nevis intrusive ring tuff by Burt and Brown (1997) due to new evidence indicating that the unit represents an ignimbrite conduit formed during caldera collapse, hence that the unit has a wholly igneous origin. The work of this study discounted a frictional melting origin for the Ben Nevis 'FCR' due to discordance with typical pseudotachylyte characteristics. Evidence found to support the volcanic origin was both due to the unit's magmatic appearance as well as its geochemical similarity to nearby volcanic units. The recognition of this analogous unit as an intrusive tuff further supports that this conclusion may be also correct for Glencoe.

A complexity to any explanation of the FCR is the presence of FCR veins (such as GC22) found within the ring intrusions (described in section 4.1.5). These veins may have brecciated contacts (GC14B), which is a sign that these veins were not passive, and instead actively injected into the units with high energy, showing that the explanations given for these veins by the authors supporting the frictional melt origin are questionable. Instead, in a volcanic setting, it is likely that towards the end of an eruptive period there may be small lenses of un-erupted liquid magma remaining in the reservoir. This magma would be highly pressurized therefore may produce veins which inject upwards through the deposited transport system to release pressure, leaving behind anastomosing networks of the crystal poor FCR material. This also explains why the more fractured second intrusion contains more veins, as the process would have preferentially exploited the pre-existing weaknesses/fractures within. Support for this theory is found when looking at the sampled FCR vein found within a fault intrusion, as the vein is poor in quartzite clasts, which accords to this theory as the moving liquid would not have yet travelled past the quartzite in order to experience any mechanical mixing. As the intrusion is crystal rich it would not require particularly high strain in order to experience brittle fracturing (Wadsworth *et al.*, 2018). In cases, described well by Garnham (1988), there are also few examples at Glencoe where the FCR veins appear to push aside the fault intrusion crystals. These are examples of where the magma is not yet cool enough or crystal rich enough to experience such brittle fracture, known as gas filter pressing or ductile intrusion.

There is banding along the main intrusion contacts. This banding is clearly a result of shear during flow, typical of similar highly welded ignimbrites. However, this study also highlights the likelihood that the causation of bands of with various colours is a result of the close relationship the FCR has with both the brecciated quartzite and the red felsite. It is proposed that the colour variations show pulses of volcanic activity where either wall erosion or red felsite eruption dominated and interacted with the main FCR body. This is supported by the occurrence of bands rich in fine quartzite xenoliths

and associated reaction rims, as well as bands bearing similarity to the red felsite. These bands would later become smeared out by flow and welding.

In conclusion this study finds that the FCR has a fragmented volcanic origin, like originally proposed by (Reynolds, 1956), but with adaptations to the overall hypothesis so that all the nuances of the unit are explained and so that it suits what we now know about caldera eruption dynamics. Such as, the FCR is a lithic rich tuff which has formed due to the fracking of wall rocks during explosive ignimbrite eruption, whereby small volumes of pyroclastics have aggregated onto the conduit walls mechanically mixed with the brecciated wall rock to create a lithic rich tuff and a mechanically mixed contact where veins project into the wall rock. The outer contacts of the intruded ring fault have become irregular due to the preferential fracking of the outer wall due to the upwards direction of explosive volcanic eruptions against the outward dipping conduit. These lithics have reacted to the new groundmass they are set within, to develop certain reactionary behaviours. The unit has an intimate relationship with the brecciated quartzite and red felsite which has resulted in a banding texture in places. The unit has cooled slowly due, become oxidised, mixed and flow banded to create the textures seen in the FCR today.

6.3.2 The red felsite

It is now an increasingly understood phenomenon that welded tuff dykes (which once behaved as feeder systems for explosive eruptions) are extremely difficult to recognise, due to the extreme welding processes that occur during conduit closure causing the ash to re-morph back into what appears as a cohesive magma structure (Wolff, 1985). We also now know that silicic magmas fragment very easily (Gonnermann, 2015) and that the pressure changes that occur during caldera collapse is extreme, therefore making the possibility of fragmented magma transport more likely (Wiebe *et al.*, 2021). This has resulted in the re-evaluation of dykes in recent years which has allowed for the recognition that these pyroclastic dykes are more common than once believed. The work of Burt and Brown (1997) concluded that the ring intrusion units of Ben Nevis (analogous to those at Glencoe) were intensely rheomorphosed pyroclastic vent fills. Deciphering the state of magma as it travels through conduits has an important control on our understanding of caldera dynamics and hazard prediction efforts due to the important effect it has on eruption explosivity. Due to this study's conclusion that the FCR is a fragmented volcanic, the study must next test the possibility that the adjacent, more crystal rich red felsite is also pyroclastic. This is also used to question whether the red felsite's eruption history has played an effect on its different colour when compared to the otherwise very similar fault intrusion. Reynolds (1956) and Roberts (1966) have previously suggested that the ring fault fill units are all fragmented but subsequent workers have not supported this. Previous

workers considering the red felsite have either disregarded the unit (Reynolds, 1956; Roberts, 1966), described it as a chilled margin of a non-fragmented ring intrusion (Bailey and Maufe, 1960), both of which Garnham (1988) disputed along with disputing that it may also be related to frictional melting of the ring intrusion. Garnham (1988) alternately suggests this unit has resulted from liquid fractionation or mixing of partial melt liquids.

Within the red felsite there is a large array of textural and petrological characteristics that are commonly associated with pyroclastic dykes. A very important indicator of fragmentation is the presence of fractured phenocrysts, these are recognised as crystals with angular shapes with acute and sharp corners that cut through crystal habits and crystal zoning (Motoki *et al.*, 2012). Fragmented crystals are very common within the red felsite, which has been noticed before (Reynolds, 1956; Roberts, 1966; Kokelaar and Moore, 2006).

The red felsite also contains many small quartzite lithics, which is another indicator that the unit is pyroclastic (Torres-Hernández *et al.*, 2006; Motoki *et al.*, 2012; Szemerédi *et al.*, 2020). These quartz clasts that comprise a small but common portion of the red felsite have been classified as xenoliths due to their sintered surfaces, their reactionary rims and their brittle shapes. Mineral aggregates are also found within the red felsite, these provide evidence that crystals have collided or welded together, hence another indicator of a fragmentary origin (Motoki *et al.*, 2012). Van Zalinge *et al.,* (2018) also describes the presence of in situ secondary crystal fragmentation (where a whole crystal can be seen in its original shape but it is broken up into multiple pieces that have had minor displacements) as another key piece of evidence of welding and compaction. There is a lot of evidence for the in situ fracturing of weaker minerals (i.e. the amphiboles and biotites) within the red felsite, hence implying it is a welded pyroclastic unit. This study did not find clear evidence of a spherulitic texture, but this may be a result of limited sample selection as the work of Garnham (1988) recorded the presence of spherulites, which is another important sign of a pyroclastic nature.

There are many more indicators of a fragmentary origin within the red felsite; a massive texture; unsorted crystals; matrix supported structure; fine, homogenous groundmass; strongly sericitized juvenile feldspar fragments; resorbed quartz; lack of deformation lamella within quartz; resorbed alkali feldspar; flow banding; lack of chilled margins; varied shape and width of intrusion, and non-straight intrusion contacts (Bachmann, 2002; Motoki *et al.*, 2012; van Zalinge, Cashman and Sparks, 2018; Szemerédi *et al.*, 2020). These characteristics may not provide evidence of fragmentation when used alone, but when considered in conjunction with each other and the previously described textures, they show the wide array of pyroclastic textures within the red felsite.

In conclusion, the red felsite contains an abundance of evidence suggesting that the unit was emplaced as a fragmented volcanic unit. This aligns well with what we know about the silicic composition of the unit and the extreme pressure changes that occur during caldera-forming eruptions, because silicic magma fragments so easily.

6.3.3 The fault intrusion

The adjacent fault intrusion is similar in appearance, however there is much less evidence for a fragmentary origin, especially when compared to the abundance of evidence within the red felsite. Whilst there are still some indicators, such as the presence of lithics and aggregates, the evidence is less obvious. It is also more challenging to imagine the physics of fragmentation of the whole fault intrusion because of the way it has blocked the majority of the very wide Glencoe ring faults. The occurrence of very wide pyroclastic dykes are however not unheard of, such as those up to 1 km described by Díaz-Bravo and Morán-Zenteno (2011), the genesis of which could be imagined by the conduit blocking process described by Wadsworth *et al.*, (2020). As the fault intrusion marks the very final material to travel through the ring fault conduit, its cohesive state matches the belief that the final stages of activity at calderas are commonly effusive. In conclusion, evidence suggests the fault intrusion was intruded as a coherent magma which has fused with the adjacent red felsite, however more research into this unit (especially considering other locations around the ring fault) could reveal more.

6.3.4 How the eruption state of each unit aligns to the overall caldera-forming eruption

The suggestion that the red felsite is fragmented, whereas the fault intrusion is not, fits well with some of the other characteristics of these units. The striking difference between the red felsite and the fault intrusion is the difference in colour (red and grey, respectively), and this colour difference is why they have been addressed differently in previous literature. However there has been no clear conclusion as to the origin of these two units and why their colours are so different. It is only when looking at the two units using the SEM, where optical colour cannot be used as guide, that it becomes clear how remarkably similar these units are. Therefore, it is recommended that a fragmentary origin for the red felsite, explains why the colour difference has occurred. A red colour is a common feature of units that have become oxidised. It is likely that a fragmented volcanic may become oxidised due to the higher surface areas that can interact with the less reducing environment within the conduit than in the magma reservoir it previously resided within. Other than colour difference, in this study (which uses fieldwork, thin sections and geochemistry, hence could be more accurately assessed in further studies with use of electron microprobe probe analysis (EMPA)) the only major change recognised

between the two units at Stob Mhic Mhartuin is the change in phenocryst texture from smaller, more broken and often aggregated crystals within the red felsite, to the larger crystals with clear habits of the fault intrusion. This change of crystals becoming increasingly more fragmented within the red felsite also fits the fragmented origin theory for the unit. It is these two major differences from the fault intrusion (colour and crystal breakage) that support the fragmented origin for the red felsite. The contact between the two units also appears to be fused (unlike the mixed contacts seen between other units), which provides further and final support that these units mark a change in state from pyroclastic to cohesive. This shows an abrupt change from an explosive to an effusive eruption, something expected to occur where complex magma reservoirs feed eruptions (Cashman and Giordano, 2014).

Not only does the temporal progression from red felsite to the fault intrusion (a.k.a. moving inwards to the centre of the fault fill) show the change from a fragmented explosive eruption to the very final effusive fault fill, but it also shows the change towards tapping varied and more crystal rich magmas. The fault intrusion is slightly richer in crystals than the red felsite, specifically plagioclase. This shows that the red felsite is a more evolved melt which has had less long to cool. Modern understanding of magma storage reservoirs suggest that they are comprised of multiple melt lenses (partially connected or completely isolated) or a zoned melt body which is rapidly assembled to feed a single eruption (Cashman and Giordano, 2014). The idea of multiple distinct/zoned melt sources with individual crystal populations matches the variation in fault intrusion composition around the ring fault, as shown by the geochemical studies of Garnham (1988), as different vents would open and different sources would be tapped in different areas of the caldera structure over the course of an eruption. Hence, a complex storage geometry matches the complex fault fill unit geometry seen. The idea of a complex storage geometry also matches the piecemeal collapse at Glencoe, as the two phenomena are expected to be related (Cashman and Giordano, 2014).

Magma storage regions are predominantly composed of a crystalline mush (which is a mixture of solidified multiphase crystals as well as some evolved silicate interstitial liquid melts) within which the melt dominant lenses exist (Bachmann and Bergantz, 2008; Cashman and Giordano, 2014; Parmigiani *et al*.,2014). The final eruptive product within the Glencoe ring faults (the fault intrusion) is much more crystal rich than the first volcanic product filling the fault (the FCR). The porphyritic nature of the fault intrusion demonstrates that this was not a slow cooled magma (where you would expect a more uniform graphic texture), but a liquid magma (which cooled quickly after emplacement) that contains crystals which solidified at an earlier stage (in the reservoir), hence making this a mobilised magma mush. Therefore, there is evidence that towards the end of large eruptions, these more crystalline and therefore more rigid magma mush bodies may become mobilised enough to feed into the eruption conduits (Wiebe *et al.*, 2021). This has been suggested by Wiebe *et al,* (2021) to occur in the Cadillac Mountain intrusive complex, USA, through a collapse driven flow caused by

the pressures of the collapsing chamber roof, which squeezed the granitic material into inactive vents. The great textural variability at Glencoe fits this model, as the change from FCR to the fault intrusion marks the progression from a crystal poor magma which was preferentially erupted and fragmented throughout the eruption, into the final stages of rigid crystal mushes passively filling the fault fill due to pressures exerted onto it within the chamber. Additional to the collapse driven flow described by Wiebe *et al.,* (2021) we suggest a further mechanism driving this magma mush intrusion. It is widely accepted that caldera ring faults are outward dipping, therefore during collapse this creates a dilation in the crust. During eruption the void in the crust is supported by the violent eruption of magma. However, as the eruption wanes it is not possible for such a void to remain in the sub-surface. Therefore the pressure gradient created by this will drive the semi-rigid magma mush to mobilise and flow into the space for it to become filled. Subsequently this creates more space in the chamber, so the squeezing of magma into the ring faults may drive further collapse which could initiate a positive feedback system whereby further intrusion is driven by the squeezing pressure of the collapse driven flow until an equilibrium is found. This system therefore explains the change from crystal poor and fragmented material into crystal rich and cohesive magma. This idea that the final fault fill represents mush regions that have squeezed into the fault and were just as active as the FCR explains the porphyritic texture of the units, as the larger crystals had long time peroids to crystalise when in the chamber before becoming mobilised amongst liquid magma which cooled more rapidly at shallow depths. This also explains the ability of FCR veins to fragment through the material, as its quicker cooling and high crystallinity allows it to experience brittle deformation (Wadsworth *et al.*, 2018).

This study suggests that the red felsite marks small volumes of magma mush material (approximately identical in original composition/origin to the fault intrusion) which have become incorporated into the main eruption along with the liquid magma FCR. This material has become fragmented due to the extreme pressure changes exerted during an eruption, this fragmentation has resulted in greater oxidation of the unit due to the material's increased surface area interaction with surrounding atmosphere (similarly to what has occurred to the FCR). The material has travelled up the conduit alongside the fragmented material which composes the FCR, hence why their relationship is very intimate and mixed. This explains why the red felsite is not always present, as various tapping and vent opening geometries would only allow this phenomena to occur at certain locations.

Understanding the Glencoe transport system requires an explanation of the outer ring fault intrusion seen at Stob Mhic Mhartuin. Previous studies have not agreed on why this ring fault has occurred, as some suggest this ring fault marks a separate, early subsidence period, whereas others have questioned this and the significance of the outer ringfault at all (Taubeneck, 1967). This study finds that due to the small size of the outer ringfault which does not encircle the whole caldera that it cannot be a significant, completely different period of activity. Instead, the presence of this extra segment of ring

fault and associated intrusion matches well with what we now know about Glencoe and caldera eruptions in general. The presence of the ring fault and intrusion, along with the many other faults seen in the area, agrees with the knowledge that Glencoe experienced a very piecemeal style of collapse. Therefore, this fault is just one of the many that contributed to the complex incremental breakup of the crust, and therefore need not be considered a separate period of activity. It is interesting that this fault was able to link up the reservoir and the atmosphere to create a vent which became exploited as a volcanic conduit. In fact, the difference in ring fault angle (the outer ring fault is steeper) may provide field evidence supporting analogue models that suggest that several generational sets of concentric outward dipping reverse faults combine to facilitate the collapse of calderas. If these new faults link with the chamber and the surface, these too would be capable of creating conduits for eruption (Kennedy *et al.*, 2004; Burchardt and Walter, 2010; Geyer and Martí-, 2014). Therefore, it is believed that this '2nd ring fault' is simply a part of the multiple, coeval active faults that are present during caldera collapse (especially in the case of a piecemeal caldera like Glencoe) which has been exploited as a conduit, therefore it would be misleading to regard it as a completely separate period of activity, and instead should be used as support for the modern research behind the presence of multiple faults at calderas. The progression of intrusions within this outer ringfault is similar even though the units are slightly different in composition, therefore this shows that caldera ring faults may all experience the same progression of events (from a fragmented crystal poor magma containing small blebs of magma mush which becomes fragmented, into a collapse driven squeezing of more rigid crystal mushes into the waning eruption conduits). The slight difference in compositions and textures is likely to be a result of when the various vents became active, and which parts of the zoned or multi-sill reservoir it tapped, hence causing slight variations in the magma travelling through the conduit. Therefore, if this fault became blocked and the intrusions cooled earlier, it may have become fractured by the strain of the pressure from the nearby main intrusion.

In conclusion, this study finds that hypothesis 2 – "The ring intrusions (the fault intrusion, the red felsite, and the FCR if hypothesis 1 is proven wrong) are fragmented. These represent the order of volcanics to travel up the conduit, in pyroclastic form, due to their near instantaneous fragmentation early in their transport. Therefore, suggesting that calderas erupt large volumes of ignimbrites until the very end of their extrusive activity travelling through their ring faults, and that fragmentation occurs below a depth of 3.5km (current level exposure depth estimation taken from Garnham 1988)" – is partially correct. There is evidence that the red felsite (a crystal rich magma mush) and the FCR (a crystal more magma melt) are fragmented (and therefore oxidised) units deposited throughout sustained explosive eruptions at Glencoe. However, the fault intrusion represents a final period of effusive activity towards the end of caldera-forming volcanism at Glencoe. Therefore, this suggests that calderas erupt large volumes of ignimbrites until their eruption wanes, and such fragmentation occurs below a depth of 3.5km.

6.4 – Final model for the sub-surface transport system of Glencoe

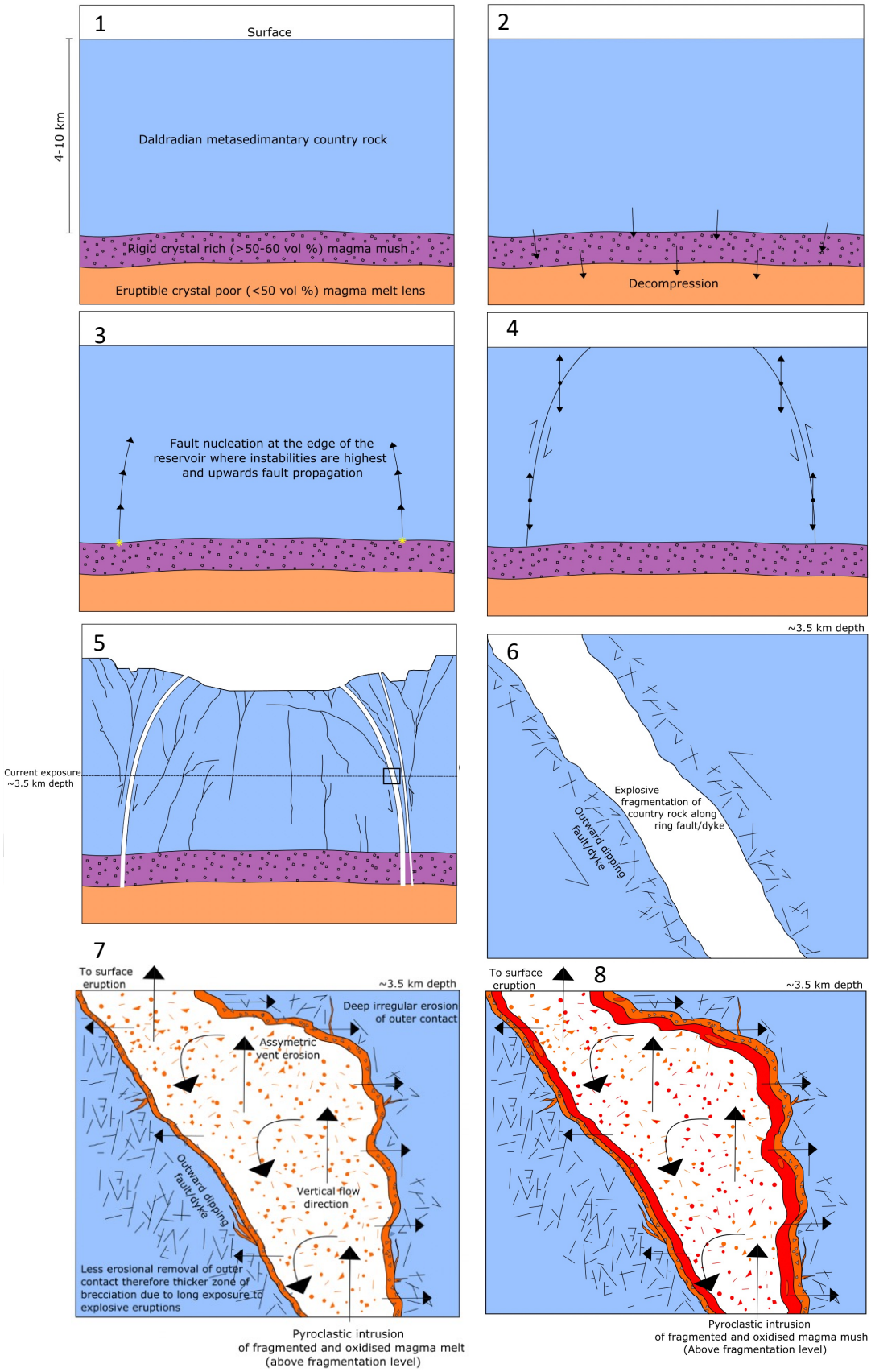

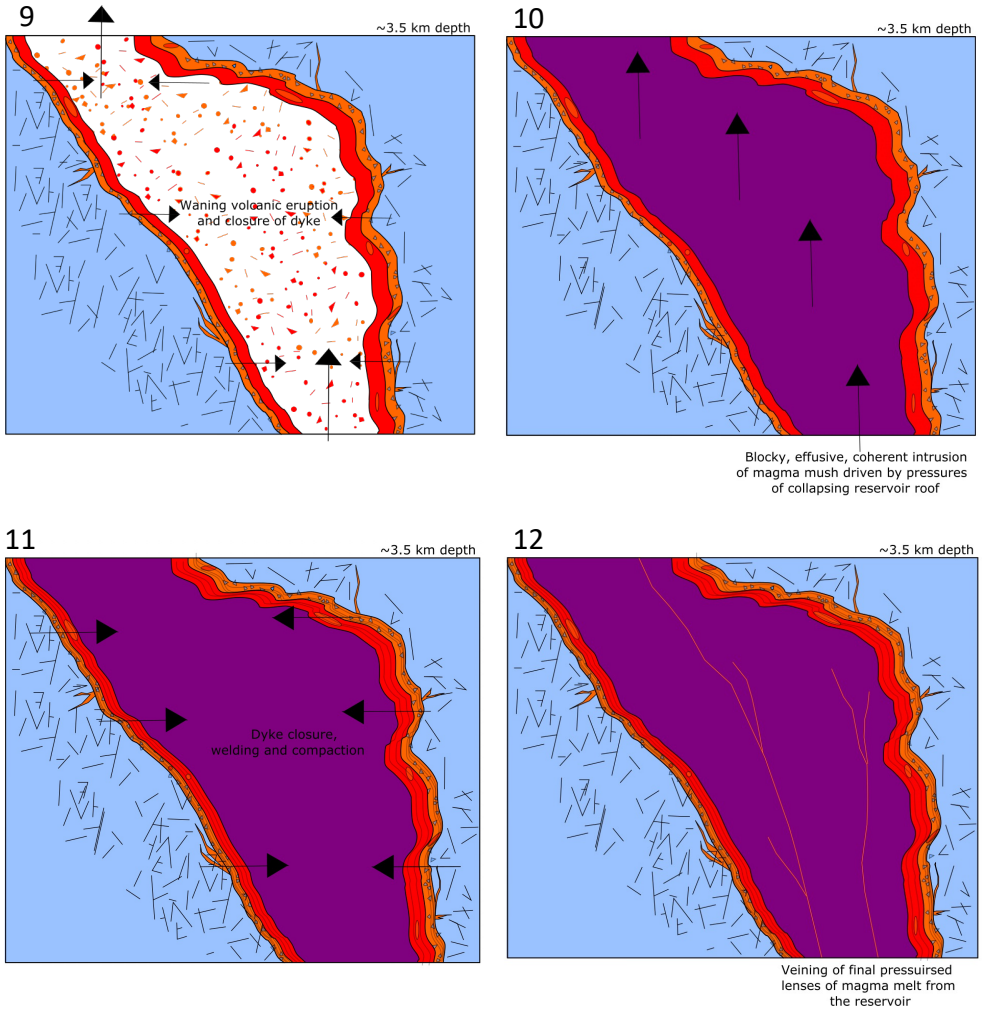

Figure 6.5 (1-12) *a model for the sequence of events of the sub-surface transport system of Glencoe. Adapted from* (Garnham, 1988; Kokelaar, 2007).

1. Eruption of magma from a single vent from the Glencoe reservoir resulted in **decompression** (Garnham, 1988; Moore, 1995)**.**
2. Once the sum of the initial shear stress plus the stress induced by magma withdrawal reached the static strength of the overlying crust, decompression of the reservoir triggered the formation of **outward dipping faults which propagate upwards** within the crustal roof towards the surface. The shape and dip of the faults was controlled by tectonic setting, reservoir geometry, host rock properties, magma volume and roof aspect ratio (Acocella, 2007; Burchardt and Walter, 2010; Cashman and

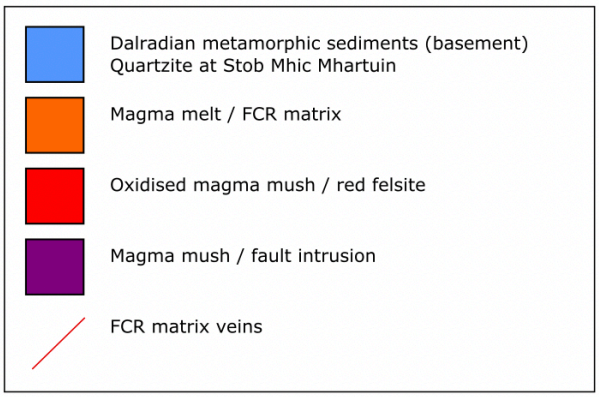

Giordano, 2014; Geyer and Martí-, 2014; Browning and Gudmundsson, 2015; Segall and Anderson, 2021).

3. The ring faults formed in **dilational or shear** movements, resulting in low friction along their surface (Figure 1.4a page 15; Holohan, 2015).
4. Coeval ring fault activity occurred as faults facilitated subsidence and a volcanic eruption
    (a) Caldera **subsidence** occured. Glencoe collapsed in a **piecemeal** nature, because the collapse of a large network of tectonically controlled faults broke up the caldera floor into multiple blocks. Pre-existing faults linked to control the collapse location and morphology (Moore and Kokelaar, 1997, 1998; Cole *et al*., 2005).
    (b) Prior to or simultaneous with collapse, **magmatic products intruded** the ring faults which connect the chamber and the surface meaning these are also ring **dykes** which form the transport system of the caldera. The '2nd ring fault' which is part of the large fault network of the piecemeal Glencoe also links with the reservoir and is intruded by volcanics with the same progression.
5. The caldera-forming volcanic activity along the ring faults began with an **explosive** phase of activity (this chronology relates to the succession of units seen at Stob Mhic Mhartuin, which varies slightly throughout the ring fault due to the opening and closing of vent/fault dynamics and variable tapping of a zoned reservoir, meaning not all phases of this eruption sequence are always recognised elsewhere).
    (a) The eruption preferentially tapped the crystal poor magma melt lenses found within the magma reservoir, the composition of the magma produced throughout the (up to) 14km wide ring fault may vary due to the tapping of isolated or zoned lenses of magma (Bachmann and Bergantz, 2008; Cashman and Giordano, 2014; Parmigiani *et al*.,2014).
    (b) Silicic magma which intrudes the fault/dykes **fragmented** almost instantaneously as a result of the pressure changes occurring during caldera collapse (Gonnermann, 2015).
    (c) The fluidised system of volcanic gas and ash travelling through the conduit **explosively fragmented**/fracked the Dalradian sediment wall rock, this resulted in **brecciated** country rock margins and **widening dyke** margins (Reynolds, 1956; Roberts, 1966; Wiebe *et al.*, 2021).
    (d) The majority of the through passing pyroclastic material travelled to the surface, to feed the **sustained, voluminous pyroclastic surface eruptions** (Kokelaar and Moore, 2006).
    (e) Relatively small volumes of ash **aggregated** and stuck onto the conduit wall, injecting along the fracked margins to create veins of FCR within the country

rock and to create a thin band of **FCR** lining the sides of the volcanic conduit (Wiebe *et al.*, 2021).

(f) The **FCR mechanically mixed with the brecciated country rock** (quartzite in the case of Stob Mhic Mhartuin), this resulted in: the attrition of some of these xenoliths; **reactionary** behaviour (for example the formation of embayment's) of some of these high silica xenoliths and their undersaturated surrounding groundmass; the creation of FCR as a **lithic rich tuff**, and, the contribution of quartzite to the banding of the FCR depending on pulses of explosive activity (Díaz-Bravo and Morán-Zenteno, 2011; Szemerédi *et al.*, 2020).

(g) In places, intermittently throughout the explosive eruption and particularly towards the end of the explosive eruption blebs of more **rigid crystal rich magma mush** were entrained into the conduit. This material **fragmented, oxidised** and aggregated onto the conduit walls to form the **red felsite**. The material was co-erupted with, and is deposited alongside, the FCR, therefore these two units were **intimately mixed** and the red felsite contributed to the flow banding seen within the FCR due to pulses of magma mush eruption.

6. The explosive activity waned and the conduit walls began to close.
7. There was an abrupt change into the final stage of **effusive** activity which was short lived compared to the sustained previous explosive activity. The now inactive ring fault vents were intruded by a less evolved, **crystal rich mush** similar in composition to the red felsite, however it travelled in a cohesive state therefore it has larger, whole crystals and no red colouration due to lack of oxidation. The crystal mush was **squeezed** up the ring faults with flow induced by the pressures of the **collapsing roof block**, resulting in **wide and blocky ring fault intrusions**. The composition of the ring fault intrusion varies throughout the (up to) 14km wide ring fault because the **tapping of different compositions** of magma mush which occurred due to **zoning and isolation of magmas** within the reservoir. Mixing and fusion occured along the contact with red felsite (Garnham, 1988; Bachmann and Bergantz, 2008; Cashman and Giordano, 2014; Parmigiani *et al*.,2014; Wiebe *et al.*, 2021).
8. The pressure changes occurred due to eruption waning and conduit closure/collapse resulted in **welding/compaction** pressures. This resulted in compaction structures within the fragmented units, including secondary fragmentation. Compaction was less strong in the red felsite as the FCR because it is more crystal rich therefore rigid. The FCR banding resulted from flow and the mixing with brecciated quartzite and red (Wolff, 1985; van Zalinge, Cashman and Sparks, 2018).
9. As the eruption settled, the final, small, remaining pressurised lenses of crystal poor magma within the reservoir injected upwards through the ring fault system in order to relieve

pressure, creating a network of **FCR veins** cutting through the intrusions. Veining exploited pre-existing weaknesses therefore there are more veins within the fractured outer ringfault.

10. Post collapse magmatism, resurgence, hydrothermal activity and mineralisation.

Chapter 7: conclusions

7.1 Glencoe

In conclusion, through microscopy and geochemical work this thesis has advanced understanding of the Glencoe ring fault by using evidence of unit origins alongside modern knowledge of caldera systems to create a model for how the Glencoe transport system evolved overtime. This has resulted in the rejection of hypothesis 1 –

> "The FCR is a frictional melt, as stated by the previous researchers Clough, Maufe and Bailey (1909); Bailey and Maufe (1916, 1960); Kokelaar and Moore (2006); Kokelaar (2007). Hence, suggesting that calderas have superfaults which experience significant friction related to subsidence on their surfaces prior to, or simultaneous with, magma transport along their planes".

and a partial acceptance of hypothesis 2 –

> **"**The ring intrusions (the FCR if hypothesis 1 is proven wrong, the red felsite, and the fault intrusion) are fragmented. These represent the order of volcanic to travel up the conduit, in pyroclastic form. Therefore, suggesting that calderas erupt large volumes of ignimbrites in wide conduits until the very end of their extrusive activity travelling through their ring faults, and that fragmentation occurs below a depth of 3.5km (current level exposure depth estimation taken from Garnham 1988)."

Because this study posits that the FCR and red felsite are fragmented magmas which represent the major phase of explosive activity at Glencoe where fragmentation occurred at depths below 3.5km and most material was erupted at the surface. This phase involved the eruption of mostly crystal poor magma melt extraction from the crystal rich reservoir which deposited thin FCR bands along the transport system. The red felsite was also erupted in this phase as an oxidised, fragmented magma mush entrained into the explosive eruption mostly towards the end. The fault intrusion however represents a final effusive period of activity which represents the collapse-driven flow of magma mush

into the inactive ring dykes. The red felsite and the fault intrusion are both magma mushes which are overall very similar, their key differences (colour and crystal size) have occurred as a result in the difference in state in which they travelled. The varying composition of the intrusion units (shown by (Garnham 1988) and their varied presence along the ring faults throughout the 14km wide caldera is a result of the tapping of various regions of a zoned or multi-chambered magma reservoir as well as the dynamic opening and closing of various vents along the ring fault throughout an eruption, which is accords with the chaotic piecemeal style of the Glencoe caldera. This suggests that volcanic fragmentation may be a process that occurs near instantaneously during a caldera-forming eruption as magma moved into a conduit, in order for the products representing the major eruption phase to be found in a fragmented state at this depth. This also shows that ring faults are capable of tapping various different magma reservoir compositions and producing various states of eruption through time, therefore suggesting that mapping of these structures should pay closer attention to the variation throughout a ring structure. This therefore
concludes that future studies of the Glencoe ring faults may wish to embrace new terminology that is less genetic or misleading when referring to the fault fill units.

7.2 Caldera systems worldwide

There are hundreds of known caldera-forming volcanoes throughout the world. A subset of these calderas have become eroded enough to show that processes producing the FCR are common (such as: Ben Nevis caldera in Scotland, Slieve Gullion ring dyke complex in Ireland, Hafnarrfjall in Iceland, Jansang caldera in Korea, Glencoe caldera in Scotland). Despite recent work supporting a frictional melt origin for some of these examples (Glencoe, Kokelaar, 2007; Jansang, Han *et al.*, 2019; Kim *et al.*, 2019) the outcomes of this detailed work at Glencoe suggests that these units are fault hosted volcanic vents. Therefore, these are not frictionally produced and slip rates may not be as high as expected, therefore the proposed idea of caldera superfaults is unlikely (Spray, 1997; Kokelaar, 2007).

This work does however show the importance of these faults as conduits for an explosive volcanic eruption. Conclusions support recent studies showing that calderas are composed of a network of concentric and cross cutting faults capable contributing to both piecemeal collapse and the transport of volcanic products. Studies of units at Glencoe have shown that calderas are capable of dynamic eruptions that change over time and tap different regions of a magma reservoir. Furthermore, this work has shown that magma mushes can become entrained into an eruption, but mostly this occurs as a collapse-driven conduit blocking process when explosive activity has waned.

To conclude, the outcome of this study poses a final question – does the naming of caldera ring faults need to be re-evaluated if their primary purpose throughout an eruption is to transport volcanic material between the reservoir and the surface, and if they are not a major, high friction superfault structure. Therefore, should we stop thinking of these surfaces primarily as faults, and instead chose a representative co-genetic name?

7.3 Future work

Further studies could be conducted in Glencoe. Firstly, supplementary analysis of the fault intrusions throughout the whole ring fault could be used in order to test that they were all deposited as a cohesive magma, or whether in fact the state of the magma changes throughout the ring fault. For example, this could be done using the size-frequency distribution analysis used by Motoki *et al.,* (2012) to test the explosivity of units. Work on the intrusions could also aid the mapping and re-naming of the fault intrusions throughout the unit due to their specific compositions. Further study fo the fault intrusions at Glencoe could, for example, provide a better understanding of what they are, how they formed, how they are (in places) so wide therefore how this initiates and evolves, and their implications for caldera formation and ignimbrite-forming eruptions. The angles of veins on either side of the intrusions at Glencoe could also be analysed to test whether this fits the hypothesis that the outer contact is more irregular due to the outward dip of ring dykes, resulting in fracking becoming more oblique along the outer contacts.

Previous studies of Glencoe, as well as this one, have heavily focused on the type locality Stob Mhic Mhartuin, due to its better outcrop exposures. However, it is important for future studies of Glencoe to repeat analyses for different locations along whole system to ensure conclusions are widely applicable and that Stob Mhic Mhartuin is a reliable 'type'. This study was heavily impacted by the affects of covid-19 by limiting data collection opportunities. Future geochemical studies could also benefit from more specific and detailed analysis from electron microprobe analysis (EMPA) with greater consideration for sample location. This type of detailed geochemical work could focus on groundmass compositions, comparison of phenocryst and oxides within units, and comparison of the two ring faults.

Finally, similar comprehensive studies such as this could be conducted for more exposed sub caldera transport systems worldwide to understand whether the volcanic FCR phenomena is applicable to calderas throughout. For example, starting with Jansang caldera where it the unit is currently believed to be a frictional melt in connection with theories that began at Glencoe.

References

Acocella, V. (2007) 'Understanding caldera structure and development: an overview of analogue models compared to natural calderas', *Earth-Science Reviews*, 85, pp. 125–160.

Bachmann, O. (2002) 'The Fish Canyon Magma Body, San Juan Volcanic Field, Colorado: Rejuvenation and Eruption of an Upper-Crustal Batholith', *Journal of Petrology*, 43(8), pp. 1469–1503. doi:10.1093/petrology/43.8.1469.

Bachmann, O. and Bergantz, G. (2008) 'The Magma Reservoirs That Feed Supereruptions', *Elements*, 4(1), pp. 17–21. doi:10.2113/GSELEMENTS.4.1.17.

Bachmann, O. and Huber, C. (2016) 'Silicic magma reservoirs in the Earth's crust', *American Mineralogist*, 101(11), pp. 2377–2404. doi:10.2138/am-2016-5675.

Bailey, E.B. and Maufe, H.B. (1916) *Ben Nevis and Glencoe*. Mem. geol. Surv. Scotland.

Bailey, E.B. and Maufe, H.B. (1960) *The geology of Ben Nevis and Glen Coe and the surrounding country*. Second. Edinburgh: H.M. Stationary Office.

Blundy, J. and Cashman, K.V. (2008) 'Petrologic reconstruction of magmatic system variables and processes', *Reviews in Mineralogy and Geochemistry*, 69(1), pp. 179–239.

Bosworth, W., Burke, K. and Strecker, M. (2003) 'Effect of stress fields on magma chamber stability and the formation of collapse calderas: STRESS FIELDS AND COLLAPSE CALDERAS', *Tectonics*, 22(4), p. n/a-n/a. doi:10.1029/2002TC001369.

Branney, M.J. (1995) 'Downsag and extension at calderas: new perspectives on collapse geometries from ice-melt, mining, and volcanic subsidence', *Springer-Verlag*, (57), pp. 303–318.

Branney, M.J. and Kokelaar, B.P. (2003) *Pyroclastic density currents and the sedimentation of ignimbrites*. London: Geological Society.

Brown, R.J., Bonadonna, C. and Durant, A.J. (2012) 'A review of volcanic ash aggregation', *Physics and Chemistry of the Earth, Parts A/B/C*, 45–46, pp. 65–78. doi:10.1016/j.pce.2011.11.001.

Brown, R.J. and Branney, M.J. (2004) 'Event-stratigraphy of a caldera-forming ignimbrite eruption on Tenerife: the 273 ka Poris Formation', *Bulletin of Volcanology*, 66(5), pp. 392–416. doi:10.1007/s00445-003-0321-y.

Browning, J. and Gudmundsson, A. (2015) 'Caldera faults capture and deflect inclined sheets: an alternative mechanism of ring dike formation', *Bulletin of Volcanology*, 77(1), p. 4. doi:10.1007/s00445-014-0889-4.

Burchardt, S. and Walter, T.R. (2010) 'Propagation, linkage, and interaction of caldera ring-faults: comparison between analogue experiments and caldera collapse at Miyakejima, Japan, in 2000', *Bulletin of Volcanology*, 72(3), pp. 297–308. doi:10.1007/s00445-009-0321-7.

Burt, R.M. and Brown, P.E. (1997) 'The Ben Nevis Intrusive Ring Tuff, Scotland: re-interpretation of the "Flinty Crush Rock" as part of an ignimbrite conduit in the roots of an ancient caldera', *Scottish Journal of Geology*, 33(2), pp. 149–155. doi:10.1144/sjg33020149.

Cashman, K.V. and Giordano, G. (2014) 'Calderas and magma reservoirs', *Journal of Volcanology and Geothermal Research*, 288, pp. 28–45. doi:10.1016/j.jvolgeores.2014.09.007.

Clayburn, J.A.P. Harmon, R.S., Pankhurst, R.J. and Brown, J.F. (1983) 'Sr, O, and Pb isotope evidence for origin and evolution olf Etive Igneous Complex, Scotland', *Nature* [Preprint].

Clough, C.T., Maufe, H.B. and Bailey, E.B. (1909) 'The Cauldron-Subsidence of Glen Coe, and the Associated Igneous Phenomena', *Quarterly Journal of the Geological Society*, 65(1–4), pp. 611–678. doi:10.1144/GSL.JGS.1909.065.01-04.35.

Cole, J.W., Milner, D.M. and Spinks, K.D. (2005) 'Calderas and caldera structures: a review', p. 26.

Costa, A., J. Suzuki, Y. and Koyaguchi, T. (2018) 'Understanding the plume dynamics of explosive super-eruptions', *Nature Communications*, 9(1), p. 654. doi:10.1038/s41467-018-02901-0.

Degruyter, W. Bachmann, O., Burgisser, A. and Manga, M., (2012) 'The effects of outgassing on the transition between effusive and explosive silicic eruptions', *Earth and Planetary Science Letters*, 349–350, pp. 161–170. doi:10.1016/j.epsl.2012.06.056.

Devenish, B.J. (2013) 'Using simple plume models to refine the source mass flux of volcanic eruptions according to atmospheric conditions', *Journal of Volcanology and Geothermal Research*, 256, pp. 118–127. doi:10.1016/j.jvolgeores.2013.02.015.

Dewey, J.F. and Strachan, R.A. (2003) 'Changing Silurian–Devonian relative plate motion in the Caledonides: sinistral transpression to sinistral transtension', *Journal of the Geological Society*, 160(2), pp. 219–229. doi:10.1144/0016-764902-085.

Di Toro, G. Han, R., Hirose, T., De Paola, N., Nielsen, S., Mizoguchi, K., Ferri, F., Cocco, M. and Shimamoto, T. (2011) 'Fault lubrication during earthquakes', *Nature*, 471(7339), pp. 494–498. doi:10.1038/nature09838.

Di Toro, G., Goldsby, D.L. and Tullis, T.E. (2004) 'Friction falls towards zero in quartz rock as slip velocity approaches seismic rates', *Nature*, 427(6973), pp. 436–439. doi:10.1038/nature02249.

Di Toro, G. and Pennacchioni, G. (2004) 'Superheated friction-induced melts in zoned pseudotachylytes within the Adamello tonalites (Italian Southern Alps)', *Journal of Structural Geology*.

Díaz-Bravo, B.A. and Morán-Zenteno, D.J. (2011) 'The exhumed Eocene Sultepec-Goleta Volcanic Center of southern Mexico: record of partial collapse and ignimbritic volcanism fed by wide pyroclastic dike complexes', *Bulletin of Volcanology*, 73(7), pp. 917–932. doi:10.1007/s00445-011-0460-5.

Emeleus, C.H. (1962) 'The Porphyritic Felsite of the Tertiary Ring Complex of Slieve Gullion, Co. Armagh', p. 28.

Fondriest, M. Mecklenburgh, J., Passelegue, F.X., Artioli, G., Nestola, F., Spagnuolo, E., Rempe, M. and Di Toro, G., (2020) 'Pseudotachylyte Alteration and the Rapid Fade of Earthquake Scars From the Geological Record', *Geophysical Research Letters* 47(22), p.e2020GL090020.

Franzson, H. (1978) 'Structure and petrochemistry of the Hafnarfjall Skardsheidi central volcano and the surrounding basalt succession, W-Iceland', *Edinburgh, Scotland, university of Edinburgh*, p. 254.

Garnham, J.A. (1988) *Ring-faulting and associated intrusions, Glencoe, Scotland*. Imperial College London.

Gautneb, H., Gudmundsson, A. and Oskarsson, N. (1989) 'Structure, petrochemistry and evolution of a sheet swarm in an Icelandic central volcano', *Geological Magazine*, 126, pp. 659–673.

Geshi, N. Yamasaki, T., Miyagi, I. and Conway, C.E., 2021. Magma chamber decompression during explosive caldera-forming eruption of Aira caldera. *Communications Earth & Environment, 2(1), pp.1-10*.

Geyer, A. and Martí, J. (2008) 'The new worldwide collapse caldera database (CCDB): A tool for studying and understanding caldera processes', *Journal of Volcanology and Geothermal Research*, 175(3), pp. 334–354. doi:10.1016/j.jvolgeores.2008.03.017.

Geyer, A. and Martí-, J. (2014) 'A short review of our current understanding of the development of ring faults during collapse caldera formation', *Frontiers in Earth Science*, 2. doi:10.3389/feart.2014.00022.

Goldsby, D.L. and Tullis, T.E. (2002) ‘Low frictional strength of quartz rocks at subseismic slip rates.’, *Geophysical research letters*, 29(17), pp. 25–1.

Gonnermann, H.M. (2015) ‘Magma Fragmentation’, *Annual Review of Earth and Planetary Sciences*, 43(1), pp. 431–458. doi:10.1146/annurev-earth-060614-105206.

Gudmundsson, M.T. Jónsdóttir, K., Hooper, A., Holohan, E.P., Halldórsson, S.A., Ófeigsson, B.G., Cesca, S., Vogfjörd, K.S., Sigmundsson, F., Högnadóttir, T. and Einarsson, P. (2016) ‘Gradual caldera collapse at Bárdarbunga volcano, Iceland, regulated by lateral magma outflow’, *Science*, 353(6296), p. aaf8988. doi:10.1126/science.aaf8988.

Han, R. Kim, J.S., Kim, C.M., Hirose, T., Jeong, J.O. and Jeong, G.Y. (2019) ‘Dynamic weakening of ring faults and catastrophic caldera collapses’, *Geology* 47(2), p. 107-110.

Hardie, W.G. (1963) ‘Expolsion-breccias near Stob Mhic Mhartuin, Glen Coe, Argyll, and their bearing on the origin of he nearby flinty crush-rcok’, *Transactions of the Geological Society of Edinbrugh* [Preprint].

Hickman, A.H. and Wright, A.E. (1983) ‘Geochemistry and chemostratigraphical correlation of slates, marbles and quartzites of the Appin Group, Argyll, Scotland’, *Transactions of the Royal Society of Edinburgh: Earth Sciences*, 73(4), pp. 251–278. doi:10.1017/S0263593300009718.

Holness, M.B. (2018) ‘Melt segregation from silicic crystal mushes: a critical appraisal of possible mechanisms and their microstructural record’, *Contributions to Mineralogy and Petrology*, 173(6), p. 48. doi:10.1007/s00410-018-1465-2.

Holohan, E.P. (2015) ‘Stress evolution during caldera collapse’, *Earth and Planetary Science Letters*, p. 13.

Huber, C., Bachmann, O. and Dufek, J. (2011) ‘Thermo-mechanical reactivation of locked crystal mushes: Melting-induced internal fracturing and assimilation processes in magmas’, *Earth and Planetary Science Letters*, 304(3–4), pp. 443–454. doi:10.1016/j.epsl.2011.02.022.

Kennedy, B., Stix, J., Vallance, J.W., Lavallée, Y. and Longpré, M.A., (2004) ‘Controls on caldera structure: Results from analogue sandbox modeling’, *Geological Society of America Bulletin*, 116(5), p. 515. doi:10.1130/B25228.1.

Kennedy, B.M., Holohan, E.P., Stix, J., Gravley, D.M., Davidson, J.R.J. and Cole, J.W., (2018) ‘Magma plumbing beneath collapse caldera volcanic systems’, *Earth-Science Reviews*, 177, pp. 404–424. doi:10.1016/j.earscirev.2017.12.002.

Kim, C.-M., Han, R., Kim, J.S., Sohn, Y.K., Jeong, J.O., Jeong, G.Y., Yi, K. and Kim, J.C., (2019) 'Fault zone processes during caldera collapse: Jangsan Caldera, Korea', *Journal of Structural Geology*, 124, pp. 197–210. doi:10.1016/j.jsg.2019.05.002.

Kokelaar, B.P. (2007) 'Friction melting, catastrophic dilation and breccia formation along caldera superfaults', *Journal of the Geological Society*, 164(4), pp. 751–754.

Kokelaar, B.P. and Moore, I. (2006) *Glencoe caldera voclano, Scotland*. Nottingham: British Geological Survey.

Maddock, R.H. (1986) 'Frictional melting in landslide-generated frictionites (hyalomylonites) and fault-generated pseudotachylytes-discussion', *Tectonophysics* [Preprint].

Magloughlin, J.F. and Spray, J.G. (1992) 'Frictional melting processes and products in geological materials: introduction and discussion', *Tectonophysics*, 204(3–4), pp. 197–204. doi:10.1016/0040-1951(92)90307-R.

Mastin, L.G., Guffanti, M., Servranckx, R., Webley, P., Barsotti, S., Dean, K., Durant, A., Ewert, J.W., Neri, A., Rose, W.I. and Schneider, D., (2009) 'A multidisciplinary effort to assign realistic source parameters to models of volcanic ash-cloud transport and dispersion during eruptions', *Journal of Volcanology and Geothermal Research*, 186(1–2), pp. 10–21. doi:10.1016/j.jvolgeores.2009.01.008.

McGarvie, D.W. (1980) 'Stob Mhic Mhartuin', *the Geological Conservation Review*, 17.

Melnik, O. and Sparks, R.S.J. (1999) 'Nonlinear dynamics of lava dome extrusion', *Nature*, 402(6757), pp. 37–41. doi:10.1038/46950.

Moore, I. (1995) *The early history of the Glencoe cauldron*. University of liverpool.

Moore, I. and Kokelaar, P. (1998) 'Tectonically controlled piecemeal caldera collapse: A case study of Glencoe volcano, Scotland', *Geological Society of America Bulletin*, p. 20.

Moore, I.A.N. and Kokelaar, P. (1997) 'Tectonic influences in piecemeal caldera collapse at Glencoe Volcano, Scotland', *Journal of the Geological Society*, 154(5), pp. 765–768. doi:10.1144/gsjgs.154.5.0765.

Motoki, A., Geraldes, M.C., Iwanuch, W., Vargas, T., Motoki, K.F., Balmant, A. and Ramos, M.N., (2012) 'The pyroclastic dyke and welded crystal tuff of the Morro dos Gatos alkaline intrusive complex, State of Rio de Janeiro, Brazil', *Rem: Revista Escola de Minas*, 65(1), pp. 35–45. doi:10.1590/S0370-44672012000100006.

Muir, R.J. (2017) ‘Moving faults and building fracture models in a digital world-an example from Glen Coe, Scotland’, *Geology Today*, 33(2), pp. 54–59. doi:10.1111/gto.12180.

Newhall, C.G. and Dzurisin, D. (1988) ‘Historical unrest at the large calderas of the world’, *Department of the Interior, US Geological Survey*, 2(1855).

Parmigiani, A., Huber, C. and Bachmann, O. (2014) ‘Mush microphysics and the reactivation of crystal-rich magma’, *Journal of Geophysical Research: Solid Earth*, 119(8), pp. 6308–6322.

Passchier, C.W. and Trouw, R.A. (2005) *Microtectonics*. Springer Science & Business Media.

Polacci, M., Vitturi, M.D.M., Fabio, A., Burton, M.R., Luca, C., Brett, C., Matteo, C., Corrado, C., Clarke, A.B., Simone, C. and Antonio, C., (2017) ‘From magma ascent to ash generation: investigating volcanic conduit processes by integrating experiments, numerical modeling, and observations’, *Annals of Geophysics*, 60(6), p. 1. doi:10.4401/ag-7449.

Reynolds, D.L. (1956) ‘Calderas and ring-complexes’, *Nederlandsch Geologisch-Mijnbouw- kundig Genootschap, Verhandelingen, Geologische Serie* [Preprint].

Richey, J.E. (1932) ‘Tertiary ring-structures in Britain’, *Transactions of the Geological Society of Glasgow*, 19, pp. 42–140.

Richey, J.E. and Thomas, H.H. (1932) ‘The Tertiary ring compelx of Slieve Gullion, Ireland’, *Quaterly Journal of the Geological Society of London*, 88, pp. 653–88.

Roberts, J.L. (1963) ‘Source of the Glencoe lgnimbrites’, 199(4896), pp. 901–901.

Roberts, J.L. (1966) ‘The Emplacement of the Main Glencoe Fault-Intrusion at Stob Mhic Mhartuin’, *Geological Magazine*, 103(4), pp. 299–316. doi:10.1017/S0016756800052973.

Roberts, L. (1974) ‘The evolution of the Glencoe Cauldron’, *The Scottish Journal of Geology*, 10(4), pp. 269–282.

Roche, O., Druitt, T.H. and Merle, O. (2000) ‘Experimental study of caldera formation’, *Journal of Geophysical Research: Solid Earth*, 105(B1), pp. 395–416. doi:10.1029/1999JB900298.

Segall, P. and Anderson, K. (2021) ‘Repeating caldera collapse events constrain fault friction at the kilometer scale’, *Proceedings of the National Academy of Sciences*, 118(30), p. e2101469118. doi:10.1073/pnas.2101469118.

Shand, J. (1916) ‘The pseudotachylyte of Paris (Orange Free State) and its relation to “Trap-Shotten Gneiss” and “Flinty Crush-Rock”’, *Quaterly Journal of the Geological Society of London* [Preprint].

Sibson, R.H. and Toy, V.G. (2006) ‘The habitat of fault-generated pseudotachylyte: Presence vs. absence of friction-melt’, in Abercrombie, R. et al., (eds) *Geophysical Monograph Series*. Washington, D. C.: American Geophysical Union, pp. 153–166. doi:10.1029/170GM16.

Sigurdsson, H., Houghton, B., McNutt, S., Rymer, H. and Stix, J. (2015) *The encyclopedia of volcanoes*. Elsevier.

Soper, N.J. *et al.,* (1992) ‘Sinistral transpression and the Silurian closure of Iapetus’, *Journal of the Geological Society*, 149(6), pp. 871–880. doi:10.1144/gsjgs.149.6.0871.

Spray, J. (1997) ‘Superfaults’, *Geology*, 25(7), pp. 579–582.

Stevenson, C.T.E. *et al.,* (2008) ‘The structure, fabrics and AMS of the Slieve Gullion ring-complex, N. Ireland: testing the ring-dyke empalcement model’, *Geological Society Special Publication*, 302, pp. 159–84.

Stix, J. and Kobayashi, T. (2008) ‘Magma dynamics and collapse mechanisms during four historic caldera-forming events’, *Journal of Geophysical Research*, 113(B9), p. B09205. doi:10.1029/2007JB005073.

Sung keun, L., Han, R., Kim, E.J., Jeong, G.Y., Khim, H. and Hirose, T., (2017) ‘Quasi-equilibrium melting of quartzite upon extreme friction.’, *Nature Geoscience*, 10.6, pp. 436–441.

Szemerédi, M., Varga, A., Szepesi, J., Pál-Molnár, E. and Lukács, R., (2020) ‘Lavas or ignimbrites? Permian felsic volcanic rocks of the Tisza Mega-unit (SE Hungary) revisited: A petrographic study’, *Central European Geology*.

Tan, W., Liu, P., He, H., Wang, C.Y. and Liang, X., (2016) ‘Mineralogy and Origin of Exsolution In Ti-Rich Magnetite From Different Magmatic Fe-Ti Oxide-Bearing Intrusions’, *The Canadian Mineralogist*, 54(3), pp. 539–553. doi:10.3749/canmin.1400069.

Taubeneck, W.H. (1967) ‘Notes on the Glen Coe Cauldron Subsidence, Argyllshire, Scotland’, *Geological Society of America Bulletin*, 78(11), p. 1295. doi:10.1130/0016-7606(1967)78[1295:NOTGCC]2.0.CO;2.

Thirlwall, M.F. (1988) ‘Geochronology of Late Caledonian magmatism in northern Britain’, *Journal of the Geological Society*, 145(6), pp. 951–967. doi:10.1144/gsjgs.145.6.0951.

Torres-Hernández, J.R. *et al.,* (2006) 'The pyroclastic dikes of the Tertiary San Luis Potosí volcanic field: Implications on the emplacement of Panalillo ignimbrite', *Geofísica Internacional*, 45(4), pp. 243–253. doi:10.22201/igeof.00167169p.2006.45.4.161.

Troll, V.R., Meade, F.C., Chew, D.M. and Emeleus, C.H., (2008) 'A new exposure of a caldera fault segment at the Slieve Gullion Igneous Centre: implications for the emplacement of the early ring-complex', *Irish Journal of Earth Sciences*, pp. 1–16.

Wadsworth, F.B., Witcher, T., Vossen, C.E., Hess, K.U., Unwin, H.E., Scheu, B., Castro, J.M. and Dingwell, D.B., (2018) 'Combined effusive-explosive silicic volcanism straddles the multiphase viscous-to-brittle transition', *Nature Communications*, 9(1), pp. 1–8.

Wadsworth, F.B., Llewellin, E.W., Vasseur, J., Gardner, J.E. and Tuffen, H., (2020) 'Explosive-effusive volcanic eruption transitions caused by sintering', *Science Advances*, 6(39), p. eaba7940. doi:10.1126/sciadv.aba7940.

Wiebe, R.A., Kolzenburg, S., Rooyakkers, S.M. and Stix, J., (2021) 'Plutonic record of a caldera-forming silicic eruption: The shatter zone of the Cadillac Mountain granite, coastal Maine', *Geosphere* [Preprint]. doi:10.1130/GES02252.1.

Wilson, C.J.N. (2001) 'The 26.5 ka Oruanui eruption, New Zealand: an introduction and overview', *Journal of Volcanology and Geothermal Research*, 112(1–4), pp. 133–174. doi:10.1016/S0377-0273(01)00239-6.

Wilson, C.J.N. (2008) 'Supereruptions and Supervolcanoes: Processes and Products', *Elements*, 4(1), pp. 29–34. doi:10.2113/GSELEMENTS.4.1.29.

Wilson, C.J.N., Cooper, G.F., Chamberlain, K.J., Barker, S.J., Myers, M.L., Illsley-Kemp, F. and Farrell, J., (2021) 'No single model for supersized eruptions and their magma bodies', *Nature Reviews Earth & Environment*. 2(9) pp,610-627 doi:10.1038/s43017-021-00191-7.

Wilson, L., Sparks, R.S.J. and Walker, G.P.L. (1980) 'Explosive volcanic eruptions -- IV. The control of magma properties and conduit geometry on eruption column behaviour', *Geophysical Journal International*, 63(1), pp. 117–148. doi:10.1111/j.1365-246X.1980.tb02613.x.

Wolff, J.A. (1985) 'Zonation, mixing and eruption of silica-undersaturated alkaline magma: a case study from Tenerife, Canary Islands', *Geological Magazine*, 122(6), pp. 623–640. doi:10.1017/S0016756800032039.

Wolff, J.A. (1986) ‘Welded-tuff dykes, conduit closure, and lava dome growth at the end of explosive eruptions’, *Journal of Volcanology and Geothermal Research*, 28(3–4), pp. 379–384. doi:10.1016/0377-0273(86)90032-6.

van Zalinge, M.E., Cashman, K.V. and Sparks, R.S.J. (2018) ‘Causes of fragmented crystals in ignimbrites: a case study of the Cardones ignimbrite, Northern Chile’, *Bulletin of Volcanology*, 80(3), p. 22. doi:10.1007/s00445-018-1196-2.

Appendix

This appendix has been made to support the work produced in the thesis in order to give background to the terminology used and the units that have been studied. This material is supplementary, not essential to the thesis. You can expect to find:

A – Nomenclature which clarifies and cross references terminology used throughout literature and in this thesis.

B – Although the history of science is not critical to this thesis, it is informative to understand the evolution of ideas at Glencoe, particularly because this study discusses a topic which has been persistently debated for over one hundred years (the debate of the origin of FCR, introduced in section 1.6 and 2.3). The origin of the petrogenesis of the FCR is an ongoing debate, dating back from when it was first described, where support has repeatedly switched between frictional melt theories and volcanic theories.

C – Provides extended background to Glencoe relevant to the discussion in the sense that placing caldera fault rocks in the widest context is really helpful for building the argument that there was a large mass of material transported through this fault that arrived at the surface in a fragmented state.

A - Nomenclature

Throughout literature on these topics, especially within studies of Glencoe, terminology has become confused and problematic, particularly due to the use of names with genetic descriptions. Therefore, this study re-clarifies the use of certain language. This may lead to future work in this area changing to new, less genetic, or unclear names. Importantly, this study supports the efforts of previous authors (Taubeneck, 1967; Garnham, 1988) to make it clear that the 'Fault Intrusion' is a catchall name used for a the ring fault fill which is very variable in composition, therefore depending on the scale of future studies, researchers may wish to re-organise language in order to break down the units further.

Unit names or phrases that have been given different names throughout literature	
The phase I will use	Other names used in previous literature
Brecciated quartzite	Breccia; microbreccia; cataclasite; quartzite breccia
Red felsite	Rhyolite
Tuffisite	Pseudotachylyte
Fragmentation	Foaming

Phrases I would like to clarify the definition of my use for the purpose of clarity	
Quartzite	A metamorphic rock formed by the metamorphism of sandstone. Part of the Dalradian basement of Glencoe, including found at Stob Mhic Mhartuin.
Brecciated quartzite	A brecciated sub-unit of quartzite found along the ring faults in Stob Mhic Mhartuin. Found at various degrees of cataclasis.
Flinty Crush rock	A fine grained, aphanitic, banded black unit which intermittently lines the contact between

	the country rock and the ring intrusions at Glencoe.
Red felsite	A red porphyritic unit which is found in lenticular bodies throughout the Glencoe ring intrusion, found in close association with the FCR and fault intrusion, commonly lying between them.
Fault intrusion	A grey, crystal rich glomeroporphyrite which intrudes the Glencoe ring fault. As recorded well by Garnham (1988) this comprises a range of compositions and therefore future studies should consider this as multiple units.
Main ring fault	The Glencoe ring fault which facilitated the caldera collapse of Glencoe and was intruded by magma. A discontinuous ring of faults which forms an elliptical shape. At Stob Mhic Mhartuin this is the ring fault further to the southeast.
Outer ring fault	A minor ring fault strand which extends from the main ring fault of Glencoe in the northeastern sector, and is also intruded by magma. At Stob Mhic Mhartuin this is the ring fault further to the northeast.
Inner ring fault/intrusion contact	The contact of the ring fault intrusion closer to the centre of the caldera. At Stob Mhic Mhartuin this is to the southeast of the intrusions and lies along a fault plane.
Outer ring fault contact	The contact of the ring fault intrusion furthest from the centre of the caldera. At Stob Mhic Mhartuin this is to the northeast of the intrusions and does not lie along a fault plane.
Groundmass/matrix	In this thesis the use of groundmass and matrix is interchangeable due to the debate over the origin/state of units. This refers to the material separating clasts/phenocrysts.
Phenocryst/clast	In this thesis the use of phenocryst and clast is interchangeable due to the debate over the origin/state of units. This refers to any particle of rock or single crystal set.
Pseudotachylyte/frictional melt	A very fine-grained or glass-like fault rock, formed by rapid displacement and melting by shear generated heating.
Fluidised/fragmented system	A volcanic product comprised of fragmented pyroclastic magma and gas entrained in a flow.
Fragment/fragmented/pyroclastic/ash	A volcanic product, formed by magma fragmentation, which takes the form of fine clasts which are broken particles.

Fracking	Gas pressure driven fracture process, physically analogous to fracking in industrial context
Tuffisite	A fine grained pyroclastic rock, comprising finely divided fragments of magma, broken phenocrysts, grains of sediment and dismembered vent wall material, which appear to have been fluidized and intruded along volcanic conduits.
Caldera	A depression in earths surface with a diameter >1.5km formed by collapse into a magma chamber that has been vacated by the eruption of migration of magma.
Storage region	A region of subsurface accumulation of magma.
Transport system	The region of magma through the subsurface through the crust, between the storage region and the surface eruption.
Surface eruption	The release of volcanic products at the earths surface from a volcano.
Ring fault	An annular fault of cylindrical shape that acts as the main surface to facilitate collapse of a central block during caldera collapse, which is vertical or outward dipping.
Ring intrusion	An annular, tabular body of cylindrical shape, exposed at the surface with a ring-shaped outcrop, formed of almost any igneous rock, with a vertical axis and vertical or outward-dipping contacts.
Caldera collapse structural system	The structure movements (i.e. fault slip and downsagging) which contribute to the downwards subsidence of the crustal roof block of the magma reservoir.
Superfault	A fault with very large displacement (>=100 m) occurring during a single-slip event at seismogenic velocity (>0.1m/s), proposed by Spray (1997) and Kokelaar (2007) to occur at caldera ring faults.

Definitions aided by:
Kearey, P., 2001. *The new Penguin dictionary of geology*. London: Penguin.
Sigurdsson, H. *et al.,* (2015) *The encyclopedia of volcanoes*. Elsevier.

B – background on the development of research at Glencoe caldera

Understanding silicic caldera-forming volcanic eruptions is important due to their capacity for widespread destruction (Cole et al., 2005; Sigurdsson *et al.*, 2015; Kennedy *et al.*, 2018; Geshi *et al.*, 2021). Silicic caldera-forming eruptions are considered to be among the largest and most hazardous

natural events on Earth, with the ability to erupt 5,000 km^3 of lavas and pyroclastic material (Cole et al., 2005; Geyer and Martí, 2008; Sigurdsson *et al.*, 2015; Kennedy *et al.*, 2018). Caldera-forming volcanoes also represent a large portion of the world's total volcanism (for example, there are >60 known calderas in North America (Newhall and Dzurisin, 1988; Geyer and Martí, 2008; Browning and Gudmundsson, 2015). Calderas are additionally important for harnessing of resources because they are common sites of geothermal activity and mineralisation therefore it is crucial to understand fluid circulation and post-eruption mineralisation (Cole et al., 2005; Kennedy *et al.*, 2018). It is for these reasons that understanding the processes (both at the surface and within the sub-surface) that occur during caldera-forming eruptions is a key aim for scientists in modern volcanology.

The pioneering work of the Glencoe volcano was conducted by Clough *et al*., (1909). Not only was it the first detailed analysis of the deeply dissected ancient Glencoe caldera, but it was also one of the first detailed analyses of its kind worldwide, where scientists saw the first thorough layout of the crustal relationships that occur between a magmatic plumbing system and the surface. This work highlighted significant structures such as the discontinuous fault intrusions (the blocky **purple** unit circling the map on Glencoe in figure 2.1a page 23), which occasionally displayed a second (found at Stob Mhic Mhartuin in the northeast of figure 2.1a) early fault, as well as the presence of the unit they named the 'flinty crush rock' (not highlighted in figure 2.1a due to its scale, but found intermittently lining the ring fault and Fault Intrusion that circles across the whole map) . This triggered a debate that would continue for years until the present day. Their study originally named the area of volcanics, along with associated rocks and structures, a 'cauldron'. The system was believed to have experienced piston-like subsidence of a coherent cylindrical block of crust along the peripheral ring fault. The 'fault-intrusion complex' was explained as the complementary magma ascent to this subsidence, exploiting the ring fault as a semicontinuous vent.

Since this work, a more detailed understanding of the Glencoe volcano has developed due to an improved general volcanological understanding, as well as further study of the Glencoe site. Some noteworthy advances in Glencoe research include: the recognition of ignimbrites within the volcanic succession (Roberts, 1963); changing constraint of the dip of the caldera faults (Taubeneck, 1967); realisation that early explosive activity resulted in asymmetric subsidence of the caldera (Roberts, 1974); and understanding that caldera structures will commonly overlie major fault zones (Moore and Kokelaar, 1997). These advancements have culminated with a detailed remapping of Glencoe. This work was undertaken by Kokelaar and Moore, (2006) who produced a 1:25,000 geological map of the entire volcanic succession (summarized in simplified form in Figure 2.1), using the improved modern day understanding of the systems involved, modifying the original interpretations. This new understanding synthesised by the remapping has resulted in a new term to be applied to the system – the Glencoe caldera-volcano complex - which encompasses all volcanic units, sedimentary units, coeaval intrusions, and volcano-tectonic structures related to the volcano's development. This development of ideas leading to a detailed picture of the Glencoe system has been an important insight to modern caldera systems worldwide, indicating that the simple system seen at the surface may not be the case at depth.

C – Glencoe magmatism and the units of Glencoe caldera

Magmatism occurred here as a result of the Caledonian orogeny (435-425 Ma; Soper *et al.*, 1992; Dewey and Strachan, 2003), which involved strike-slip faulting, uplift and erosion, and culminated in the closure of the Iapetus Ocean (Kokelaar and Moore, 2006). This period of activity resulted in the development of NE-SW orientation structures. Two intersecting basement/crustal discontinuities are what have influenced the formation of orthogonal faults and related grabens, as well as the magmatic plumbing system (Moore and Kokelaar, 1997). This crossing is the explanation given by Moore and Kokelaar for why magmatism was focused in Glencoe. The tectonic framework played a substantial control in the magmatic plumbing and location of vents, the direction and location of faults, the caldera depocenters and the developments of through going rivers (Moore and Kokelaar, 1997). The faults all correspond to a regional transpressional regime, which has been linked by Moore and Kokelaar to the effects of post-Caledonian Orogenesis in Britain. The shift in vents and depocentres

seen throughout Glencoes multiple collapse history reflects the interplay that occurred between regional tectonism and volcano tectonic collapse (Moore and Kokelaar, 1998). Moore and Kokelaar have related the apparent magnitude of tectonism to the most actively subsiding pull apart sedimentary basins known, with an expected 2-3km/myr rate.

The Glencoe basement, which composes part of the downfaulted block outlined by the ring fault, consists of Dalradian rock (Late Precambrian – Cambrian times, 700-500myr; Garnham, 1988), as part of the Dalradian supergroup which dominates the Grampian Terrane. This foundation of intensely deformed metasedimentary rocks has become exposed due to the deep dissection of the rugged terrain. The basement rocks in this region, found on both sides of the ring fault, are commonly quartzites and pelites. A compressional tectonic regime during the Ordovician (500-490myr) also caused this basement to become folded and metamorphosed (Garnham, 1988). This basement is significantly fragmented by the faults of the Glencoe graben, as well as additional segmentary faults. The basement is overlain by some pre-caldera successions of volcanics (extrusive and intrusive andesites) and sedimentary rocks, before the >1 km thick intra-caldera units deposited during the period of collapse. The former cover of basalt-andesite lavas and sills, as well as sedimentary rocks, (seen at the stratigraphically lowest volcanic unit in figure 2.1b) were substantially eroded prior to the explosive intra-caldera volcanism. The period between this early magmatism and the later caldera-volcanism may have lasted for longer than hundreds of thousands of years (Kokelaar and Moore, 2006).

Caldera collapse here was piecemeal and incremental, involving numerous crustal blocks, with each major slip event being marked by the deposition of an ignimbrite unit. Studies showing the complex collapse and infilling structures are what reconciled Glencoe with a non-coherent subsidence structure. Each eruption event caused rapid large-scale subduction on graben and cross graben faults and flexures. Prior to collapse, tectonically controlled faults broke up the caldera floor into many blocks and provided lines of weakenss for caldera collapse to preferentially exploit, which resulted in Glencoe's piecemeal collapse style.

The extrusive and intrusive intra-caldera volcanics range from basalt/gabbro to rhyolite/granite in bulk composition (seen in the centre of the map of Glencoe in figure 2.1a, as deposits tend to collect and stay preserved in the collapsed caldera centre). The extrusive volcanic deposits consist of silicic pyroclastic rocks, and intermediate-silicic lavas (Garnham, 1988). The intra-caldera volcanic rocks are ~1.3 km in thickness (Kokelaar, 2007) and do contact with the metamorphic basement along the steep ring fault. There are 7 thick major ignimbrite units dominating the volcanic succession at Glencoe. These 100-150 m thick ignimbrite units each represent an episode of major caldera-forming explosive eruptions accompanied by volcano-tectonic subsidence and piecemeal caldera collapse (Moore and Kokelaar, 1998; Kokelaar and Moore, 2006). The ignimbrites have been assigned to 3 different members - the Etive Member, the Three Sisters Member, and the Dalness Member – each named according to the areas where its thickness is greatest. This variation in thickness is a result of the constantly changing form of the tectonically controlled graben. The start of an eruption is marked by a phreatomagmatic tuff cone and associated distal layers developed around the vent. The reason for each eruption initiating with phreatomagmatism is due to the channelling of ascending magma through water saturated sediments in the tectonic depocenter (Moore and Kokelaar, 1997). The initiation of caldera collapse events is marked by the explosive eruption of rhyolite which formed flows built from fountaining pyroclastics from one or more vents which were large and dilated during caldera subsidence. As a testament to the very piecemeal and incremental nature of Glencoe's caldera collapse, the volcanic succession is found to have varying thicknesses and numerous scarps. These units accumulated in local depocentres which were controlled by the ongoing downsag and orthogonal faulting (Moore and Kokelaar, 1997). The volcanic rocks are considered to have been derived from more than one centre, due to their bimodal nature (andesite and rhyolite) and thickness variations of units according to area (Garnham, 1988).
There are numerous intra-caldera mingled (andesite-rhyolite) magma sills also found amongst the succession. These are up to 100m thick and were accommodated by incremental periods of subsidence (Moore and Kokelaar, 1998).

The roughly oval shaped caldera ring fault system is associated with intrusions of gabbros, diorites, tonalites, monzonites and granites – the Glencoe fault intrusions. They are blocky and variable in width (up to 1.5 km at their widest, Figure 2.1a) (Garnham, 1988; Kokelaar, 2007). The fault intrusions are 419+-5.4Ma (Neilson et al., 2009). The red felsite and the flinty crush rock (FCR) are two units associated with the ring fault intrusions at Glencoe. They are smaller (so not seen in Figure 2.1a) and are not always present along the ring fault. The ring intrusions and associated fault rocks are variably exposed (partly due to the later destruction by granitoid plutonism – the Rannoch Moor Pluton 422.5+-0.5 Ma, the Clach leathad Plutons 417+-0.9 Ma, and the Etive Pluton 414.9+-0.7 Ma (Neilson et al., 2009)), forming an irregular and near continuous ring that surrounds the downfaulted central caldera block consisting of country rock and volcanic deposits.

Sedimentary units are found between the volcanics which were deposited as a result of alluvial deposition. There are also numerous erosional unconformities formed due to the incising action of the fluid pathways. These sedimentary features developed between periods of extrusive volcanism where rivers and fluvial palaeocanyons exploited small basins (grabens or half-grabens) created by the continued tectonic faulting. It is believed that these periods of volcanic quiescence may have been up to many tens of thousands of years long. Tectonism producing dynamic graben structures played a key control on intra-caldera sedimentation. Frequent changes in drainage and sedimentation systems (represented by changing location and character of sedimentary deposits in the geological record) resulted as an unsurprising outcome of the tectonic complexity and ever-changing structural configuration of Glencoe's activity (Moore and Kokelaar, 1997; Kokelaar and Moore, 2006). Sediments even had an influence on the eruption styles and shallow level sill emplacements, creating a feedback system between the processes of tectonism, volcanism and sedimentation (Moore and Kokelaar, 1997).

Hydrothermal activity has been rife throughout the region meaning that the majority of the rocks have been significantly hydrothermally altered to look quite different from when they were originally deposited. Reactivation of faulting and presence of a hydrothermal system is evident through fractures and quartz, epidote, white mica and commonly oxidised pyrite veins (Bailey and Maufe, 1960; Kokelaar, 2007). Additionally, the effects of significant burial and weathering has affected their appearance further.

There are no absolute constraints on the durations of eruptions and periods of quiescence between them. The 7 major ignimbrites of the volcanic succession are believed to represent single sustained eruption deposits, some may have been long lived lasting multiple days (Moore and Kokelaar, 1998). Significant enough intervals occurred between these eruptions in order to allow cooling, erosion, deep fluvial canyon incision, and subsequent development of lakes and fans. Following intrusion events, seen to cut through the complex, produce slightly younger ages 412-401 million years ago (Clayburn *et al.*, 1983; Thirlwall, 1988). To allow more detailed insight into the timeline of volcanism at Glencoe, Moore and Kokelaar (1998) use a modern comparison of the Taupo Volcanic Zone. These systems are considered similar due to their rapid tectonic extension and resulting high frequency of caldera eruptions. Therefore, this implies possible constraints of Glencoe's tectonic downthrow rate to be around >0.5km/myr and minimum intervals between caldera-forming eruptions to be ~10^3-10^5 years. The expected slip rate of >0.5km/myr is typical of the most actively subsiding sedimentary basins.

D – Pseudotachylytes

A pseudotachylyte is a rock formed from a frictional melt of the wall rocks (in this case the crustal reservoir roof cut by the caldera ring faults) which occurs as a dynamic weakening mechanism in reaction to the high friction caused by rapid frictional sliding, resulting in a dramatic drop in friction along the fault surface (Di Toro *et al.*, 2011). Frictional melts are known to occur during the faulting of anhydrous, non-porous crustal crystalline rocks which are under a high strain rate (>95% of host rocks are crystalline metamorphic or plutonic (Magloughlin and Spray, 1992)). These are similar

conditions to those inferred for caldera collapse. Frictional melting is occurs out of equilibrium, rapidly in a single slip event, at temperatures around 1200°C (Sibson and Toy, 2006). The process is believed to occur within or near the base of the upper crustal seismogenic zone (1-2 km to >20 km). Sibson and Toy (2006) demonstrate that to produce just 10 mm thickness of pseudotachylyte ~40 MJ/m^2 energy dissipation is required, hence, they are rare in the geological record. The chemical composition of pseudotachylytes should be almost identical to their host rocks, with few minor exceptions (Magloughlin and Spray, 1992).

The resulting pseudotachylytes rocks have a fairly distinct appearance – they are generally cohesive, dark, fine, aphanitic (Magloughlin and Spray, 1992; Sibson and Toy, 2006; Fondriest *et al.*, 2020). Generally there are isolated fragments contained within a homogenous and fine matrix. Some characteristic microstructures of pseudotachylytes include; veining, devitrified glasses (i.e. microlites/spherulites), isotropic, sulphide droplets, thermally shocked clasts (cracks with melt inside), a dark homogenous matrix, minor inclusions of wall rock fragments, compositional layering which may be folded, amygdales, embayed clasts, vesicles (Magloughlin and Spray, 1992; Fondriest *et al.*, 2020). Micas, Fe-Mg Al silicates and feldspars are commonly lacking in pseudotachylytes due to their preferential dissolution, whereas quartz tends to resist melting therefore is seen as angular fragments with internal fractures and fluid inclusion planes. Typically pseudotachylytes are thin, rarely exceeding a few centimetres, with 75% of them having thicknesses of less than 25 mm (Passchier and Trouw, 2005; Sibson and Toy, 2006). Veins greater than 6 mm are zoned to develop more spherulitic central domains (Di Toro and Pennacchioni, 2004). The contact of pseudotachylytes with their wall rock are sharp and straight, never showing progressive intensity of brittle deformation. The wall rock may be occasionally cataclasted. Often there is evidence of injection veins offshooting from the plane of origin.

E – Pyroclastic conduits

Pyroclastic conduits and tuffisites are a well-studied phenomenon (Wolff, 1985; Torres-Hernández *et al.*, 2006; Díaz-Bravo and Morán-Zenteno, 2011; van Zalinge, Cashman and Sparks, 2018; Szemerédi *et al.*, 2020). Indeed, Wadsworth et al., (2020) have suggested that the majority of dense rhyolite interpreted to be lavas at the Earth's surface, may in fact be the product of in-conduit welding. This was expanded on by Schipper et al., (2021). Once produced, pyroclasts may re-weld, effectively undoing fragmentation and producing dense magma again (e.g. Sparks et al., 1999; Wadsworth et al., 2021). This has led to some very high-grade, densely-welded ignimbrites – the product of pyroclast welding – to be misinterpreted as lavas – dense bodies of volcanic rock (see Branney & Kokelaar, 1992). Clearly therefore, volcanic welding can obscure and confound unique interpretations, and lead to debate. Burt and Brown (1997) provide an example at Ben Nevis Caldera in Scotland, for ignimbrites lining the edges of a caldera ring fault conduit in place of where a pseudotachylyte might otherwise be expected.